ANALYSIS OF PHENOL OXIDATION PRODUCTS BY *SCYTALIDIUM THERMOPHILUM* BIFUNCTIONAL CATALASE/PHENOL OXIDASE (CATPO)

A THESIS SUBMITTED TO
THE GRADUATE OF NATURAL AND APPLIED SCIENCES
OF
MIDDLE EAST TECHNICAL UNIVERSITY

BY

GÜLDEN AVCI

IN PARTIAL FULFILLMENT OF THE REQUIREMENTS
FOR
THE DEGREE OF DOCTOR OF PHILOSOPHY
IN
BIOTECHNOLOGY

JUNE 2011

Approval of the thesis:

ANALYSIS OF PHENOL OXIDATION PRODUCTS BY *SCYTALIDIUM THERMOPHILUM* BIFUNCTIONAL CATALASE/PHENOL OXIDASE (CATPO)

submitted by **GÜLDEN AVCI** in partial fulfilment of the requirements for the degree of **Doctor of Philosophy in Biotechnology Department, Middle East Technical University** by,

Prof. Dr. Canan Özgen ———————————
Dean, Graduate School of **Natural and Applied Sciences**

Prof. Dr. İnci Eroğlu ———————————
Head of Department, **Biotechnology**

Prof. Dr. Zümrüt B. Ögel ———————————
Supervisor, **Food Engineering Dept**., **METU**

Prof. Dr. Gürkan Karakaş ———————————
Co-Supervisor, **Chemical Engineering Dept., METU**

Examining Committee Members:

Prof. Dr. Ufuk Bakır ———————————
Chemical Engineering Dept., METU

Prof. Dr. Zümrüt B. Ögel ———————————
Food Engineering Dept., METU

Prof. Dr. Aziz Tekin ———————————
Food Engineering Dept., Ankara Univ

Assoc. Prof. Dr. Nursen Çoruh ———————————
Chemistry Dept., METU

Prof. Dr. Gülüm Şumnu ———————————
Food Engineering Dept., METU
.

                               Date: 10.06.2011

I hereby declare that all information in this document has been obtained and presented in accordance with academic rules and ethical conduct. I also declare that, as required by these rules and conduct, I have fully cited and referenced all material and results that are not original to this work.

Name, Last name : Gülden Avcı

Signature　　　　　 :

ABSTRACT

ANALYSIS OF PHENOL OXIDATION PRODUCTS BY *SCYTALIDIUM THERMOPHILUM* BIFUNCTIONAL CATALASE/PHENOL OXIDASE (CATPO)

Avcı, Gülden

Ph.D., Department of Biotechnology

Supervisor: Prof. Dr. Zümrüt Begüm Ögel

Co-Supervisor: Prof. Dr. Gürkan Karakaş

June 2011, 160 pages

This thesis was aimed to analyze phenol oxidation by the bifunctional catalase/phenol oxidase of the thermophilic fungus *Scytalidium thermophilum.* Several reactive oxygen species (ROS) are continuously produced in fungi under oxidative stress. Depending on the nature of the ROS species, some are highly toxic and are rapidly detoxified by various cellular enzymatic mechanisms, including the production of catalase. *S. thermophilum* produces a novel bifunctional catalase-phenol oxidase (CATPO) which is capable of oxidizing phenolics in the absence of hydrogen peroxide. Phenol oxidases convert phenolic compounds to quinones, which are then polymerized mainly by free- radical mediated reactions. In this study, 14 phenolic compounds were selected according to their different chemical structures and functional properties and were analyzed as substrates of CATPO. Among 14 phenolic compounds, only in catechol, chlorogenic acid, catechin and caffeic acid distinct oxidation products were observed by HPLC. The oxidation products of catechol, caffeic acid, chlorogenic acid and catechin were characterized by LC-ESI-MS. Dimer, trimer, tetramer and oligomer formations were detected. While the maximum conversion efficiency, at 1 hour of reaction, was observed with catechin, minimum conversion efficiency was attained by caffeic acid, under the specified conditions. The oxidation products observed after oxidation of catechol, chlorogenic

acid, catechin and caffeic acid by CATPO was compared with the same phenolic compounds oxidation products oxidized by laccase and tyrosinase. CATPO was incapable of oxidizing tyrosinase and laccase-specific substrates tyrosine and ABTS respectively. However, the oxidizing spectrum of substrates indicates that the nature of phenol oxidation by CATPO appears to resemble mainly those of laccase.

ÖZ

SCYTALIDIUM THERMOPHILUM ÇİFT AKTİVİTELİ KATALAZ/FENOL OKSİDAZI (CATPO) İLE FENOL OKSİDASYON ÜRÜNLERİNİN ANALİZİ

Avcı, Gülden

Doktora, Biyoteknoloji Bölümü

Tez Danışmanı: Prof. Dr. Zümrüt Begüm Ögel

Yardımcı Tez Danışmanı: Prof. Dr. Gürkan Karakaş

Haziran 2011, 160 sayfa

Bu tez, *S. thermophilum*'un çift aktiviteli katalaz/fenol oksidaz enziminin fenol oksidasyonunun analiz edilmesini amaçlamaktadır. Birçok reaktif oksijen türleri (ROS) oksidatif stres altında mantarlarda sürekli olarak meydana gelmektedir. ROS türlerinin niteliğine bağlı olarak, bazıları oldukça toksik olup hücresel kalatazı da içeren çeşitli enzimatik mekanizmalar tarafından çabucak detoksifiye edilmektedir. *Scytalidium thermophilum* tarafından üretilen çift aktiviteli katalaz-fenol oksidaz enzimi (CATPO), fenolik maddeleri hidrojen peroksit yokluğunda okside edebilmektedir. Fenol oksidazlar fenolik maddeleri kinonlara dönüştürebilmekte ve oluşan bu kinonlar daha sonra serbest radikal reaksiyonları ile polimerize olmaktadırlar. Bu çalışmada, kimyasal yapı ve fonksiyonel özelliklerine göre seçilmiş olan 14 farklı fenolik maddenin CATPO için uygun sübstrat olup olmadığı araştırılmıştır. Bu 14 fenolik madde içinde, HPLC ile katekol, klorojenik asit, katekin ve kafeik asitin oksidasyon ürünleri gözlemlenmiştir. Katekol, klorojenik asit, kafeik asit ve katekinin oksidasyon ürünleri LC-ESI-MS ile analiz edilmiştir. Dimer, trimer, tetramer ve oligomer oluşumları saptanmıştır. 1 saatlik oksidasyon reaksiyonu sonucu en yükek dönüşüm verimi katekin için gözlemlenirken, en düşük dönüşüm verimi kafeik asit için gözlemlenmiştir. CATPO'nun katekol, klorojenik asit, katekin ve kafeik asit ile verdiği oksidasyon ürünleri, lakkaz ve tirosinaz enzimlerinin aynı

fenolik maddeleri okside ederek verdiği oksidasyon ürünleri ile karşılaştırılmıştır ve oluşan ürünler açısından CATPO'nun lakkaz ile daha fazla benzerlik gösterdiği belirlenmiştir.

Anahtar Kelimeler: *Scytalidium thermophilum*, fenolik maddeler, CATPO, biyolojik dönüşüm

To My Family

ACKNOWLEDGMENTS

TABLE OF CONTENTS

LIST OF TABLES

TABLES

LIST OF FIGURES

FIGURES

CHAPTER 1

INTRODUCTION

1.1 Catalases

During aerobic respiration, both eukaryotic and prokaryotic organisms use molecular oxygen (O_2) and generate Reactive Oxygen Species (ROS) as the by-products of their metabolism (Aguirre *et al.,* 2005). ROS have damaging effects on the macromolecules of the cell as nucleic acids, lipids and proteins. Aerobic organisms protect themselves from oxidative injury, by both enzymatic and non-enzymatic defense systems. The enzymatic system includes superoxide dismutases (SODs) catalase-peroxidases, peroxiredoxins and catalases (Aguirre *et al.,* 2005; Angelova *et al.,* 2005).

Catalase is one of the most studied classes of enzymes. It was first characterized and named as catalase in 1900 (Nicholls *et al.*, 2001). Today, many represents of catalases are known in both prokaryotes and eukaryotes (Zamochy *et al.,* 1999).

Catalase shows its antioxidant action via dismutation of H_2O_2. The overall reaction catalyzed by catalase is very simple and includes disproportionation of two molecules of hydrogen peroxide to water and oxygen (Reaction 1) (Nicholls *et al.*, 2001).

$$2H_2O_2 \rightarrow 2H_2O + O_2 \tag{1}$$

According to the present knowledge, this simple overall reaction can be separated into two stages, but what is involved in each of the stages depends on the type of catalase. In the first step, hydrogen peroxide is reduced to water leaving the heme iron in an oxyferryl intermediate to form compound I, an oxyferryl species with one oxidation equivalent located on the iron and a second oxidation equivalent delocalized in a heme cation radical (Reaction 2) (Nicholls *et al.*, 2001; Mate *et al.,* 1999).

$$Enz\ (Por\text{-}Fe^{III}) + H_2O_2 \longrightarrow Cpd\ I\ (Por^{+\cdot}\text{-}Fe^{IV} = O) + H_2O \qquad\qquad (2)$$
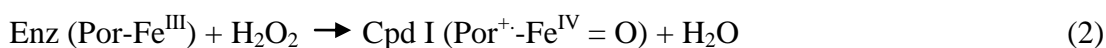
In the second step, second hydrogen peroxide molecule is used as an electron donor and compound I is reduced to regenerate the resting-state enzyme, oxygen and water (Reaction 3) (Nicholls *et al.*, 2001; Mate *et al.,* 1999).

$$Cpd\ I\ (Por^{+\cdot}\text{-}Fe^{IV} = O) + H_2O_2 \longrightarrow Enz\ (Por\text{-}Fe^{III}) + H_2O + O_2 \qquad (3)$$

This is the general reaction but there are great differences in reactive capability among the members of this family of enzymes (Chelicani *et al.,* 2004).

Some catalases can also function as a peroxidase, if there is a suitable small organic compound. However generally it is a minor activity except for catalase-peroxidases (Reaction 4) (Nicholls *et al.*, 2001; Mate *et al.,* 1999).

$$Cpd\ I\ (Por{+}\cdot\text{–}Fe^{IV}{=}O) + AH_2 \rightarrow Cpd\ II\ (Por\text{–}Fe^{IV}\text{–}OH) + AH\cdot \qquad (4)$$
$$Cpd\ II\ (Por\text{–}Fe^{IV}\text{–}OH) + AH_2 \rightarrow Enz\ (Por\text{–}Fe^{III}) + AH$$
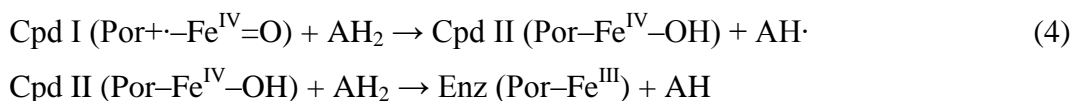
1.1.2 Classification of Catalases

Generally, catalases can be organized into four main groups according to the variety of subunit sizes, the different heme prosthetic groups, and the variety of sequence groups (Klots *et al.,* 2003).

(1) The heme-containing monofunctional catalases for which hydrogen peroxide is both the electron donor and acceptor,

(2) The heme containing bifunctional catalase-peroxidases in which the catalatic activity is much higher than the peroxidatic activity,

(3) The nonheme-containing catalases, and

(4) A miscellaneous group catalases with minor catalatic activities (Mate *et al*., 2001; Nicholls *et al.,* 2001).

1.1.2.1 Monofunctional Catalases

Members of this largest and most extensively studied group of catalases are found both in prokaryotic and eukaryotic aerobic organisms. Monofunctional catalases degrade hydrogen peroxide to oxygen and water by a two-step mechanism. They can also undergo peroxidatic activity by using organic reductants, but the peroxidatic reaction is minor and usually restricted to small organic substrates because of a limited accessibility to the active site (Klots *et al.,* 2003).

Depending on the subunit size it is possible to divide the monofunctional catalases into two subgroups (Mayer, 2006). One of the subgroups which is heme b-associated, contains small subunit enzymes (55 to 69 kDa), and the other one which is heme d-associated, contains large subunit enzymes (75 to 84 kDa). Monofunctional catalases can be active as tetramers, but other reported dimer and heterotrimetic types of enzymes have also been reported. (Mayer, 2006).

The phylogenetic analysis in 1997 including 74 monofunctional catalase sequences, showed a clear division into three clades (Chelicani *et al.,* 2004). Clade I catalases predominantly contain the plant enzymes, one subgroup of bacterial catalase and one algal representative. Clade II catalases contain large subunit enzymes of bacterial and fungal origin. Clade III catalases are small subunit enzymes that contain a third group of bacterial enzymes as well as fungal, archaeal and animal origin enzymes (Chelicani *et al.,* 2004).
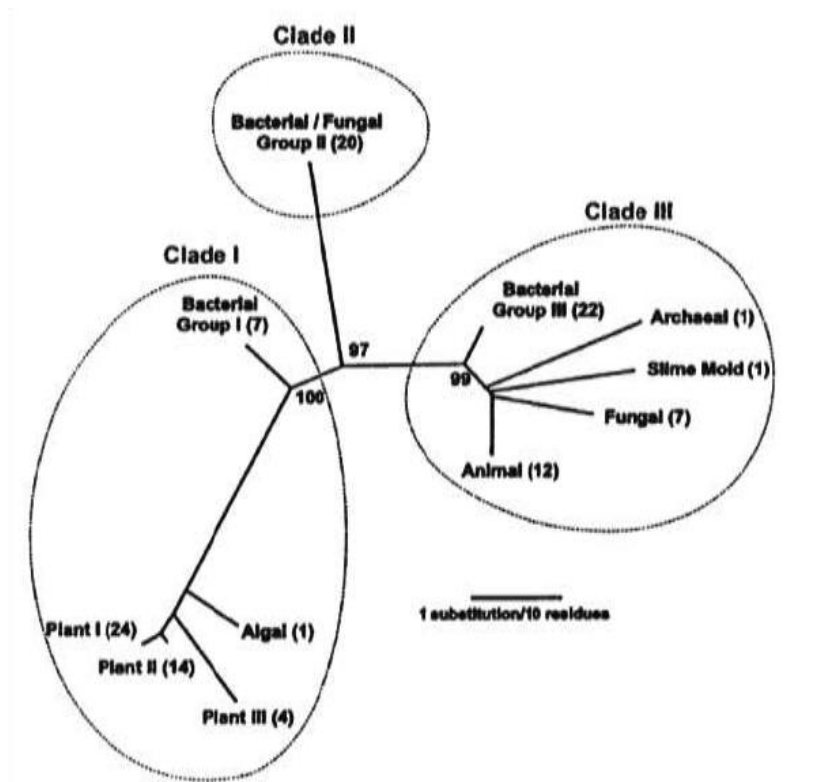
Figure 1.1 Phylogenetic tree of monofunctional catalases (Nicholls *et al*., 2001)

1.1.2.2 Heme-Containing Catalase-Peroxidases

Catalase-peroxidases show a predominant catalatic activity but they are biochemically different from the monofunctional catalase by showing a significant peroxidatic activity (Thomas, Morris, and Hager 1970; Sun *et al.,* 1994). Therefore, catalase–peroxidases are known as bifunctional enzymes. In the low level of H_2O_2 and the presence of suitable organic substrates, the peroxidase activity gains importance (Reaction 5) (Chelicani *et al*., 2004).

$$\text{Cpd I}(Por^{+\cdot}\text{-}Fe^{IV} = O) + 2AH_2 \rightarrow \text{Enz}(Por\text{-}Fe^{III}) + 2AH^{\bullet} + H_2O \qquad (5)$$

Catalase-peroxidases have been characterized in both fungi and bacteria and have shown sequence similarity with plant and fungal peroxidases (Fraajie *et al.,* 1996; Levy *et al.,* 1992). They are generally active as homodimer but homo-tetramer structures are also reported. Their molecular weight varies from 120 to 340 kDa (Obinger *et al.,* 1997; Nagy *et al.,* 1997). Furthermore, unlike the typical catalases,

reversible dimer-tetramer association of catalase-peroxidases has been reported (Billman *et al.,* 1996).

1.1.2.3 Nonheme Catalases (manganese-containing catalases)

Nonheme catalases contain manganese in their active sites. For this reason, they were initially referred to as pseudo-catalases. Now they are called more accurately as nonheme catalases or Mn-containing catalases. The nonheme catalases make up a small group of enzymes (Chelicani *et al.,* 2004). So far only three nonheme catalases have been purified and characterized, one from lactic acid bacteria (*Lactobacillus plantarum*; Wayne, Beyer and Fridovich, 1985) and two from thermophilic organisms. (*Thermoleophilum album, and Thermus thermophilus*; Allgood *et al*., 1986; Waldo *et al*., 1991).

A manganese-rich reaction center was identified as the active site, which is a dimanganese group, in each of the three characterized enzymes. They are active as tetramers or hexamers with a molecular mass of 30 kDa per subunit (Chelicani *et al.,* 2004).

Catalatic activity of the Mg-containing catalases is similar to the heme containingcatalases and constitutes two stages. The overall reaction requires two-electron redox cycling of the binuclear manganese cluster between the divalent and trivalent states, $Mn^{II}–Mn^{II}\leftrightarrow Mn^{III}–Mn^{III}$. There is no temporal order to the oxidation and reduction stages due to the equally stability of the oxidation state of dimangenese cluster. If H_2O_2 encounters Mn^{II}-Mn^{II}, it acts as an oxidant (Reaction 6) and if $Mn^{III}–Mn^{III}$ is encountered, the H_2O_2 act as a reductant (Reaction7) (Chelicani *et al.,* 2004).

$$H_2O_2 + Mn^{II}\text{-}Mn^{II} (2H^+) \rightarrow Mn^{III}\text{-}Mn^{III} + 2\ H_2O \tag{6}$$

$$H_2O_2 + Mn^{III}\text{-}Mn^{III} \rightarrow Mn^{II}\text{-}Mn^{II} (2H^+) + O_2 \tag{7}$$
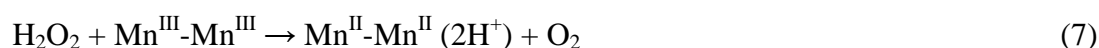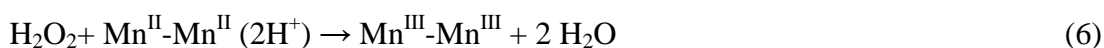
Reaction 6 and 7 are shown as equivalent of reactions 2 and 3 in heme-containing catalases. However, there are two distinctive differences in the reaction mechanisms of heme and nonheme catalases. One is that the reactive intermediate is not produced

during the oxidation of the reaction centre of the nonheme catalases. The second is that both water products are formed in reaction 6, whereas water is produced in each of reactions 2 and 3 in heme catalases. The catalytic mechanism of nonheme catalases is currently under investigation (Chelicani *et al.*, 2004).

1.1.2.4 Minor Catalase

Minor catalases include heme-containing proteins. These enzymes show low levels of catalatic and peroxidatic activity in the presence of the chloride and hydrogen peroxide and have ability to chlorinate organic substrates. On the other hand, enzyme has peroxidatic and catalatic activity in the absence of chloride. Minor catalase is active as a monomer and has a 42-kDa molecular weight. Chloroperoxidase from *Caldariomyces fumago* is an example of this type of enzyme (Mate *et al.,* 2003).

1.1.3 Biological Functions of Catalase

Catalase is known as an antioxidant enzyme because of its ability to remove hydrogen peroxide before it has a negative effect on cells (Fridovich, 1995). Although O_2 is crucial for aerobic organisms, reactive oxygen species (ROS), such as hydrogen peroxide (H_2O_2), superoxide anion radical (O_2^-), and hydroxyl radicals (OH^-) are produced during usage of O_2 for respiration and energy supply. Therefore, there will be an oxidative stress, when there is an imbalance between the production of free radicals and a biological system's ability to readily detoxify the reactive intermediates. Enzymatic or non-enzymatic systems are used to detoxify these radicals in both prokaryotic and eukaryotic organisms (Fridovich, 1995).

Oxidative stress responses are often part of more general stress responses to temperature, salinity or starvation among the prokaryotes (Loewen, 1997). Catalases can also be an important factor in bacterial virulence because hydrogen peroxide is used as an antimicrobial agent during the infection of the cells with a pathogen. For instance, pathogens that are catalase positive such as *Staphylococcus aureus, Mycobacterium tuberculosis, Legionella pneumophila,* and *Campylobacter jejuni* require catalase to inactivate the peroxide radicals in order to survive within the host (Loewen, 2000; Boerjan *et al.,* 2003).

In the eukaryotes, pathogenesis, radiation, hormones, temperature extremes and extreme oxygen concentrations have all been observed to effect catalase levels (Scandalios *et al.*, 1994). Under physiological conditions, catalase may also play a role in the compartmentalization of hydrogen peroxide (Mullen *et al.*, 1997), which is gaining attention in signaling as a potential second messenger.

1.1.4 Structure of Catalase

The crystal structures of six heme-containing catalases have been solved and structural information is now available. Four of the representatives are from clade III including small subunits. These are; *Micrococcus lysodeikticus* catalase (MLC; Murshudov *et al.*, 1992), *Proteus mirabilis* catalase (PMC; Gouet *et al.*, 1995), bovine liver catalase (BLC; Murthy *et al.,* 1981; Fita *et al.,* 1986) and *Saccharomyces cerevisiae* catalase (SCC; Berthet *et al.,* 1997). Two of the representatives are from clade II including large subunits. These are; bacterial *Eshericia coli* hydroperoxidase II (HPII; Bravo *et al.,* 1995) and fungal *Penicillium vitale* catalase (PVC; Vainshtein *et al.,* 1981; Melik - Adamyan *et al.,* 1986). Despite differences in size and primer structure of these six catalases, they share common well conserved three dimensional structures. In small subunit enzymes four distinct regions can be identified (Figure 1.2). These are;

a) an amino terminal arm
b) a β-barrel domain
c) wrapping domain
d) α-helical domain

The amino-terminal domain is variable in length and includes 50 residues (53 residues in PMC) to 127 residues (127 residues in HPII) (Mate *et al.*, 2001; Melik-Adamyan *et al.*, 1986). This domain is involved in extensive inter-subunit interactions and residues from this region contribute to define the heme pocket of a symmetry related subunit. The extent of the inter-subunit interactions increases with the length of domain showing the molecular stability of catalases (Mate *et al.*, 2001). This arm extends from the globular (β-barrel) region of one subunit, but at about half of its length bends back in an 'elbow' like structure. The distal histidine in this arm

contributes to proper binding and the reduction of a peroxide molecule. It is invariantly situated at the C-terminus of the N-terminal arm and its reactivity is controlled by the highly conserved side chain architecture of residues from the β-barrel domain, which allows the formation of a specific hydrogen-bonding network (Zamochy and Koller, 1999).

The antiparallel β-barrel largest domain is the core of the subunit. It extends from essential histidine and includes 250 residues. The first half of the β-barrel provides most of the residues involved in forming the cavity on the hemes distal side. The second half of the β-barrel contributes to the NADP(H) binding pocket in small subunit catalases. This domain also includes at least six helices located along the polypeptide chain in two long insertions between β-strands (Fita and Rossmann, 1986; Mate *et al*., 2001; Melik-Adamyan *et al*., 1986).

The third region is the wrapping loop including 110 residues that connects the β-barrel and α-helical regions. This region lacks the secondary structure in long stretch of polypeptide chain between residues 366-420, but it contains the essential helix (α_9) defining the heme proximal side including tyrosine residue. This portion of polypeptide chain participates in various inter-domain and inter-subunit interactions particularly with residues from the amino terminal arm region from another subunit (Fita and Rossmann, 1986; Mate *et al*., 2001; Melik- Adamyan *et al*., 1986).

The fourth is α-helical region containing 60 residues organized in four anti-parallel α-helices that are close to some of the helices from the β-barrel domain to stabilize the structure (Mate *et al*., 2001; Melik-Adamyan *et al*., 1986).
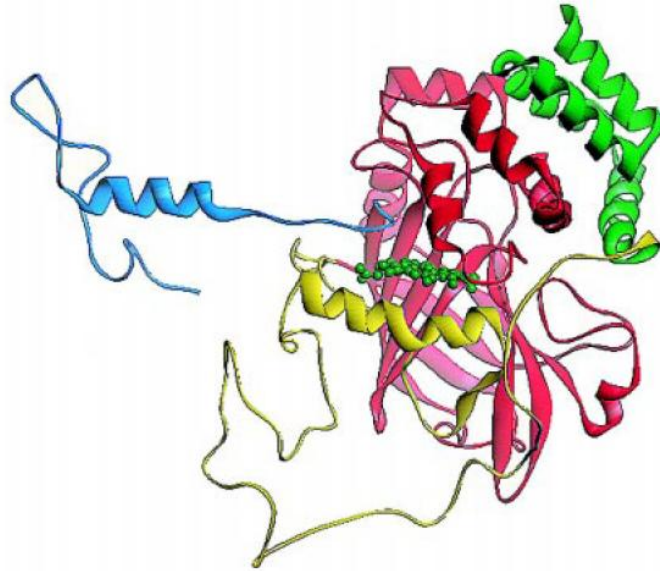
Figure 1.2 Three-dimentional structure of *S. cerevisiae* catalase among Clade II small subunit enzymes (Zamocky *et al*., 1999) A color scheme: dark green-heme group, cyan-N-terminal arm, red-b-barrel domain, yellow- domain connection, green- α helical domain.

Unlike BLC, the structures of PVC and HPII present an extra carboxy-terminal domain including roughly 150 residues with a high content of secondary structure elements organized with a "flavodoxin-like" topology (Figure 1.3). The possible role of this extra domain in PVC remains unknown (Mate *et al*., 2001). In BLC, prior to the flavodoxin like domain is occupied by an NADP(H) molecule (Fita and Rossmann, 1986). Although PVC and HPII share common structural similarities, HPII differs by the presence of 60 residues at N-terminal end, which increases the contact area between subunits (Bravo *et al*., 1995).

All of the seven catalases that have been characterized exist as homotetramers. The catalase tetramer has a rather compact arrangement of subunits, revealing an extensive and complex pattern of interactions (Figure 1.4). Some of these interactions virtually are incompatible with a simple way of tetramer assembly by combining four pre-folded monomers (Vainshtein *et al*., 1981). The most interesting structural feature of the assembled protein is the pseudo-knot such that the N-terminal end of each subunit is overlapped through a loop formed by the C-terminus of the adjacent unit. In the large subunits 80 residues, in the small subunits 25

residues are trapped. This interaction is important for the stability of the quaternary structure of the enzyme and in this case HPII dimers do not dissociate at temperatures up to 95°C.
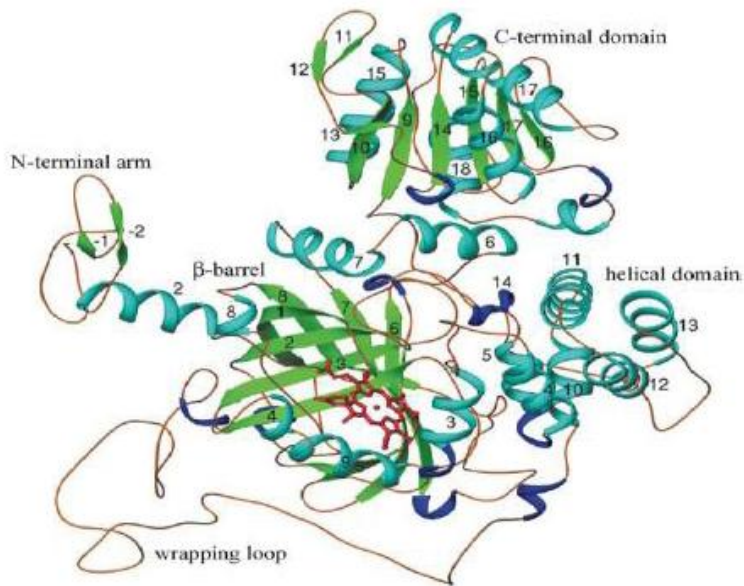
Figure 1.3 Schematic drawing of large subunits of *N. crassa* catalase (Diaz *et al.*, 2004)
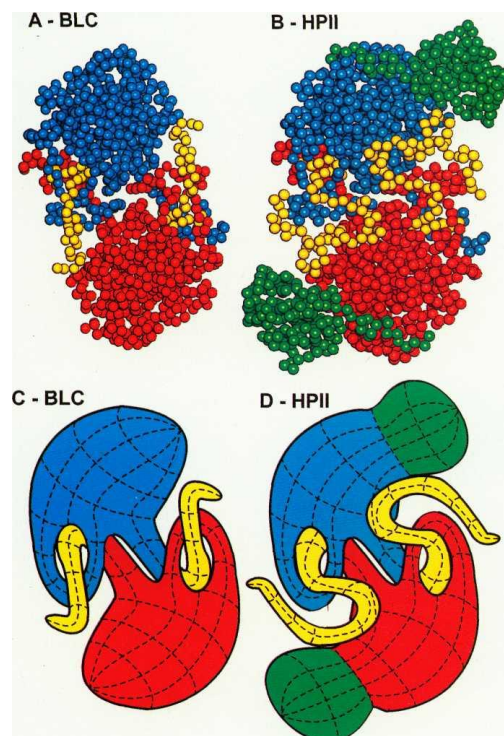
Figure 1.4 Comparison of the structures of the intertwined dimers of monofunctional catalases with small (A-BLC) and large (B-HPII) subunits (Nicholls *et al.,* 2001)

The core of the subunits with a common structure and similar sequence is shown in either blue or red. The C-terminal extension on HPII is shown in green in B. The yellow segments are the N-terminal portions of both enzymes that are red through a loop on the adjacent subunit, 25 residues in the case of BLC and 80 residues in the case of HPII. Panels C and D contain a cartoon to illustrate the interwoven structure (Lowen *et al.*, 2000).

1.1.5 Heme Orientation

Besides size, the small- and large-subunit catalases have characteristic differences (Figure 1.5). Small-subunit enzymes contain heme b, which in large-subunit enzymes is converted to heme d. In heme d, ring III is oxidized to a cis-hydroxyspirolactone. Initially heme b is bound to both enzymes during assembly and it is subsequently oxidized by the catalase itself during the early rounds of catalases. Loewen and colleagues (1993) reported that this conversion happens in the presence of hydrogen peroxide. Another possible conversion of proto-heme to heme *d* is provided by Díaz *et al.*, 2005. They postulated a mechanism in which singlet oxygen, produced catalytically or by photosensitization, may hydroxylate C5 and C6 of pyrrole ring III and causes the γ-spirolactone formation in C6 (Diaz *et al.*, 2005).
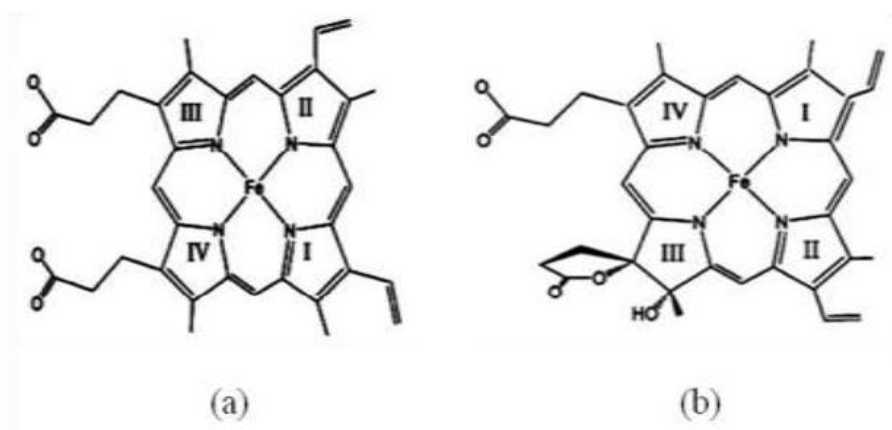
Figure 1.5 Structures of heme b (a) and heme d (b) (Alfonso-Prieto *et al.,* 2007)

The heme d of HPII and PVC is flipped 180° relative to the heme b of SCC, BLC, MLC and PMC. This is another important difference between the small and the large

subunit catalases. This difference is the result of the residues that form the heme pocket.

The first catalase structures which are BLC and MLC, had a common heme orientation. In this structure His situated in the active site was above ring III of the heme (referred to as the His-III orientation), leading to the conclusion that this was the normal orientation for heme in catalases (Chelikani *et al*, 2004). Heme contacting residues are rather found to be different for heme *d* and protoheme enzymes. Such residues for PVC involve Ile41, Val209, Pro291, and Leu342 and for HPII contain Ile114, Ile279, Pro356, and Leu407, while analogous residues for BLC are Met60, Ser216, Leu298 and Met349 (Figure 1.6). These differences may also determine heme orientation (Mate *et al*., 1998; Murshudov *et al*., 1995).

Heme groups are deeply buried inside the catalase tetramer with iron atoms situated at about 20 Å from the nearest molecular surface. Heme pockets show extensive structural similarities among different catalases. Tyrosine on the proximal side of the heme (Tyr415 in HPII), histidine (His 128 in HPII) and asparagine on the distal side (Asn201 in HPII), are believed to be essential for catalysis (Mate *et al*., 2001). The oxygen of the phenolic hydroxyl group of tyrosine is the proximal ligand of the heme iron and is most likely deprotonated having negative charge so that can contribute to the stabilization of the high oxidation states of iron. The bond between the imidazole ring of His 392 and the β-carbon of Tyr 415 is correlated with heme oxidation. The histidine and asparagine residues on the distal side of the heme make the environment strongly hydrophobic (Mate *et al*., 2001). Mutation on His 128 in HPII resulted in no detectable activity, confirming that the His residue is essential for the activity. A conserved serine residue (Ser167 in HPII) is also found to be hydrogen bonded to the N^{δ} of the essential histidine and might facilitate the enzymatic mechanism (Bravo *et al*., 1999). On the other hand, replacements of either Asn201 or Ser167 resulted in low level of activity, revealing that these residues facilitated the catalytic activity but were not essential for activity (Nicholls *et al.,* 2001).
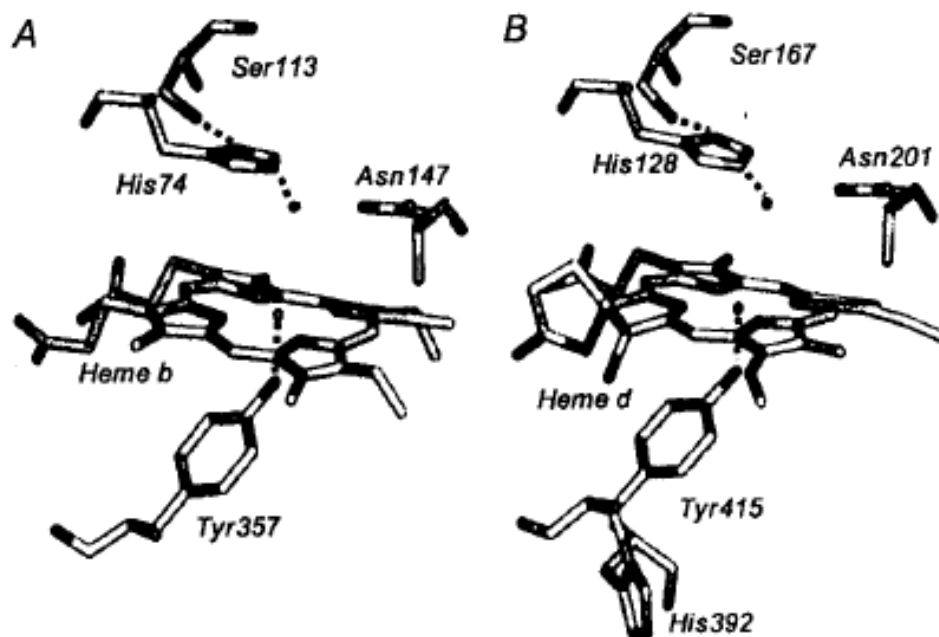
Figure 1.6 Comparison of the active site residues in a small subunit catalase BLC (A) and large subunit catalase HPII (B) (Nicholls *et al.,* 2001)

1.1.6 NADPH Binding

Small-subunit catalases as in bacterial (PMC), yeast (SCC-A) and mammalian (BLC) enzymes, all contain NADPH in some fraction of their subunits. The NADPH binding pockets of BLC, HEC, CATA and PMC contain a His, an Arg, a Val and a His (193, 202, 301 and 304, respectively (Chelicani *et al.,* 2004), and are localized at a side about 20 Å from the heme iron that is highly conserved among the small subunit enzymes. This may be considered as a signature for NADPH binding (Nicholls *et al.,* 2001).

It is believed that NADPH serves as an electron source and protects the enzyme from the formation of the compound II that is formed at low peroxide concentration or to convert the inactive compound II back to the Fe^{III} state. In addition to NADPH role in the recycling mechanism, experiments with SCC-A indicate that binding of NADPH stabilizes the quaternary structure. Not only the reduced form, but to a lesser extent also the oxidized form of the dinucleotide (and, moderately, even NADH and NAD^+) contribute to the conformational stabilization (Herzog *et al.,* 1997). This is in agreement with Gouet (1995), who propose that NADPH binding in

PMC causes slight structural changes. In large subunit enzymes such as HPII the cavity filled by NADPH in small subunit enzymes is partially filled by a segment of the α-helical and linking regions (Zamochy *et al.*, 1999).

1.2 Phenol Oxidases

The general terms phenolase or polyphenol oxidases are used to describe enzymes, which catalyze the oxidation of aromatic compounds in the presence of molecular oxygen, which are also substrates for phenol oxidase. The three major groups of these enzymes are laccases (E.C. 1.10.3.2, p-benzenediol: oxygen oxidoreductase), catechol oxidases (E.C. 1.10.3.1) and tyrosinases (E.C. 1.14.18.1, monophenol monooxygenase) (Griffith, 1994).

Phenol oxidases represent a major group of enzymes involved in secondary metabolic activity, most commonly being associated with the production of melanins and other pigments.

1.2.1 Phenolic Compounds

Phenols are compounds with a hydroxyl group (–OH) attached to a six membered aromatic ring, including their functional derivatives. Phenols are bifunctional compounds; hydroxyl group and aromatic ring interact strongly, leading to novel properties of phenols (Kaptan, 2004).

Although they share the same functional group with alcohols, where the –OH group is attached to an aliphatic carbon, the chemistry of phenols is very different from that of alcohols. Intramolecular hydrogen bonding is possible in some ortho-substituted phenols. This intramolecular hydrogen bonding reduces water solubility and increases volatility.

Phenolic compounds (polyphenols) are secondary metabolites of plants and essential for growth and reproduction of plants. They are involved in defense against radiation or aggression by pathogens. Their contribution to pigmentation of plants foods is also well recognized. They are effective free radical scavengers and metal chelators,

which are mediated by the presence of *para*-hydroxyl groups. Their occurrence in animal tissues and non-plant materials is due to ingestion of plant foods. Many of the food phenolics are soluble in water and organic solvents. Recognition of symbionts may also be related to the presence of polyphenols in plants (Manach *et al.*, 2004).

Phenolics can be classified into different groups as a function of the number of phenolic rings and of the structural elements that bind these rings to one another (Manach *et al.*, 2004). These are; simple phenols, phenolic acids, flavonoids, stilbenes and lignans.

1.2.1.1 Simple Phenols

Simple phenols in foods may originate by microbial activity, thermal degradation of lignin or decorboxylation of phenolic carboxylic acids. The dihydroxylbenzenes representatives of simple phenols include hydroquinone, catechol and resorcinol (Figure 1.7) (Maga, J.A, 1978).
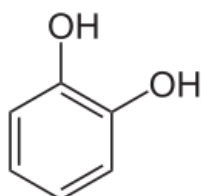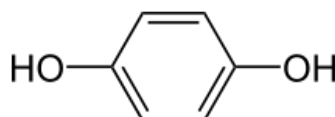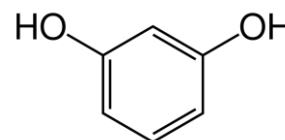
Catechol   **Hydroquinone**   **Resorcinol**

Figure 1.7 Structures of catechol, hydroquinone and recorcinol

Catechol also named as pyrocatechol is an organic compound with the molecular formula $C_6H_4(OH)_2$. This colorless compound occurs naturally in small amounts in fruits and vegetables. Catechol was first isolated in 1839 by H. Reinsch by distilling catechin**.** Catechol is produced industrially by the hydroxylation of phenol using hydrogen peroxide (Fiegel *et al.,* 2002).

Hydroquinone also named as benzene-1, 4-diol is an aromatic organic compound with chemical formula $C_6H_4(OH)_2$. Hydroquinone is produced industrially by hydroxylation of phenols (Hudnall *et al*., 2002). Hydroquinone is thought to be the active toxin in *Agaricus hondensis* mushrooms. Hydroquinone and hydrogen peroxide are two primary reagents in the defensive glands of bombardier beetles (Klots *et al*., 2003).

Resorcinol is a dihydroxy benzene and 1, 3-isomer of benzenediol with molecular formula $C_6H_4(OH)_2$. Resorcinol can be regarded as a phenol derivative. in a hydrogen atom is substituted by a hydroxyl group in the meta position to the OH. The resorcinol has been found in a wide variety of natural products as in broad bean (*Vicia faba*) and flavour-forming compound in the honey mushroom (*Armillaria mellea*) (Dressler *et al.,* 1994).

1.2.1.2 Phenolic Acids

Derivatives of hyrdroxybenzoic acid and hydroxycinnamic acid are distinguished within the group of phenolic acids.

Hydroxybenzoic acids are components of hydrolysable tannins such as gallotannins and ellagitannins and lignin and commonly present in bound form. The content of them in foods of plants origin is very low. Exceptions are blackberry, and strawberry (Stohr and Herrmann, 1975) as well as vegetables such as onions and horseradish (Schmidtlein and Herrmann, 1975). Gallic acid is the most representative compound of hyrdroxybenzoic acids. It is generally present in tea, red fruits, black radish and onions. Gallic acid is found both free and as part of tannins. Gallic acid is thought to have anti-fungal and anti-viral properties. Gallic acid is proposed to protect our cells against oxidative damage by acting as an antioxidant compound and act as a cytotoxicity against cancer cells, without harming healthy cells. Gallic acid is also used to treat albuminuria and diabetes (Sakaguchi *et al.,* 1998).

Hydroxycinnamic acids are more common and found in plants as bound form and rarely in free form. The main representative of this class is caffeic acid. It is found in all plants because it is a key intermediate in the biosynthesis of lignin. It constitutes

over 75% of total hydroxycinnamic acid found in apples, tomatoes, apricots and blueberries (Macheix *et al.,* 1989). Caffeic acid is biosynthesized by hydroxylation of coumaroyl ester of quinic ester. Caffeic acid has been shown to inhibit carcinogenesis. It is known to have antioxidant effects and reduce aflatoxin production by more than 95 percent (Olthof *et al.,* 2001). Caffeic acid also shows immunomodulatory and anti-inflammatory activity. This opens the door to using natural anti-fungicide methods by supplementing trees with antioxidants. Caffeic and quinic acid combine to form chlorogenic acid, which is found in high concentrations in coffee (Manach *et al*., 2004). Chlorogenic acid is the precursor to ferulic acid, which is significant building block in lignin (Boerjan *et al.,* 2003). It is found in many foods including apples, blackberries, peaches, pears and avocado. Chlorogenic acid is the key polyphenol for enzymatic browning, particularly in apples and pears. Chlorogenic acid is also known as antioxidant because of its positive effects on Type 2 Diabetes Mellitus and cardiovascular disease (Paynter *et al.,* 2006; Morton *et al*., 2000). It is claimed to have antiviral, antibacterial and antifungal effects with relatively low toxicity and side effects, alongside properties that do not lead to antimicrobial resistance (Jassim *et al.,* 2003; Satillo *et al.,* 1998).

1.2.1.3 Flavonoids

Flavonoids have the basic skeleton of diphenylpropanes with different oxidation level of the central pyran ring, which is open in the case of chalcones. Of these, flavonoids can be divided into the six classes; anthocyanins, flavonols, flavones, isoflavones, flavanones and flavanols (Table 1.1) (Cimpoiu, 2006).

Anthocyanins are water soluble vacuolar pigments responsible for red, purple or blue found in many species of plant kingdom according to pH. They are found in blackberries, blueberries, cherries, red grapes and cranberries (Hall and Stark, 1972) Anthocyanins are stable to the light and pH, and stabilized by glycosylation, esterification with other flavonoids. Cyanidin is the main component of the anthocyanins (Cimpoiu, 2006).

Flavonols have the 3-hydroxyflavone backbone and possess a double bond between C-2 and C-3. They also possess a hydroxyl group in the 3-position, in addition to this

may also be hyrdoxylated in the 5- and 7- positions. Number and positions of the hydroxyl groups in their B-ring can be different. Kaempferol, quercetin and myricetin are commonly found flavonols. They are generally presented in glycosylated forms. Flavonols are found in fruit and vegetables, especially in grapes, berries and potatoes (Cimpoiu, 2006; Macheix *et al.*, 1989).

Flavones also possess a double bond between C-2 and C-3 as flavonols but not a hydroxyl group in the 3-position. Flavones are less common then flavonolsin plants. The main representatives are luteolin and apigenin (Cimpoiu, 2006; Herrman, 1976).

Isoflavones and flavanones are characterized by the presence of a saturated 3-C chain and an oxygen atom in the 4-position. Isoflavanones differ from flavanones by having a hydroxyl group in the 3-position. Both are mainly found in citrus fruits. The main isoflavones are geinstein and daidzein and the main flavanones are naringenin and hesperitin (Cimpoiu, 2006).

Flavanols include a saturated 3-C chain with hydroxyl groups. They are found in fruits and leguminous plants, either in the monomer form (catechins) or in the polymer form (proanthocyanidins). The main sources are chocolate and green tea. The main representatives are catechin and gallocatechin. Catechin is responsible for the enzymatic browning of the fruits and vegetables (Cimpoiu, 2006).

Table 1.1 Structures of the most common polyphenolic compounds of (Cimpoiu, 2006)
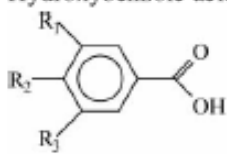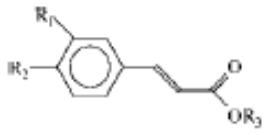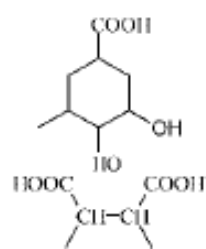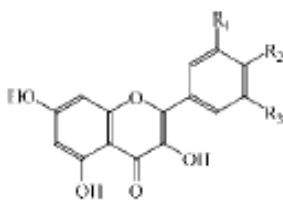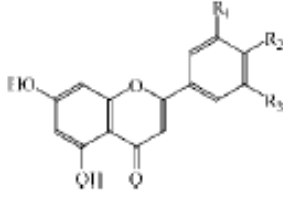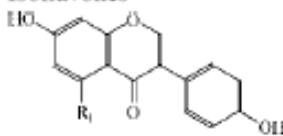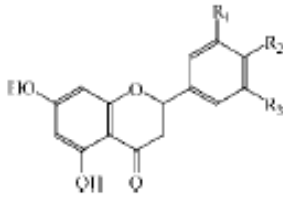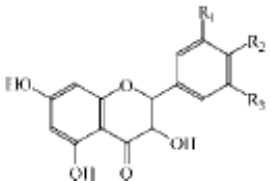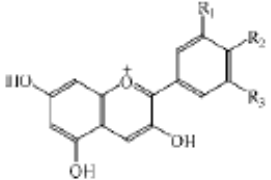
Group	Compound	R_1	R_2	R_3
Hydroxybenzoic acids	Protocatechuic acid	OH	OH	H
	Gallic acid	OH	OH	OH
Hydroxycinnamic acids	Coumaric acid	OH	H	
	Caffeic acid	OH	OH	
	Ferulic acid	OCH$_3$	OH	
	Chlorogenic acid			
	Chicoric acid (dimer of caffeic acid)	OH	OH	
Flavonols	Kaempferol	H	OH	H
	Quercitin	OH	OH	H
	Myricetin	OH	OH	OH
	Morin	OH	H	OH
	Datiscetin	OH	H	H
	Galangin	H	H	H
	Kaempferide	H	OCH$_3$	H
	Isorhamnetin	OCH$_3$	H	H
Flavones	Apigenin	H	OH	H
	Luteolin	OH	OH	H
	Chrisyn	H	H	H
	Acacetin	H	OCH$_3$	H
Isoflavones	Daidzein	H		
	Genistein	OH		
Flavanones	Naringenin	H	OH	H
	Eriodictyol	OH	OH	H
	Hesperetin	OH	OCH$_3$	H
	Pinocembrin	H	H	H
	Isosakuranetin	H	OCH$_3$	H

Table 1.1 Structures of the most common polyphenolic compounds of (Cimpoiu, 2006) (continued)

Group	Compound	R_1	R_2	R_3
Flavanols	Catechin	OH	OH	H
	Gallocatechin	OH	OH	OH
	Pinobanksin	H	H	H
	Procyanidin	H	OH	OH
Anthocyanidins	Pelargonidin	H	OH	H
	Cyanidin	OH	OH	H
	Delphinidin	OH	OH	OH
	Petunidin	OCH_3	OH	OH
	Malvidin	OCH_3	OH	OCH_3
	Peonidin	OCH_3	OH	H

1.2.2 Classification of Phenol Oxidases

As mentioned, the three major groups of these enzymes are laccases (E.C. 1.10.3.2, p-benzenediol: oxygen oxidoreductase), catechol oxidases (E.C. 1.10.3.1, o-diphenol oxidoreductase), and tyrosinases (E.C. 1.14.18.1, monophenol monooxygenase).

1.2.2.1 Laccase

Laccases (benzediol: oxygen oxidoreductases, EC 1.10.3.2) is multicopper containing enzyme which have been extensively studied since 18th century (Sharma and Kuhad, 2008). It was first described by Yoshida in 1883 and characterized as a metal containing enzyme by Bertrand in 1985 (Mayer and Staples, 2002).

Laccase is widely distributed among fungi, higher plants and insects (Mayer and Staples, 2002). The presence of this protein with a characteristic feature of multi-copper oxidase enzymes family was also reported in bacteria (Alexandre and Zulin, 2000). The first bacterial laccase was detected in the *Azospirillum lipoferum* the plant root associated bacterium, where it was shown to be involved in melanin formation. The occurrence of laccases in higher plants is more limited than fungi. Laccase from

Rhus vernicifera has been characterized and well documented (Hutteramann *et al.,* 2001).

The plant origin laccases are proposed to have an important role in lignin biosynthesis via oxidizing monolignols in the early stages of lignification (De Marco and Roublelakis-Angelakis, 1997; Thurston, 1994; Mayer and Staples, 2002). On the other hand, fungal laccases are the part of the lignin-degrading enzyme system. The presence of laccase in non-lignolytic fungi also has been demonstrated. Besides degradation of biopolymers, fungal laccases are suggested to contribute to several other functions, such as pigmentation, fruiting body formation, sporulation and pathogenesis (Leatham and Stahmann, 1981; Thurston, 1994; Nagai *et al*., 2003; Langfelder *et al*., 2003). Laccases in plant-pathogenic fungi are proposed to detoxify the toxic components generated by the plant defense systems (Mayer and Staples, 2002). Although Arakane *et al*. (2005) reported that laccase activity may have a more significant role in cuticle tanning in certain invertebrates than tyrosinase activity, generally in insects laccase activity is referred to sclerotization (Dittmer *et al*., 2004). Bacterial laccases have also been suggested to have a role in pigmentation (Martins *et al.,* 2002).

1.2.2.1.1 Structure of Laccase

Rhus vernicifera and *Trametes versicolor* laccases are the most comprehensive studied enzymes among *more* than 60 laccases detected from various plant, insect, bacterial, and fungal sources (Mayer and Staples, 2000). The structure of the active site seems to be conserved in all the fungal laccases. On the other hand, the rest of the protein structure shows great diversity. The laccase molecule, as an active holoenzyme form, is a dimeric or tetrameric glycoprotein usually containing four copper atoms per monomer, bound to three redox sites (type 1, type 2, and type 3 Cu pair) (Farver and Pecht, 1984). The four Cu atoms differ from each other in their characteristic electronic paramagnetic resonance (EPR) signals. Two of them belong to the strongly coupled type 3 site, with an EPR signal usually activated by strong anion binding. Type 1 copper has strong electronic adsorption and well characterized EPR signals. Type 2 copper shows no absorption in the visible spectrum and reveals paramagnetic properties in EPR studies. Type 2 and type 3 form a trinuclear cluster,

where reduction of molecular oxygen and release of water takes place. Type 2 copper is coordinated by two and type 3 copper atoms by six histidines (Duran *et al.,* 2002). Laccase catalysis is believed to comprise three major steps (Figure 1.8):

1. Type 1 Cu reduction by reducing substrate.
2. Internal electron transfer from type 1 Cu to type 2 and type 3 Cu trinuclear cluster.
3. O_2 reduction (to water) at type 2 and type 3 Cu (Thurston, 1994)
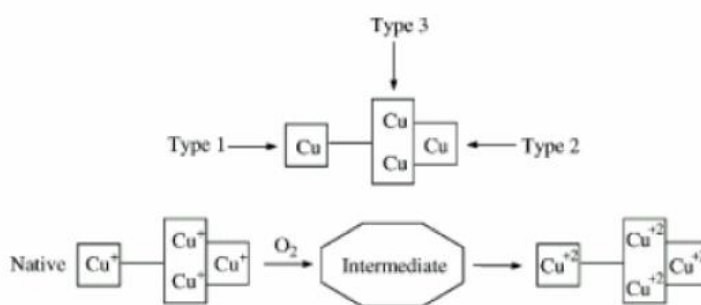
Figure 1. 8 Reactivity of laccase derivatives with oxygen (Duran *et al.,* 2002**)**

Four ungapped sequence regions L1-L4 were found by multiple sequence alignments of more than 100 laccases. Enzyme includes 12 amino acid residues which are serving as the copper ligands and housed within these conserved regions (Figure 1.9). The amino acid ligands of the trinuclear cluster are the eight histidines, which occur in a highly conserved pattern of four HXH motifs (Figure 1.10). In one of these motifs, X is the cysteine bound to the type1 copper while each of the histidines is bound to one of the two type 3 coppers. Intraprotein homologies between signatures L1 and L3 between L2 and L4 suggest the occurrence of duplication events (Claus, 2003).
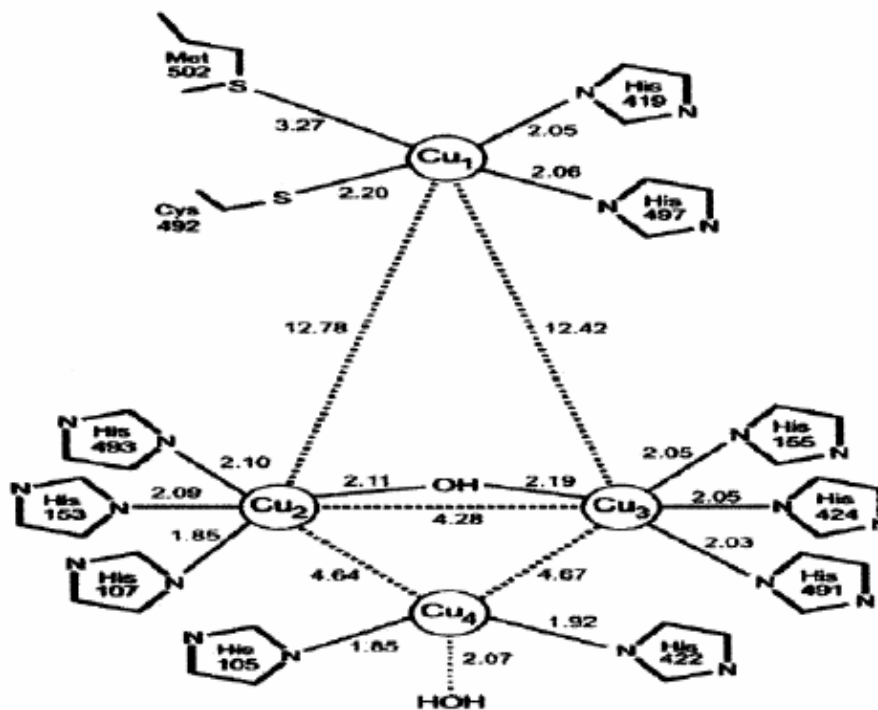
Figure 1.9 Copper centers of the laccase from *B. subtilitis* (adapted from Enguita *et al.*, 2003
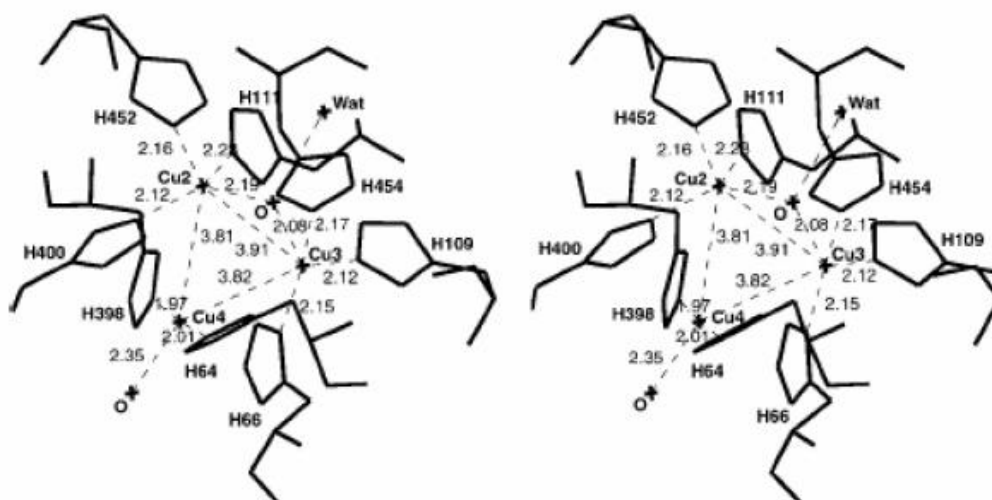
Figure 1.10 Stereo views of the T2/T3 coppers and their close environment in laccase of *Trametes versicolor* (Piontek *et al.*, 2002)

1.2.2.1.2 Reaction Mechanism and Substrate Specificity of Laccase

Laccase could oxidize any substrate with characteristics similar to a *p*-diphenol, but actually recent studies show that laccases are remarkably non-specific as to their reducing substrates, and the range of substrates oxidized varies from one laccase to another. Laccase has broad substrate specificity and has ability to catalyze the one-electron oxidation of a wide variety of organic and inorganic substrates, including polyphenols, methoxy-substituted phenols, aromatic compounds containing hydroxyl and amine groups and ascorbate with the concomitant four-electron reduction of oxygen to water (Reinhammar & Malmstrom, 1981). Substrate oxidation by laccase is a one-electron reaction generating a free radical (Figure 1.11) (Reinhammar & Malmstrom, 1981). The initial product is typically unstable and may undergo second-enzyme catalyzed oxidation (conversion phenols to quinines), or may undergo non-enzymatic reactions such as hydration or disproportionation *and/or* may undergo in a polymerization reaction giving an amorphous insoluble melanin-like product (Thurston, 1994) (Figure 1.12).
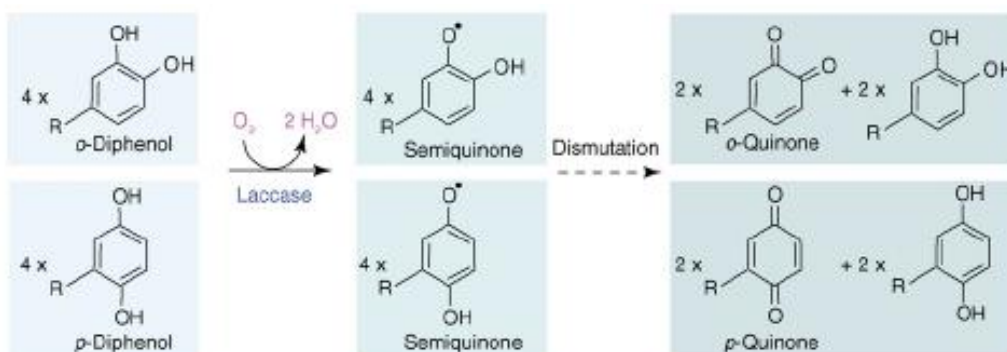
Figure 1.11 The typical laccase reaction, where a diphenol undergoes a one-electron oxidation to form an oxygen-centered free radical. This species can be converted to the quinone in a second enzyme-catalyzed step or by spontaneous disproportionation (Pourcel *et al*. 2006)
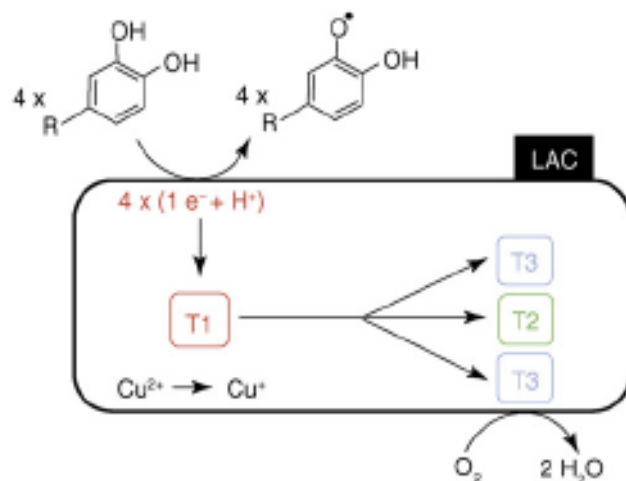
Figure 1.12 Catalytic mechanisms for the laccase and copper binding sites (Pourcel *et al.,* 2006)

Laccase has broad substrate specificity and affinity of the enzyme.can vary with changes in pH (Table 1.2). Some substrates such as ferrocyanide, oxidation reactions does not involve proton exchange. In this type of reactions the enzymatic activity of laccase often decreases as pH increases, whereas for substrates whose oxidation involves proton exchange (such as phenol), the pH-activity profile of laccase can exhibit an optimal pH whose value depends on laccase rather than substrate (Bourbonnais and Paice, 1992). For phenols, the optimal pH range is between 3 and 7 for fungal laccases. (Bollag and Leonowicz, 1984). The main substrate for *Trametes versicolor* laccase is catechol and optimum pH is 4.6.

Table 1.2 Specific substrates and optimum pH values for oxidation of substrates of some laccases (Gianfreda *et al*., 2010)

Species	Substrate	pH opt
Armillaria mellea	*p*-Phenyldiamine	3.5
Botrytis cinerea	2,6-Dimethylphenol	3.5
	Chlorogenic acid	
Ceriporiopsis subvermispora I,II	Guaiacol	3.5
Myceliophthora parasitica	Syringaldazine	7
Pleurotus ostreatus	Syringaldazine	6.5
Podospora anseria	Dopamine	5.5
Polyporus versicolor	Hydoquinone	4.6
	Catechin	
Trametes versicolor	Catechol	4.6

1.2.2.2 Tyrosinase

Tyrosinases (monophenol, o-diphenol: oxygen oxidoreductase, EC 1.14.18.1) often also referred to as polyphenol oxidase (PPO), is a copper-containing mono-oxygenase, present in a diverse range of organisms.

Tyrosinases are widely distributed enzymes in nature. Tyrosinases are found in mammals, invertebrates, plants, fungi and microganisms. The most extensively investigated tyrosinases are, from mammals (Kwon *et al*., 1987, 1988; Spritz *et al*., 1997). The fungal tyrosinases from *Neurospora crassa* (Lerch, 1983) and *Agaricus bisporus* (Wichers *et al*., 1996) have also both been characterized in detail from the structural and functional points of view. Mushroom tyrosinase is popular among researchers because of it is commercially availability. *Streptomyces* tyrosinases are the most thoroughly characterized enzymes of bacterial origin (Della-Cioppa *et al*., 1998a and 1998b; Matoba *et al*., 2006). Most of the reported laccases are mostly secreted, extracellular enzymes whereas tyrosinases are intracellular enzymes. The

characterized plant and fungal tyrosinases have possibly bound to organelles or membrane structures. Bacterial *Streptomyces* tyrosinases, however, are found to be secreted.

The role of tyrosinases in nature is considered as fundamental enzymes in diverse defense systems, especially in melanogenesis. The melanin pigment is heterogeneous polyphenolic polymers occurring in all living organisms. In the reaction melanogenesis tyrosine is first oxidized to dopaquinone, which either cyclises to give a dihydroxyindole precursor of black or brownish eumelanins, or reacts with cysteine to give a precursor of reddish brown pheomelanin (Mason, 1948) by tyrosinase. In mammals, tyrosinase-related melanogenesis is responsible for pigmentation in skin, eye, and hair, which contributes an essential part of the protective function of the skin by absorption of UV radiation (Hearing and Tsukamoto, 1991). In plants tyrosinases play an important role in wound healing systems and in regulation of oxidation reduction potential (Mayer, 1987; Walker and Ferrar, 1998). The defense mechanisms of tyrosinases in plants are suggested to be related to the non-enzymatic reactions of quinones.

1.2.2.2.1 Structure of Tyrosinase

In 1969, five different forms (I, Ia, II–IV), (Figure 1.13) ranging from monomers to octamers, were described by Jolley *et al*. 1969, who suggested that the predominant enzyme was tetrameric and composed of four identical sub-units of 32 kDa. Tyrosinases belong to the copper-proteins including an active site that contain a type 3 centre. In active site of the tyrosinase, metal atoms are coordinated by histidine residues. Binding of dioxygen in the copper proteins includes mononuclear (type 1), dinuclear (type 3) and trinuclear (combination of type 2 and type 3) copper centres. Type 1 and 3 coppers show absorption maxima at about 600 and 330.345 nm, respectively, whereas type 2 copper has undetectable absorption (Gerdemann *et al*., 2002; Solomon *et al*., 1996). Type 1 and 2 coppers show an EPR spectrum, whereas type 3 copper gives no EPR signal due to a pair of copper ions, which are antiferromagnetically coupled (Makino *et al*., 1974; Bento *et al*., 2006).
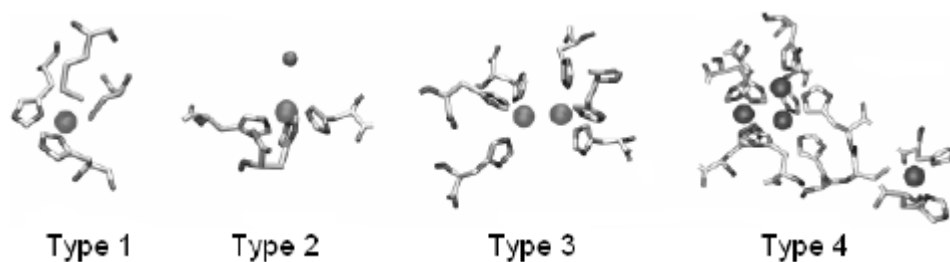
Figure 1.13 Structures of the copper sites of type 1-4 copper proteins (modified from Tepper, 2005)

1.2.2.2.2 Reaction Mechanism and Substrate Specificity of Tyrosinase

Tyrosinases are bifunctional enzymes as they catalyze *ortho*-hydroxylation of monophenols (monophenolase activity) and subsequent oxidation of diphenols to *ortho*-quinones (diphenolase activity). Quinones are highly susceptible to non-enzymatic reactions, which may lead to formation of mixed melanins and heterogeneous polymers (Lerch, 1983). Tyrosinases catalyze oxidation of substrates using molecular oxygen as a terminal electron acceptor with concomitant reduction of oxygen to water two type 3 copper atoms shuttling electrons from substrate to oxygen (Bento *et al.,* 2006; Bertrand *et al.,* 2002). Tyrosinases oxidize their substrates by removing a pair of electrons from the substrates a type 3 copper-protein, the type 4 copper proteins, laccases, oxidize their substrates with a single electron removal mechanism (Figure 1.15).
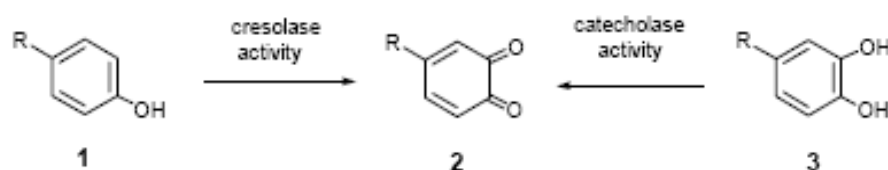
Figure 1.14 Reactions on phenolic compounds catalyzed by tyrosinases (Land *et al.,* 2008)

Tyrosinase oxidizes phenolic compounds such as catechol to *ortho*-quinones but the mechanisms of these biotransformations are different. Oxidation of phenols 1 to *ortho*-quinones 2 is referred to as cresolase activity and oxidation of catechols 3 to *ortho*-quinones 2 is referred to as catecholoxidase or catecholase activity. Other

28

enzymes can catalyse one or other of these processes but only tyrosinase catalyses both reactions (Figure 1.14) (Land *et al.*, 2008).
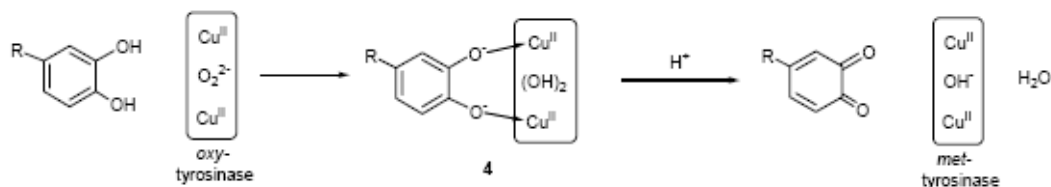
Figure 1.15 Catalytic mechanisms for the tyrosinase and copper binding sites

Tyrosinase is able to use mono-, di-, and trihydroxyphenols as substrates but exhibit greater affinity for dihydroxyphenols. Furthermore, it was also reported that among the monohydroxyphenols (p-cresol and tyrosine), dihdyroxyphenols (catechol, L-dopa, D-dopa, catechin and chlorogenic acid), and trihdyroxyphenols (pyrogallol, catechol) showed maximum activity, indicating that the enzyme is most active with catechol as substrates (Zhang *et al.*, 1999). Many microbial tyrosinases have their pH optima in the neutral and slightly acidic pH range, e.g. *N. crassa* and *A. flavipes* at pH 6.0 (Gukasyan, 1999) and *P. sanguineus* at pH 6.5 (Halaouli *et al.*, 2005). However, optimum activity in the alkaline pH range has been reported for *Thermomicrobium roseum* (pH 9), and pine needle tyrosinase (pH 9.5) (Kong *et al.*, 1998). Tyrosinases are in general reported to not to be very thermostable enzymes.

1.2.2.3 Catechol Oxidases

The activity of catechol oxidase (CO), the third member of the type-3 class of dicopper proteins, has been less well studied (Eicken *et al.*, 1999). Catechol oxidase is strongly related to both tyrosinase and hemocyanin, which all have a dinuclear copper complex with histidine ligands at the active site (Siegbahn, 2004). The classification and specificity of catechol oxidase and tyrosinase remains an area of confusion. Originally, they were classified as oxygen oxidoreductases. Cresolase activity was later given the classification of monophenol monooxygenase and catecholase activity became diphenol oxygen: oxidoreductase (Eicken *et al.*, 1999).

Catechol oxidase mainly has diphenolase activity, but monophenolase activity has also been demonstrated (Siegbahn, 2004).

Catechol oxidase is found in higher plants. It has been isolated from leaves, fruits, flowers and tubers. The physiological role of CO is not yet clear. A role in photosynthesis appears very likely since catechol oxidase is often found tightly bound in the thylakoid membrane. There is also growing evidence for a role of catechol oxidase in the defence of plants against insects and diseases. The oxidation reaction resulting by polymerization of orthoquinones and melanins formation, which have been suggested to protect plants from external attacts. Roles for catechol oxidases in the biosynthesis of diphenols and in the hardening of seed coats have also been proposed (Siegbahn, 2004).

1.2.2.3.1 Structure of Catechol Oxidase

The structure of the monomeric 39 kDa CO from sweet potatoes was solved and refined to 2.5 Å in the dicupric Cu(II)-Cu(II) state. The secondary structure is primarily α-helical, with the core of the enzyme formed by a four-helix bundle composed of helices α2, α3, α6 and α7. The helix bundle accommodates the catalytic dinuclear copper center and is surrounded by two α helices, α1 and α4, and several short β strands. Both of the two active site coppers were clearly visible in the electron density maps and each is coordinated by three histidine residues contributed by the helix bundle. Significant structural changes were observed around the active site, indicating that access to the copper dimer is primarily controlled by the aromatic ring of Phe261 (Eicken *et al*., 1999; Siegbahn, 2004).

1.2.2.3.2 Reaction Mechanism of Catechol Oxidase

The catalytic cycle of the CO begins with the oxidized *met* form. The monodentate binding of the diphenolic substrate to CuB seems to be most likely to reduce the Cu(II) Cu(II) form to the Cu(I) Cu(I) which is dicuprous state. CuB would be coordinated by H240, H244 and the dioxygen molecule in the tetragonal planar coordination. Catechol substrate and H274 would occupy the two axial positions in this distorted octahedral coordination, as favored by Cu(II) with nine electrons. The

CuA site would retain tetragonal pyramidal coordination, with H88 and H118 in equatorial positions, dioxygen, H109 in an axial position and a vacant nonsolvent accessible sixth coordination site. Ternary CO–O2^{2-} substrate complex would occur and than, two electrons could be transferred from the substrate (catechol) to the peroxide, followed by cleavage of the O–O bond, loss of water and separation of the *o*-quinone product. Binding of the catechol substrate to the reduced CO without the binding of oxygen seems less likely, as the incubation of reduced crystals did not show any catechol affinity, potentially indicating the low binding affinity of the substrate for the Cu(I)–Cu(I) center. After oxidation of the second substrate molecule and loss of the bound water, the dicopper center is in its *met* form again and ready to undergo another catalytic cycle (Figure 1.16) (Eicken *et al.,* 1999).
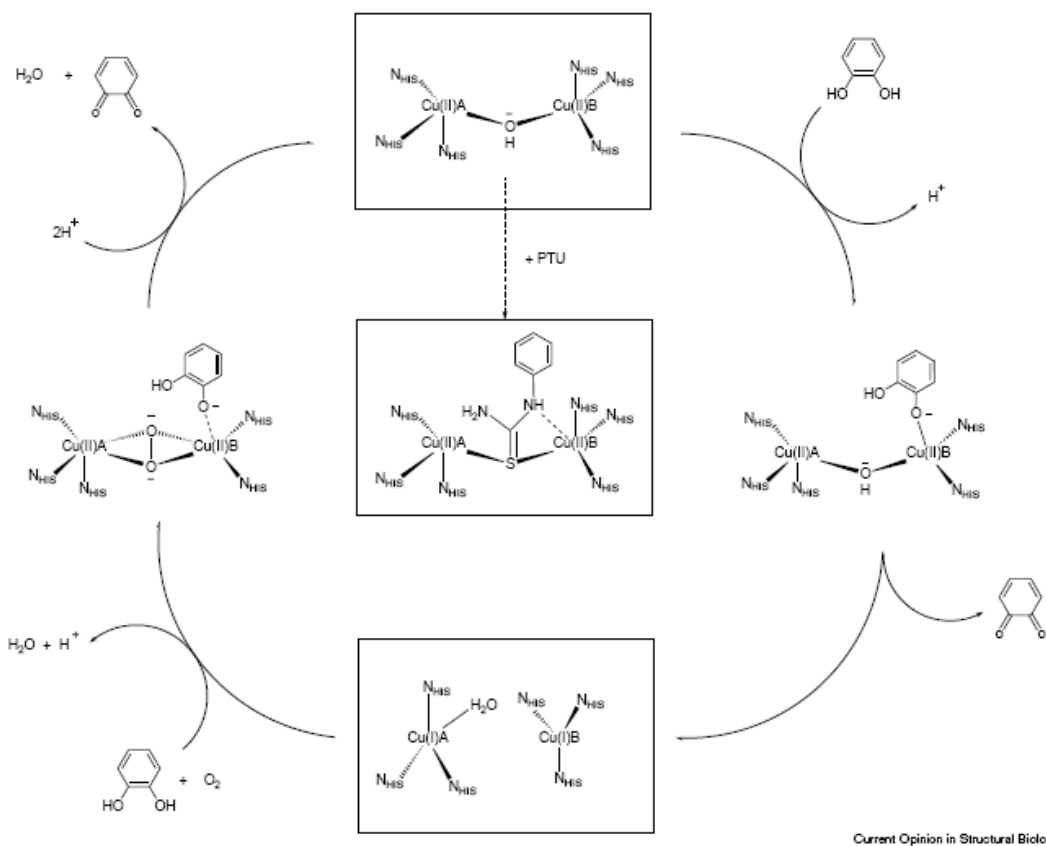
Figure 1.16 The catalytic cycle of catechol oxidation by catechol oxidase from sweet potatoes (Eicken *et al.,* 1999)

1.2.3 Oxidation of Phenolic Compounds by Phenol Oxidases

Phenols are naturally occurring plant secondary metabolites. As mentioned above, they are involved in the defense of plants against invading pathogens. So, they are widely used in plant-derived foods to stabilize the color, flavor, and taste, nutritional and aesthetic value. They are known to show beneficial effects as scavengers of oxygen radicals due to their antioxidants properties (Dugan *et al.*, 1980; Rice-Evans *et al.*, 1996). Oxidation of phenolic compounds leads to of quinone formation. These types of reactions are responsible for the enzymatic browning process. Enzymatic browning occurs by the action of polyphenoloxidases (monophenol monoxygenase or tyrosinase) and laccase. These enzymes play important role to produce insoluble polymers from phenolic compounds via quinones, which serve as a barrier that prevents spreading of infection of plants by viruses or bacteria. On the contrary, this type of browning is the major cause of quality degradation of fruits during handling, storage and processing (Coseteng *et al.*, 1987; Matheis *et al.*, 1987). Depending of the type of the phenolic compounds, these enzymes can show cresolase activity when monophenol is converted to o-diphenol and catecholase activity when o-diphenol is oxidized to o-quinone. These quinonic compounds are very unstable and so quickly polymerized to melanin like pigments (Pierpoint, 1966).

Melanins are complex bio-polymers formed by the oxidative polymerization of phenolic or indolic compounds. Melanin production consequence of the browning of fruits and vegetables but at the same time it is the phenomenon responsible for skin, hair and eye pigmentation in mammals (Munoz *et al.*, 2009). Its accumulation or deficiency cause illnesses such as melanoma and albinisim. In fungi, several different types of melanin have been identified to date. The most important types are DHN and DOPA melanin. Both types of DHN and DOPA melanin have been implicated in pathogenesis (Hamilton and Gomez, 2002; Jacobson, 2000; Kwon-Chung *et al.*, 1982; Wheeler and Bell, 1988). The proposed functions of fungal melanins include protection against UV irradiation, enzymatic lysis, oxidants, and in some instances extremes of temperatures. In addition, melanins have been shown to bind metals, function as a physiological redox buffer, thereby possibly acting as a sink for harmful unpaired electrons, and provide structural rigidity to cell walls, and store water and ions, thus helping to prevent desiccation (Jacobson, 2000). On the other

hand, phenolic compounds are very abundant environmental pollutants. Besides the natural sources they also enter the environment as waste from several types of industrial and agricultural activities (Gianfreda and Bollag 2002; Gianfreda *et al.*, 2006). In wastewater treatment systems, oxidoreductive enzymes are used to transform phenols through oxidative coupling reactions with the production of polymeric products, which are proposed to be easier removed by sedimentation and filtration (Krastanov, 2000; Aktas and Tanyolac, 2003a,b).

1.3 Bi-functional Enzymes

Bifunctional enzymes are unusual multifunctional proteins (Moore, 2004). Catalase-peroxidases, or KatGs, are good example for multifunctional enzymes present in bacteria, archaebacteria and some fungi. They show both catalase and peroxidase activity. The catalase and peroxidase reactions can be broken down into two stages. The common reaction is to both the catalase and peroxidase is the formation of compound I, classically a porphyrin cation radical, but the other stage of reactions depends on the reducing substrate that is available. The catalase reaction proceeds in the presence of high H_2O_2 concentrations, whereas at low H_2O_2 concentrations or if Cpd I is generated from an organic peroxide such as peroxyacetic acid, the peroxidase reaction take place (Figure 1.17) (Rahul Singh *et al.*, 2008).
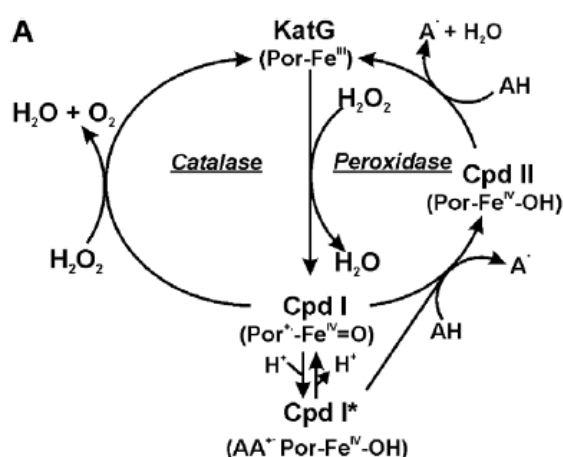
Figure 1.17 Scheme outlining the various reactions catalyzed by KatGs (Rahul Singh *et al.*, 2008)

Besides catalase-peroxidases, there are numbers of reports available showing that catalase and phenol oxidase activities somehow overlap in such a way that catalases possess additional phenol oxidase activity and phenol oxidases exhibit further catalase activity. This relationship might be clarified by the release of hydrogen peroxide because of polyphenol oxidation (Akagawa *et al.*, 2003). Aoshima and Ayebe (2007) also reported hydrogen peroxide generation by phenol oxidation. They observed high concentrations of H_2O_2 in beverages like tea or coffee immediately after opening caps due to oxygen. The mushroom tyrosinase exhibiting catalase activity in the presence of hydrogen peroxide was first introduced by Jolley *et al.*, 1974. Later, this bifunctional activity of tyrosinase was also investigated by Garcia-Molina *et al.*, (2005) and Yamazaki *et al.*, (2004). Besides this novel tyrosinase, one isozyme of catechol oxidase from sweet potatoes (*Ipomoea batatas*) was found to have catalase-like activity (Gerdemann *et al.*, 2001). There are also examples of phenol oxidases such as catechol oxidase from sweet potatoes (*Ipomoea batatas*) (Gerdemann *et al.*. 2001) displaying additional catalase activity. On the other hand, there is only one study describing phenol oxidase activity of a mammalian catalase; however, lack of characterization makes it difficult to classify the enzyme (Vetrano *et al.*, 2005). This is a homotetrameric heme-containing enzyme, known for its ability to convert hydrogen peroxide into water and oxygen (catalatic activity), and in the presence of low concentrations of hydrogen peroxide to oxidize low molecular weight alcohols (peroxidatic activity). This enzyme also shows an oxidative activity in the absence of hydrogen peroxide. Catalytic activity includes the interaction of the enzyme heme group and substrate, which is a hydrogen peroxide. This results in the formation of a transient oxyferryl porphyrin centered radical, which is a compound I. After binding the second hydrogen peroxide compound I is broken down and molecular oxygen and water is released. On the other hands, peroxidative activity includes interaction of compound I and low molecular weight alcohols. This results in substrate oxidation. In the oxidase activity the catalase heme interact with strong reducing substrate such as benzidine and molecular oxygen results in formation of a compound II like intermediate in the absence of hydrogen peroxide (Figure 1.18) (Vetrano *et al.*. 2005).
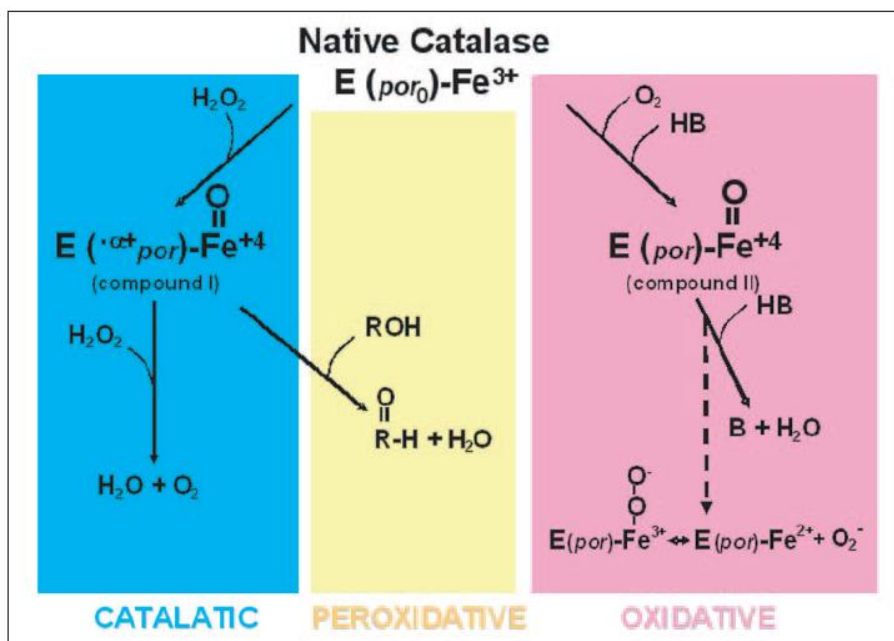
Figure 1.18 Scheme outlining the various reactions catalyzed by Native Catalase(Vetrano *et al*., 2005)

1.4 Thermophilic Fungi

The ability of organisms to live at high temperatures is described as thermophilicity. The capacity of the organisms to survive at high temperature differs and the upper temperature limit of viability increases in the sequence animals-plants-fungi-prokaryotes from 38 to 100°C and higher (Feofilova and Tershina, 1999). Among the fungi, thermophilic ones are the one that capable of surviving at the maximal or nearly maximal temperature characteristic to its taxonomic group. Thermophilic fungi are a small taxonomic group that do not grow at a temperature below 20°C and higher than 60-62 ^{o}C. *Thermomyces lanuginosus* was the first thermophilic fungus that described in 1899 (Feofilova and Tershina, 1999). At present about 30 thermophilic species from Zygomycetes, Ascomycetes, Deuteromycetes and Basidiomycetes most of which originally were isolated from composts are known. They are found in habitats where decomposition of plant materials takes place. In these habitats thermophiles may occur either as resting propagules or asactive mycelia depending on the availability of nutrients and favorable environmental conditions (Maheshwari *et al*., 2000).

1.4.1 *Scytalidium thermophilum*

Scytalidium thermophilum is a thermophilic organism from Deuteromycete, and a member of the *Torula-Humicola* complex, which is dominant species in mushroom compost. The effects of this fungus on the growth of the mushroom mycelium have been described at three distinct levels. First, this fungus decreases the concentration of ammonia in the mushroom compost, which otherwise would counteract the growth of the mushroom mycelium. Second, it immobilizes nutrients so that nutrient is available to the mushroom mycelium, and third, it may have a growth promoting effect on the mushroom mycelium, as has been demonstrated for *Scytalidium thermophilum* and for several other thermophilic fungi (Wiegant, W. M. 1992).

1.4.1.1 Catalase of *Scytalidium thermophilum* (Catalase-Phenol Oxidase CATPO)

Scytalidium thermophilum bifunctional catalase with an additional phenol oxidase activity was isolate and biochemically characterized. This *Scytalidium thermophilum* catalase (CATPO) is tetrameric, heme containing protein and has a molecular weight of 320 kDa with four 80 kDa subunit. Isoelectric point of the protein is 5.0. The most stable catalase and phenol oxidase activities were found at pH 7.0 and these activities are maximum at 60°C (Kocabas *et al.*, 2008). This enzyme was purified by anion exchange chromatography followed by gel filtration. Purified enzyme was assayed against various phenolic compounds as substrate. The pure CATPO could oxidize o-diphenols such as catechol, caffeic acid, and L-DOPA in the absence of hydrogen peroxide. The highest phenol oxidase activity of CATPO was observed against catechol. No activity was detected against tyrosine and ABTS which are specific substrates of tyrosinase and laccase respectively. Common catechol oxidase inhibitors, salicylhydroxamic acid and p-coumaric acid, inhibit the oxidase activity *Scytalidium thermophilum* produces bifunctional catalase-phenol oxidase enzyme (CATPO) which is capable of oxidizing phenolics in the absence of hydrogen peroxide on the contrary of the other catalase-peroxidases (Kocabas *et al.*, 2008).

1.5 Scope of the Study

This study aims to analyze the bioconversion products of the phenol oxidase activity of CATPO. The phenolic compounds are selected according to different chemical structure and functional properties. *Scytalidium thermophilum* produces bifunctional catalase-phenol oxidase enzyme (CATPO) which is capable of oxidizing phenolics in the absence of hydrogen peroxide on the contrary of the other catalase-peroxidases. The secretion of CATPO is enhanced in the presence of phenolic compounds such as gallic acid. This suggests, CATPO is possibly produced for defense against toxicity of phenolics and that it's oxidizing activity has a role in this process. The bifunctional CATPO from *S. thermophilum* was first discovered by our group. Therefore, the phenol oxidation spectrum of the bioconversion products is largely unknown. CATPO was purified from *S. thermophilum* and activity against compounds including flavonoids, derivatives of cinnamic acid, stilbenes and phenolic acids was analyzed and bioconversion products were characterized by HPLC and LC-MS. Thus, this study contributes to a better understanding of the mechanism of phenol oxidation by CATPO, and allows having more insights into a possible antioxidant role for CATPO and specially its phenol oxidase activity.

CHAPTER 2

MATERIALS AND METHODS

2.1 Materials

2.1.1 Fungal Strains

Scytalidium thermophilum (type culture *Humicola insolens*) was provided by Dr. Mehmet BATUM from ORBA Inc.

2.1.2 Chemicals, Enzymes and Equipment

The list of chemicals, enzymes, equipments and their suppliers are given in Appendix A.

2.1.3 Growth Media, Buffers and Solutions

The preparation of the growth media, buffers and solutions used are given in Appendix B.

2.1.4 Phenolic Materials

14 different phenolic compounds were analyzed as possible substrates of CATPO (Table 2.1.).

Table 2.1 Analyzed Phenolic Compounds

Analyzed Phenolic Compounds	
Catechol	Coumaric acid
Hydroquinone	Quercetin
Resorcinol	Resveratrol
Gallic acid	Kaempferol
Vanillic acid	Catechin
Caffeic acid	Myricetin
Chlorogenic acid	Epicatechin

2.2 Methods

2.2.1 Microbial Cultivations

Scytalidium thermophilum was inoculated onto YpSs agar plates as described in Appendix B (Cooney and Emerson, 1964) and plates were incubated at 45 °C for 4-5 days until sporulation and were stored at 20°C for maximum 2 months to use as stock cultures. Spores from these stock cultures were inoculated into 10 mL liquid preculture media, consisting of YpSs medium broth (Appendix B), containing glucose instead of starch. After 24 hs of incubation at 45°C, the preculture was transferred into the main culture. Preculture volume was 2 % of the main culture volume. Cultures were incubated in a shaker incubator at 45°C at 155 rpm shaking rate. On the 5th day of their growth, biomass was separated from culture supernatant by filtration through Whatmann No.1 filter paper. The filtrate was centrifuged at 10,000 rpm for 10 min. The supernatant was either used as crude enzyme solution for assay experiments or enzyme purification (section 2.5).

2.3 Determination of Total Protein Content

Total protein was determined according to the Bradford method (1976) by using bovine serum albumin (BSA) as standard. This method is based on dye-binding assay

in which a differential shift of absorbance of the Coomassie Brilliant Blue G-250 dye (from 465 nm to 595 nm) occurs in response to protein concentration.

Standard concentrations of BSA were prepared with distilled water (Appendix C). After addition of 1.0 mL of Coomassie Blue to each tube, the tubes were vortexed and mixed well Tubes were kept in dark for 10 minutes. The spectrophotometer wavelength was adjusted to 595 nm. The optical density was monitored. According the results a standard curve was attained. The optical density of the sample protein was measured for different amounts until the value read from the spectrophotometer fell into the range between the values obtained from standard curve.

2.4 Enzyme Assays

S. thermophilum CATPO catalase and phenol oxidase activities were determined spectrophotometrically. Catalase activity was analysed at 60 °C in 100 mM sodium phosphate buffer (pH 7). 10 μl sample was mixed with 10 mM hydrogen peroxide (H_2O_2) in a total volume of 1 mL and the disappearance of hydrogen peroxide was monitored at 240 nm. Both buffer and enzyme solutions were pre-incubated for 5 min at 60°C in a water-bath. Enzyme activity was determined using the initial rate of the reaction and the extinction coefficient for H_2O_2 was taken as 39.4 M-1 cm-1 (Merle *et al*., 2007). One enzyme unit was defined as the amount of enzyme that catalyzes the decomposition of 1 μmol H_2O_2 per minute.

Phenol oxidase activity was determined at 60 °C in 100 mM sodium phosphate buffer (pH 7). 10 μl sample was mixed with 100 mM catechol in a total volume of 1 mL and the oxidation products were monitored at 420 nm. Both buffer and enzyme solutions were pre-incubated for 5 min at 60°C in water-bath. Enzyme activity was determined using the initial rate of the reaction and the extinction coefficient was taken as 3450 $M^{-1}cm^{-1}$ for catechol (Ögel *et al*., 2006) and one enzyme unit was defined as the amount of enzyme required for the formation of one nanomole of product per min.

2.5 Protein Purification

2.5.1 CATPO Purification

S. thermophilum extracelular catalase phenol oxidase (CATPO) purification was performed with the AKTA Prime FPLC system, (Amersham Biosciences, Sweden) (Kocabas *et al*., 2008). According to this system, purification was done by a two step technique including anion exchange and gel filtration. Crude CATPO solution was prepared by centrifugation of 5th day culture supernatant at 8,000 x g for 5 minutes. Supernatant was taken and filtered through Whatman no.1 filter paper. The first step of the purification was anion exchange chromatography which was performed in a 20 mL prepacked HiPrep 16/60 Q XL column (Amersham Biosciences, USA). All solutions were filtered through a 0.45 μm filter before use. The column was operated at 50 mM pH 8.0 Tris-HCl buffer at 2 mL/min flow rate. Enzyme was eluted by collecting 3 mL fractions with a salt gradient in the range of 0-1 M sodium chloride (NaCl), prepared in the same buffer. All fractions were checked for both catalase and phenol oxidase activities.

The second step of purification was gel filtration chromatography, which was performed in a pre-packed HiPrep 16/60 or 26/60 Sephacryl S-100 high resolution gel filtration column (Amersham Biosciences, USA). Equbiliration of the column was done with 50 mM pH 8.0 Tris-HCl buffer. The flow rate was at 1 mL/min. All solutions were filtered through a 0.45 μm vacuum filter before use. 3 mL fractions were collected in 200 mL elution volume. Each fraction was tested for both catalase and catechol oxidase activities.

2.5.2 SDS-Polyacrylamide Gel Electrophoresis

SDS-PAGE was done according to the standard protocol of Laemmli (1970) and the manufactures instruction via Blue Vertical 102 and Blue Power 500 Electrophoresis System, Serva Blue Flash S, 15x28x8.5 cm (Appendix D).

2.5.2.1 Preparing Acrylamide Gels

Before preparation of the gels, 2 combs 4 spacers, 2 gel plates were cleaned with dH$_2$O and ethanol then, dried. After spacers were placed, large gel plate and small gel plate were overlaid to create a sandwich. The glass plate sandwich was slid into the electrophoresis unit.

After assembling the plates, a suitable separating gel was prepared by combining the components in a small centrifuge tube. TEMED and freshly made APS were added just before the gel was ready to pour to prevent polymerization in the tube. Using a Pasteur pipette, the gel mixture was poured between the plates up to the level indicated. After overlaying with water, the gel was left for polymerization for 30 min-1 h.

Stacking gel was prepared by combining the components in a plastic bijoux or flask. Water overlay was poured off and the area above gel was dried by using 3MM filter paper. It was poured above separating gel after addition of proper amounts of TEMED and APS. Combs were inserted by avoiding bubble formation and allowed to set for approximately 30 minutes.

For 0.75 cm spacers and 10-well comb, maximum volume of sample was 35 μL. Samples were boiled for 5 min and allowed to cool, then were centrifuged at 12500 rpm at room temperature for 5 min Constant voltage of 150 V was applied and current at approximately 60 mA per gel. The gel was run for about normally 2 hs. Preceding staining with Coomassie Blue R250, the gel was fixed with 20% trichloroacetic acid for 30 min at room temperature (Appendix E). Then it was rinsed with dH$_2$O 2-3 times for 3 minutes. The gel was transferred to 50-100 mL staining solution and stained for overnight. The gel was destained with 100 mL destained solution for 45 min and photograph of the gel was taken.

2.6 Biotransformation Assays of Different Substrates with CATPO

2.6.1 Preparation of Standard Solution

Standard solutions 5 mM, 10 mM, 20 mM and 40 mM of 14 different phenolic compounds were prepared by dissolving them in 2 mL HPLC grade methanol, and by mixing with 3 mL of 100 mM potassium phosphate buffer pH 7.0. Standard solutions were filtered through a 0.45 μm filter prior to injection (30 μL) into the HPLC system. The standard mixtures of phenolic compounds (10 mM) were prepared just before HPLC analysis, in order to avoid decomposition. Standard solutions were incubated at room temperature and 60 ºC from 10 min to overnight and analyzed by HPLC to detect autoxidation.

2.6.2 Preparation of Samples

The reaction mixture used for biotransformation assay with CATPO, consisted of 2 mL of 10 mM phenolic compound solution in methanol, 2 mL 100 mM potassium phosphate buffer pH 7.0 and 1 mL pure enzyme (3.6 U/μg).

First, to choose the appropriate time to analyze the oxidation products, different time sections (1 min, 10 min, 30 min, 1 h and 24 hs) were applied and subsequently analyzed by HPLC. After this experiment, 1 h was decided to use to analyze the oxidation products and reaction mixtures were incubated at 60°C for 1 h. After 1 h, 50 mM acetic acid was used to stop the reaction. Each reaction mixture was filtered through a 0.45 μm filter prior to injection (30 μL) to the HPLC system.

2.6.3 High Performance Liquid Chromatography Analysis

HPLC analyses were done on a Shimadzu SIL-20AHT instrument with a pump, a variable wavelength absorbance detector (UV-Vis detector) set a 254 nm and reversed phase C18 column. Column temperature was maintained at 40ºC.

Standard solution and reaction mixtures were transferred into screw cap vials and vials were closed with blue screw caps for HPLC analysis. Injection volume was 30 μL. Gradient system was applied using; the solvent system A composed of 0.04% acetic acid in water and the solvent system B composed of acetonitril, methanol and H_2O (52:37:11). Elution was done a linear gradient. It was started with 100% solvent A and applied for 2 min, followed by rapid increase by 12% B in 5 min at a flow rate of 1 mL/min. Detailed information about gradient system is given in Table 2.2.

Table 2.2 Gradient system applied on HPLC

Time	Conc. of solvent B	Time	Conc. of solvent B
0.1min	0%	17 min	35%
2 min	0%	20 min	50%
5 min	12%	22 min	50%
7 min	12%	25 min	20%
10 min	18%	26 min	0%
15 min	18%	28 min	STOP

First; the standard solutions at different molarities were injected to the HPLC system. The wavelength was set at 254 nm. The spectrum of each compound was examined. Then the retention times of each phenolic compound were determined.

Second, samples consist of reaction mixtures at 1 h were injected to the HPLC system with one injection of standard mixture after each injections of samples consist of reaction mixture, in order to control whether there is a deviation in the retention times of standards or not. By comparing the retention times of standard peaks with that of the sample peaks. Peaks in chromatograms of the samples were determined. Then, spectrum of each peak at chromatogram of sample was viewed and compared with spectrum of the analyte eluted within the same minute. Spectrum of peak was laid over the spectrum of the analyte to control that phenolic compounds unreacted by enzyme and the biotransformation products.

Having qualitatively determined the analytes in samples; quantitative analysis was performed. For the samples containing one or more of the analytes; comparing the peak area of the analyte at chromatogram of the standard mixture with that of the peak area of the analyte at chromatogram of the sample and using direct proportionation between two areas, concentration of the analyte in the sample was determined.

2.6.4 ESI- LC/MS Analysis

Biotransformation products were examined in liquid chromatography mass spectrometry (LC-MS) in TÜBİTAK ATAL laboratory. LCMS analyses were done on Agilent 1100 series LC-MSD instrument with a Waters Spherisorb S5ODS2 (25cm X 4.6 mm ıd) column (adjust to 25 ^{o}C).

Two different mobile phase wad used to apply gradient. These were % 0.05 acetic acid and asetonitril: methanol: ddwater (52:37:11). The source was operated in negative electrospray mode. Drying gas flow 0.6mL/min, nebulizer pressure 40 psig, drying gas temperature 350°C, capillary voltage 3 kV and fragmentor 70 eV. Mass spectra were collected in a scan range of 100-1000 m/z.

2.7 Effects of Reaction Conditions on CATPO Catalyzed Oxidation Products of Catechol

2.7.1 Effects of Initial Catechol Concentration on CATPO Catalyzed Oxidation Products of Catechol

To determine the effect of initial catechol concentration on the oxidation products catalyzed by CATPO, biotransformation assays were performed at various catechol concentration values as 10^{-2}, 10^{-1}, 1, 10 and 100 mM. The enzyme concentration, temperature, pH, time and methanol content were kept constant as stated in standard assay condition.

2.7.2 Effects of Enzyme Concentration on CATPO Catalyzed Oxidation Products of Catechol

The effect of enzyme concentration was evaluated with a series of runs conducted at a constant initial catechol concentration of 10 mM, temperature, 60 ^{o}C and pH 7.0 in a 40% (v/v) methanol potassium-phosphate reaction medium by using various enzyme content as 1 µg, 10 µg and 100 µg.

2.7.3 Effects of Methanol Concentration on CATPO Catalyzed Oxidation Products of Catechol

The effect of methanol content was determined bu using various methanol concentration as 0%, 20%, 40%, 60%, and 80% (v/v) for fixed initial concentrations of catechol and enzyme. The experiments were at 60 ^{o}C, pH 7.0 and with 320 U total CATPO activity.

2.7.4 Effects of pH on CATPO Catalyzed Oxidation Products of Catechol

To determine the effect of pH on CATPO catalyzed oxidation products of catechol the oxidation assay were performed at various pH values in 5.0, 6.0, 7.0, 8.0 and 9.0 using 100 mM of the following buffers: citrate-sodium phosphate (pH 5.0), potassium phosphate (pH 6.0-8.0) and Tris-HCl (pH 9.0). Enzyme concentration, initial catechol concentration were kept constant. The experiments were at 60 ^{o}C, pH 7.0 and with 320 U total CATPO activity.

2.7.5 Effects of Temperature on CATPO Catalyzed Oxidation Products of Catechol

The CATPO-catalyzed oxidation products of catechol experiments were repeated at five temperatures of 40, 50, 60, 70 and 80 ^{o}C, at pH 7 in 40% (v/v) methanol-potassium phosphate buffer medium. Constant 10 mM catechol was used each time as the substrate and CATPO (320 U in total) was added to start the polymerization reaction.

2.7.6 Effects of Reaction Time on CATPO Catalyzed Oxidation Products of Catechol

The effect of the reaction time of catechol by CATPO on oxidation products, 1 min, 10 min, 30 min, 1 h and 24 hs oxidation reaction were repeated. The enzyme concentration, catechol concentration, temperature, pH, and methanol content were kept constant as stated in standard assay condition.

2.8 Biotransformation Assays of Different Substrates with Laccase

Tramates versicolor laccae enzyme (23.1 U/mg) was used in biotransformation assays. Enzymes Isoelectric point (pI) is 4.1. Optimum pH is 4.8.

2.8.1 Preparation of Standard Solution

Standard solutions of phenolic compounds were prepared by using 10 mM from each and dissolving them in 2 mL HPLC grade methanol. After dissolving the phenolics, 3 mL 100 mM phosphate citrate buffer pH 4.8 was added to each of them. The standard mixtures of phenolic compounds were prepared just before HPLC analysis in order to avoid decomposition of standards.

2.8.2 Preparation of Samples

The reaction mixture used for biotransform prepared by mixing 10 mM phenolic compounds in 2 mL methanol and pure enzyme (10 μg) dissolved in 3 mL 100 mM potassium citrate buffer pH 4.8. To analyze the oxidation products, reaction mixtures were incubated at 25°C for 1 h. After 1 h, 50 mM acetic acid was used to stop the reaction. Each reaction mixture was filtered through a 0.45 μm filter prior to injection (30 μL) to the HPLC system and stored at -20 ºC after use.

2.9 Biotransformation Assays of Different Substrates with Tyrosinase

Agaricus bisphorus tyrosinase (mushroom tyrosinase) (4.2 U/μg) was used in biotransformation assays. Enzymes Isoelectric point (pI) is 4.7. Optimum pH is 6.7.

2.9.1 Preparation of Standard Solution

Standard solutions of 4 different phenolic compounds were prepared by using 10 mM from each and dissolving them in 2 mL HPLC grade methanol. After dissolving the phenolics 3 mL 100 mM potassium phosphate buffer pH 6.5 was added to each of them. Standard solutions were filtered through a 0.45 µm filter prior to injection (30 µL) to the HPLC system. The standard mixtures of phenolic compounds (10 mM) were prepared just before HPLC analysis in order to avoid decomposition.

2.9.2 Preparation of Samples

The reaction mixture used for biotransformation assay with tyrosinase, consisted of 2 mL of 10 mM phenolic compound solution in methanol, 3 mL 100 mM potassium phosphate buffer pH 6.5 enzyme solution (10 µg). To analyze the oxidation products, reaction mixtures were incubated at 25°C for 1 h. After 1 h, 50 mM acetic acid was used to stop the reaction. Each reaction mixture was filtered through a 0.45 µm filter prior to injection (30µL) to the HPLC system and stored at -20 ºC after use.

CHAPTER 3

RESULTS AND DISCUSSION

3.1 Experimental Strategies for Analysis of Oxidation of Phenolic Compounds by the Bifunctional Catalase-Phenol Oxidase from *Scytalidium thermophilum*

In this study, it was aimed to analyze the oxidation of various phenolic compounds by the extracellular bifunctional Catalase-Phenol Oxidase (CATPO) from *S. thermophilum*. CATPO is a novel enzyme and the range of phenolic compounds oxidized by CATPO and the resulting products are unknown. The experimental strategy used in this study is outlined in Figure 3.1.

First, CATPO was purified to perform oxidation reactions in the absence of any possible contaminating molecules that may interfere with the reactions, although this is unlikely due to the fact that CATPO is the only phenol oxidase produced under the defined growth conditions (Mete, 2003 and Kaptan 2004). Purification was performed by using a two-step column chromatography technique, involving anion exchange and gel filtration. After purification of CATPO, catalase and phenol oxidase activities were analyzed spectrophotometrically. Bioconversion profiles of 14 phenolic compounds including flavonoids, derivatives of cinnamic acid, stilbenes and phenolic acids were analyzed by HPLC and products were characterized by LC-ESI-MS. The phenolic compounds that were oxidized by CATPO, hence yielding oxidation products by HPLC, were also analyzed by using two commercial enzymes, namely *T. versicolor* laccase and *A. bisphorus* tyrosinase. The UV-Visible spectrums, HPLC and LC-MS profile of the oxidation products of CATPO, laccase and tyrosinase were compared. In previous studies by Yüzügüllü (2010) and Kocabas (2008), the phenol oxidase activity of CATPO was shown to resemble mainly catechol oxidases (tyrosinases) but the enzyme also displayed some of the properties of laccases. As CATPO is a novel phenol oxidase with a heme group at

the catalase active site and no copper atoms, as opposed to the tyrosinases and laccases, these novel features were not surprising. Nevertheless, both laccases and tyrosinases are important enzymes of industrial applications and it is, therefore, of interest to make a more precise comparison of these enzymes based on the chemistry of their oxidation products.
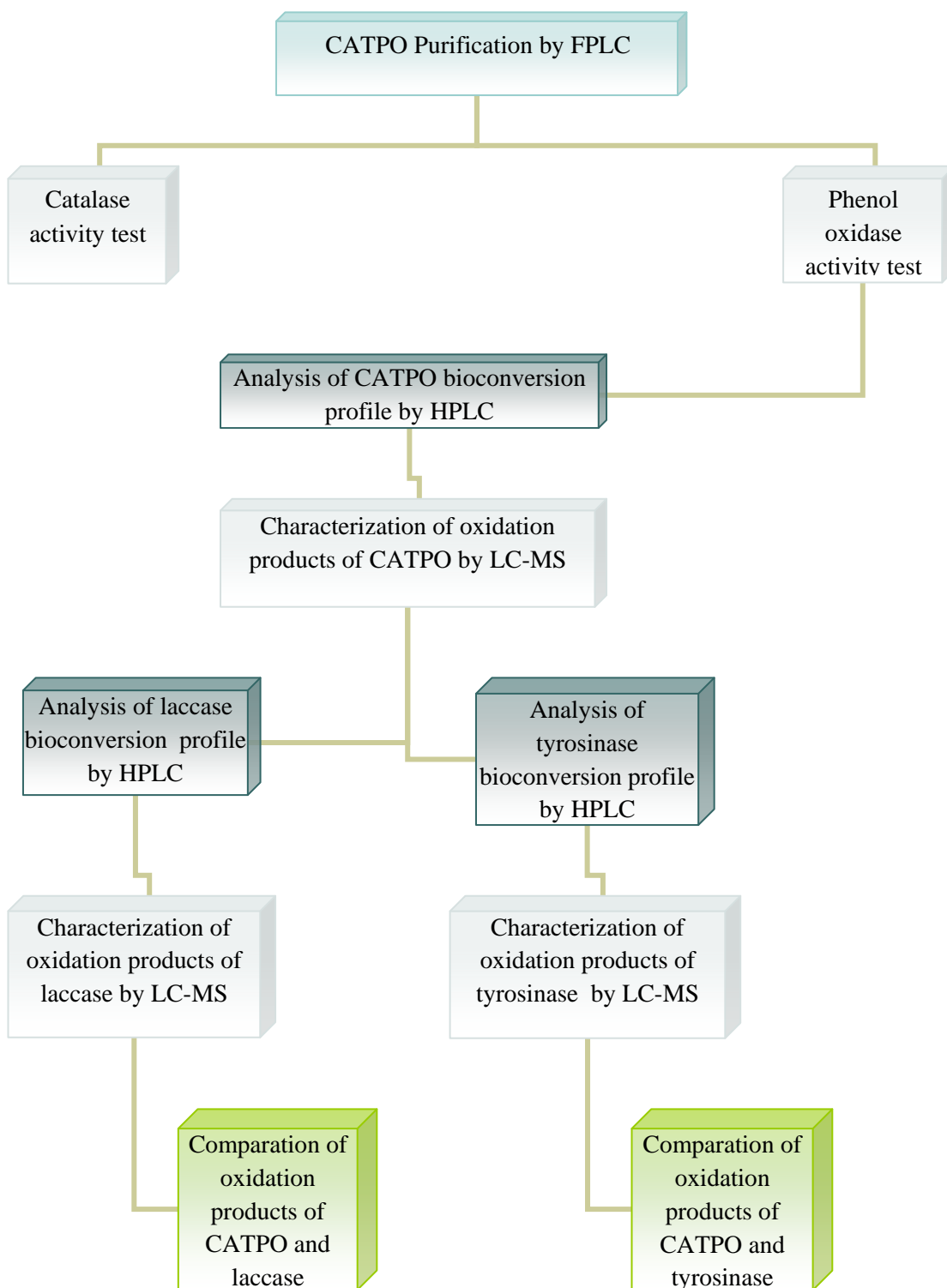
Figure 3.1 Flowchart of the experimental strategies

3.2 CATPO purification

CATPO purification was performed using a two-step column chromatography technique including anion exchange and gel filtration as previously described by Kocabas *et al.,* (2008). Both catalase and phenol oxidase activities were followed in the eluted fractions and the yield and purification fold values were calculated using both catalase and phenol oxidase data.

Anion exchange was performed as described in section 2.5.1. CATPO was bound to the anion exchange column at pH 8.0, so, the enzyme was separated from many other proteins having negative charge at this pH. To predict CATPO activity, each fraction was tested for catalase and phenol oxidase activities. Fractions showing catalase and phenol oxidase activities at the same time were combined, mixed and concentrated by vacuum centrifugation.

Gel filtration was performed as described in section 2.5.1. Fractions containing CATPO were detected as described above, for anion-exchange chromatography. Purification data are shown in Tables 3.1 and 3.2. Purity and molecular weight of CATPO was checked by SDS-PAGE using coomassie blue staining, as described in section 2.5.2. CATPO was observed as a single band with an expected size of 80 kDa (Figure 3.2 and Figure 3.3), corresponding to its monomeric form. The enzyme was previously shown to be a tetramer of 320 kDa (Sutay, 2007).
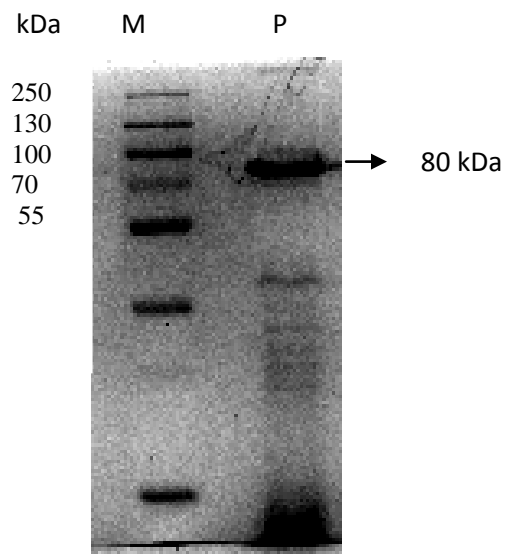
Figure 3.2 SDS-PAGE of *S. thermophilum* CATPO from anion exchange. Lanes; M: Markers and P: Purified CATPO
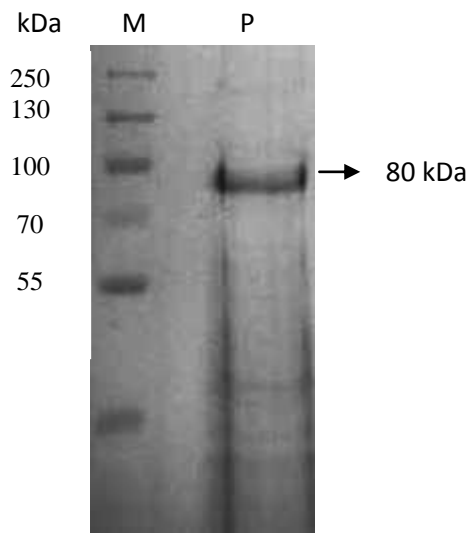
Figure 3.3 SDS-PAGE of *S. thermophilum* CATPO from gel-filtration. Lanes; M: Markers and P: Purified CATPO

Table 3.1 Two step purification results of *S. thermophilum* CATPO based on phenol oxidase actvity

Enzyme Purification Steps	Volume (mL)	Phenol oxidase activity (U/mL)	Total activity (U)	Protein concentration (mg/mL)	Total Protein (mg)	Specific activity (U/mg)	Yield (%)	Purification fold
Crude enzyme	20	37	740	0.0911	1.822	406	100	1.0
Anion Exchange Chromarography	24	21	480	0.0254	0.6096	787.4	64	1.9
Gel Filtration Chromatography	8	34	320	0.011	0.088	3633	43	8.9

Table 3.2 Two step purification results of *S. thermophilum* CATPO based on catalase actvity

Enzyme Purification Steps	Volume (mL)	Catalase activity (U/mL)	Total activity (U)	Protein concentration (mg/mL)	Total Protein (mg)	Specific activity (U/mg)	Yield (%)	Purification fold
Crude enzyme	20	3.2	64	0.0911	1.822	35	100	1.0
Anion Exchange Chromarography	24	2.1	50.4	0.0254	0.6096	84	78	2.4
Gel Filtration Chromatography	8	3.4	27.2	0.011	0.088	306	42	8.7

Anion exchange was resulted in 78 % activity recovery and 2.4-fold purification for CATPO catalase (Table 3.2) and 64 % activity recovery and 1.9-fold purification for CATPO phenol oxidase (Table 3.1) respectively. The difference in the recovery and purification fold values between two activities of the enzyme can be due the higher sensitivity of the catalase. Without performing dialysis after anion exchange, activity assays were performed activity assays were performed in fractions containing 0.3 M NaCl, which might affect the observed enzyme activity (Sutay, 2007).

At the end of gel filtration, 42 % activity recovery and 8.7-fold purification was observed for CATPO catalase (Table 3.2) and 43 % activity recovery and 8.9-fold purification for CATPO phenol oxidase (Table 3.1), respectively. These results are as expected and support the above suggestion for the NaCl sensitivity of the catalase, but not the phenol oxidase activities.

3.3 Oxidation of Phenolic Compounds by CATPO

The oxidation of 14 different phenolic compounds by CATPO and the oxidation products were analyzed by RP-HPLC (Shimadzu SIL-20AHT). Reactions were performed in methanol-potassium phosphate (2:3 v/v) buffer for 1 h at 60 ^{o}C, which were determined as the best conditions for the detection of products.

The 14 phenolic compounds were selected according to their different chemistry and functionality. The molecular formulas of these compounds are given in Table 3.3. All the selected phenolic compounds are plant-derived antioxidants, even though these antioxidants may turn out to be pro-oxidants leading to oxidative stress, thus, becoming the cause of the generation of reactive oxygen species (ROS) in some cases (Heim *et al*., 2002). The oxidized forms of phenolics, such as the semiquinone radical or benzoquinone, have also been documented as a source of ROS (Heim *et al*., 2002). The oxidation of phenolic compounds and formation of oligomers or polymers could make phenolic compounds more stable. This type of a polymerization also could decrease the pro-oxidant/toxic effect of phenolics (Heim *et al*., 2002).

Several studies have reported that these phenolic compounds of plant origin have antimicrobial and antiviral activity besides their antioxidant potential. The *o*-quinones, the products of phenol oxidation, have been shown to possess antimicrobial activity (Lule and Xia, 2005). Some anthocyanidins has shown to be highly effective agents against both fungi and bacteria (Schutt and Netzly, 1991). These phenolic compounds effect on the growth of *S. thermophilum* was studied previously by Yüzügüllü (2010). Some phenolic compounds (catechol, hydroquinone, coumaric acid, myricetin) were indeed found to have a negative effect on growth. Some of them, like catechol, showed negative effect on growth only at high concentrations. Except catechol, the phenolics having negative effects on growth were not oxidized by CATPO.

The phenolic compounds, which had either no effect or a positive effect on growth, were recorsinol, vanillic acid, gallic acid, caffeic acid, chlorogenic acid, catechin, epicatechin, resveratrol, phenyllactic acid. Among these compounds, only in catechol, chlorogenic acid, catechin and caffeic acid distinct oxidation products were observed by HPLC, although a wider range of compounds appeared to be oxidized by previous spectrophotometric measurements (Yüzügüllü, 2010). In the spectrophotometric analysis of Yüzügüllü (2010), a number of different substrates such as catechol, *p*-hydroquinone, tyrosine, caffeic acid, gallic acid and tannic acid were used to analyze the catalytic properties of CATPO-phenol oxidase activity. According to the results, higher activities were observed with catechol, and caffeic acid, but tyrosine hydroxylation was not detected. This result exhibited the lack of cresolase activity. CATPO oxidized neither ABTS nor guaiacol, which are known as laccase-specific substrates (Burton, 2003). There was low catalytic activity observed on the *p*-diphenolic compound, hydroquinone. In the TLC analysis of Yüzügüllü (2010), catechol, hydroquinone, gallic acid, caffeic acid, chlorogenic acid, resveratrol and hydrobenzoin have shown to give oxidation products. In the color-change test of Söyler (unpublished data), a number of different substrates such as catechol, *p*-hydroquinone, caffeic acid, gallic acid, recorsinol, chlorogenic acid, vanillic acid, phenyllactic acid, quercetin and catechin were used to analyze the CATPO-phenol oxidase activity. According to the results, catechol, hyroquinone, chlorogenic acid, caffeic acid, gallic acid and L-DOPA have shown color changes in test tubes. The results of this study were not exactly consistent with previous studies reported by

Yüzügüllü (2010) and the unpublished data of Söyler. This could be due to the differences of applied methods during the analysis of phenol oxidation of different substrates by CATPO. In the spectrophotometric and TLC analysis of Yüzügüllü (2010), and color-change analysis of Söyler, culture-supernatant was used for oxidation analysis whereas in HPLC analysis two-step purified CATPO was used. On the other hand, in HPLC analysis 1 h oxidized phenolic compounds were analyzed, whereas in the color-change analysis and in the TLC analysis 24 hs oxidized phenolic compounds were analyzed. Oxidation of phenolic compounds with culture-supernatant for 24 hs, could cause auto-oxidation and induce artificial oxidation product formation.

Epicatechin is an isomer of catechin but it was not oxidized by CATPO. This indicates that, CATPO shows stereospecificity on the substrates.

The common feature of catechol, catechin, caffeic acid and chlorogenic acid, which clearly resulted product peaks by HPLC, appears to be the presence of two hydroxyl groups in the *ortho-* position. This suggests that the phenol oxidase activity of CATPO requires the presence of two hydroxyl groups in the *ortho-* position, although this is clearly not the only criteria for oxidation to take place. The results also suggest that the range of phenolic compounds oxidized by CATPO is not limited to catechol, but larger MW polyphenolic compounds are also oxidized. Interestingly, all the 4 compounds oxidized by CATPO are well known for their strong antioxidant capacities (Andersan, 2006).

Table 3.3 Phenolic compounds biotransformation results and their structure
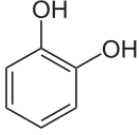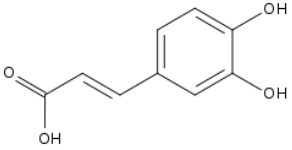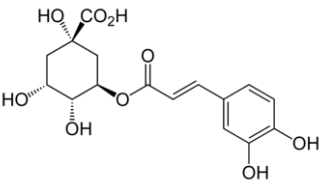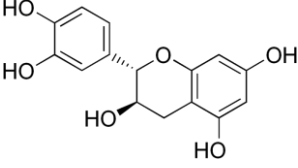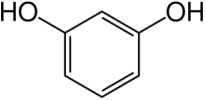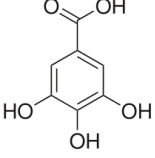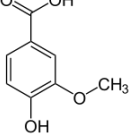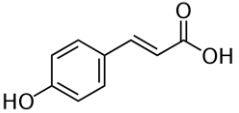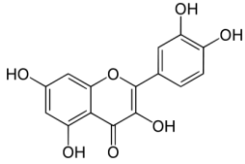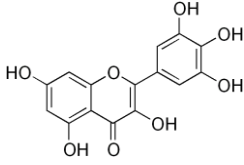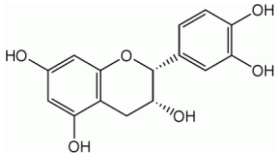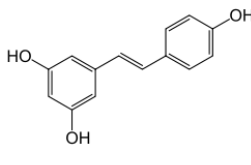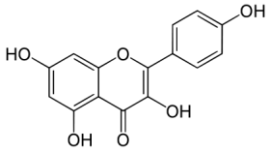
Phenolic Compounds (10 mM)	Structures	HPLC Results
Catechol		+
Caffeic acid		+
Chlorogenic acid		+
Catechin		+
Hdyroquinone		–
Resorcinol		–
Gallic acid		–
Vanillic acid		–
Coumaric acid		–

Table 3.3 Phenolic compounds biotransformation results and their structure (continued)

Phenolic Compounds (10 mM)	Structures	HPLC Results
Quercetin		–
Myricetin		–
Epicatechin		–
Resveratrol		–
Kaempferol		–

3.3.1 Oxidation of Catechol by CATPO

3.3.1.1 Analysis of the Standards and the Auto-oxidation of Catechol

Different concentrations (5, 10, 20 and 40 mM) of catechol solutions in methanol were prepared, injected and run on RP-HPLC, both to see the retention time of the catechol and areas of different concentrations on the chromatogram. Before running the HPLC, mobile phases (methanol, ddH$_2$O and acetonitrile) and samples were filtered through a 0.45 µm filter to avoid the plugging of the column. The chromatograms of different concentrations of catechol are shown below (Figure 3.4).

For all 4 phenolic compounds (catechol, caffeic acid, chlorogenic acid and catechin) the same method was used. The catechol peaks appeared at 15.7±0.1 min (Table 3.4).
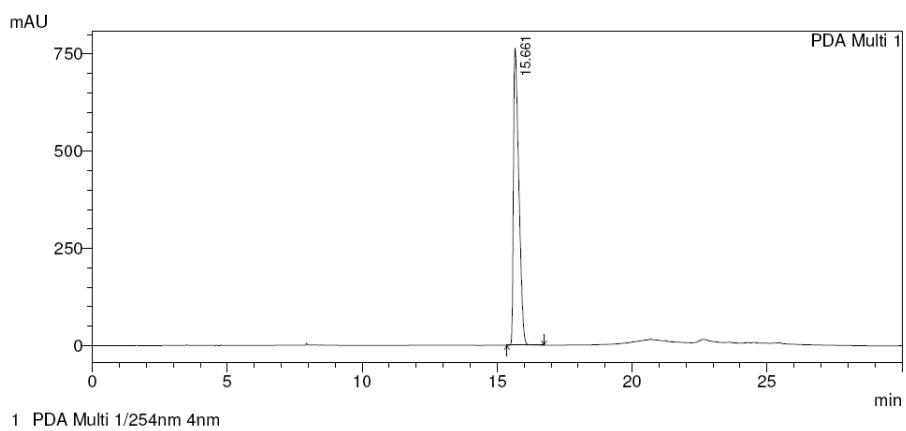
(a)
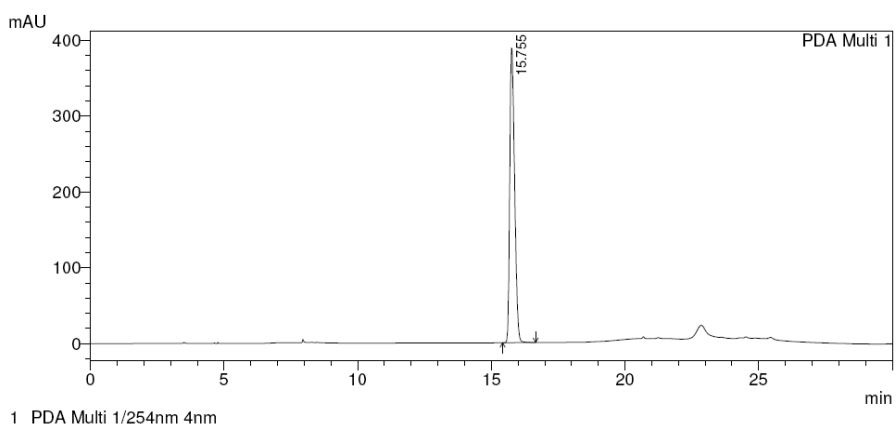
(b)
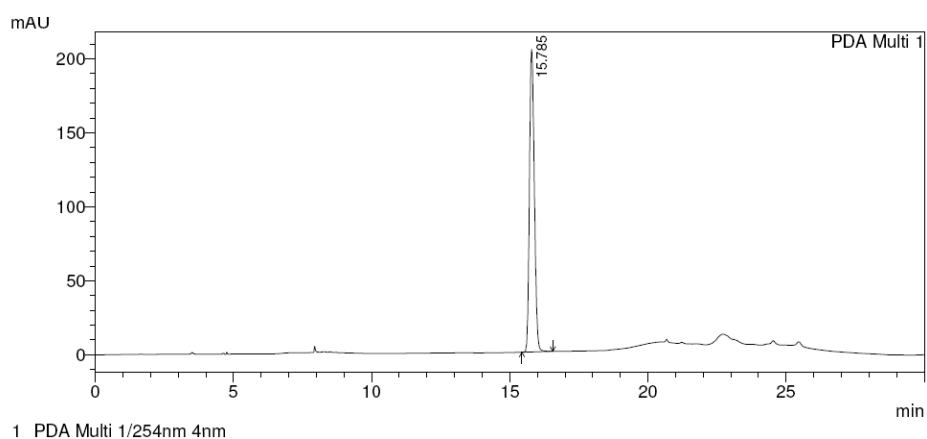
(c)

Figure 3.4 HPLC profile of (a) 40 mM, (b) 20 mM, (c) 10 mM and (d) 5 mM catechol in methanol
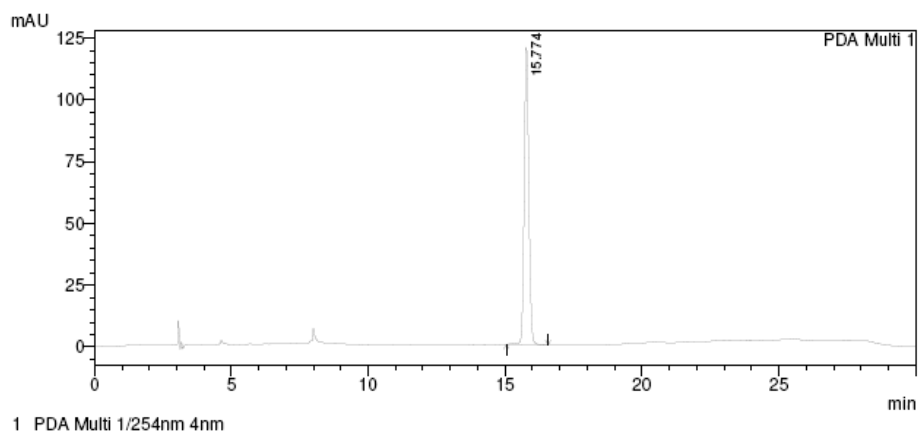
(d)

Figure 3.5 HPLC profile of (a) 40 mM, (b) 20 mM, (c) 10 mM and (d) 5 mM catechol in methanol (continued)

Table 3.4 Retention times and areas of 40, 20, 10 and 5 mM catechol

Figure	Ret.time (min)	Area Unit	Concentration (mM)
a (cat.)	15.661	10520505	40
b (cat.)	15.755	4902010	20
c (cat.)	15.785	2521512	10
d (cat.)	15.774	1402207	5

The calibration curve is a graph showing the response of an analytical technique to known quantities of an analyte and allows the determination of the concentration of an unknown sample. It can also be used to calculate the bioconversion value of the analyte after oxidation by enzymes. Here, different molarities of catechol were used as the standards. After reacting catechol with CATPO, these standards were used to calculate the concentration of catechol oxidized.

Based on these chromatograms for the different molarities of catechol, concentration versus area curve was drawn (Figure 3.5). The R^2 value of the linear correlation was

significantly high, proving the reliability of the standard curve for the catechol oxidation analysis.

The R^2 value of caffeic acid, chlorogenic acid and catechin were also calculated and listed on Appendix F.

Area Unit

Catechol Concentration (mM)
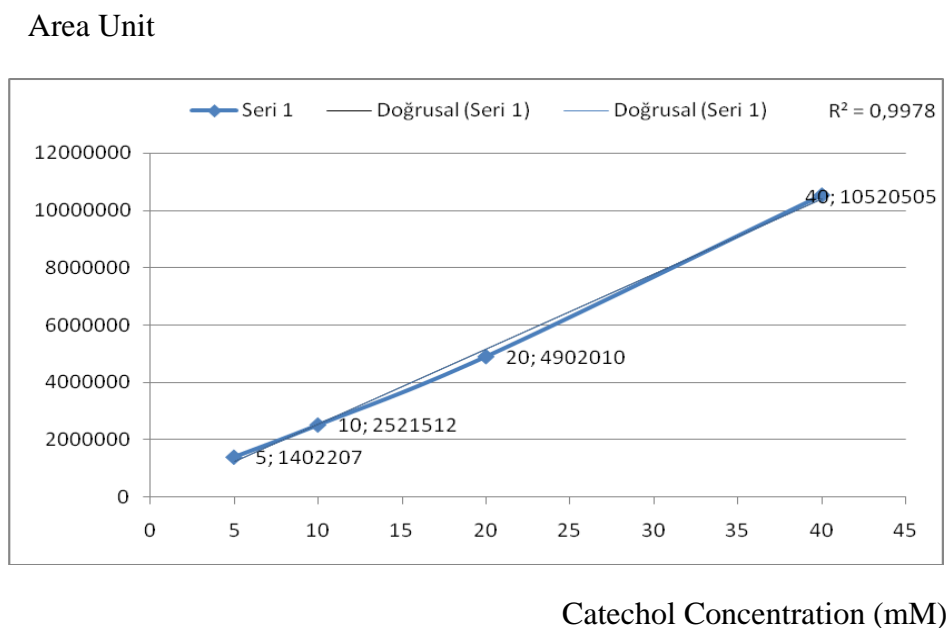
Figure 3.6 Area unit versus concentration curve of catechol of different molarities

To analyze the auto-oxidation of catechol 10 mM standard solution was incubated at 60 ºC from 10 min to overnight and analyzed by HPLC. Chromatogram that belongs to 1 h incubated catechol without enzyme can be seen below (Figure 3.6).
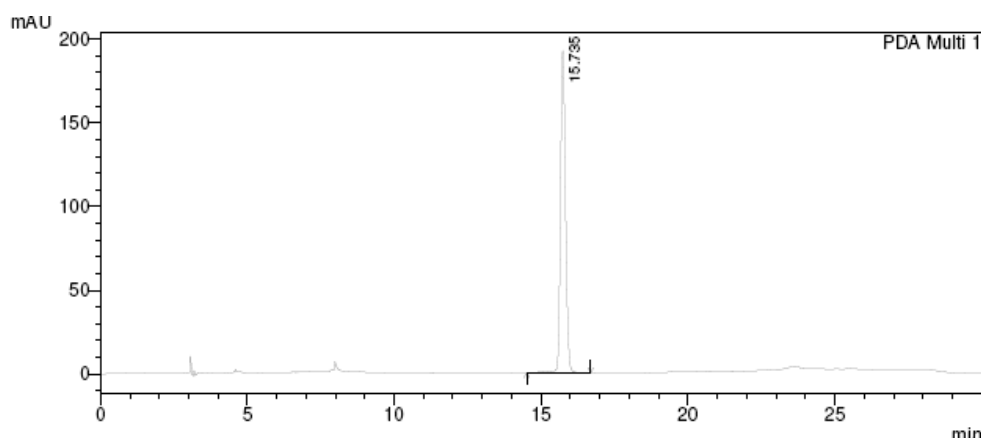
Figure 3.7 Catechol sample after 1 h incubation at 60 ºC

After 10 min, 30 min, and 1 h incubation, no auto-oxidation was seen but after 1 h catechol started to decompose (Appendix G), so in biotransformation assays 1min, 10 min, 30 min and 1 h incubated reaction mixtures were analyzed to avoid auto-oxidation. Also 24 hs oxidation of catechol by CATPO was analyzed to see the difference between the products profile and concentrations.

3.3.1.2 Analysis of the Oxidation Products of Catechol

3.3.1.2.1 Effect of Reaction Time on CATPO Catalyzed Oxidation Products of Catechol

The reaction mixture used for the oxidation of catechol by CATPO, was performed in methanol-potassium phosphate buffer (2:3 v/v) as described in section 2.6.2. Reaction mixtures were incubated at 60°C for 1 min, 10 min, 30 min, 1 h and 24 hs. Reactions were terminated with acetic acid (50 mM). Reaction products were analyzed by HPLC and stored at -20 $^{\circ}$C until LC-ESI-MS analysis.

Figure 3.8 HPLC profile of 10 mM catechol oxidized by CATPO (3.63U/µg) for 10 min at 60 $^{\circ}$C

Table 3.5 Retention times and areas of the reaction products of catechol oxidized by CATPO (3.63U/µg) for 10 min at 60 °C

Peak	Ret. Time (min)	Area (%)
1 (catechol)	15.8	83
2 (Pcat-1)	21.2	12
3 (Pcat-2)	24.2	5

At 1 min reaction, no product peak was detected. The lack of product peak can be due to the low yield of products. Thus, 1 min appears to be not sufficient to observe the oxidation products of catechol by HPLC. In the spectrophotometric analysis at 1 min reaction the conversion of catechol to quinones could be measurable but in HPLC to intercept the quinones is affirmative because of the very unstable structure of the quinones.

At 10 min reaction, two major oxidation products were detected, one at 21. 2 (Pcat-1) and another one at 24.2 min (Pcat-2) (Figure 3.8 and Table 3.5). The area percentage of the products indicate that the concentration of the Pcat-1 is higher than Pcat-2 at 10 min of the reaction. It is most likely that Pcat-1 is the first oxidation product and polarity of the Pcat-1 is higher than Pcat-2. The difference of the percentage of the areas of catechol at 1 min and 10 min, 100 % to 83 % respectively shows that 17% of the initial amount of catechol was oxidized by CATPO within 10 min.
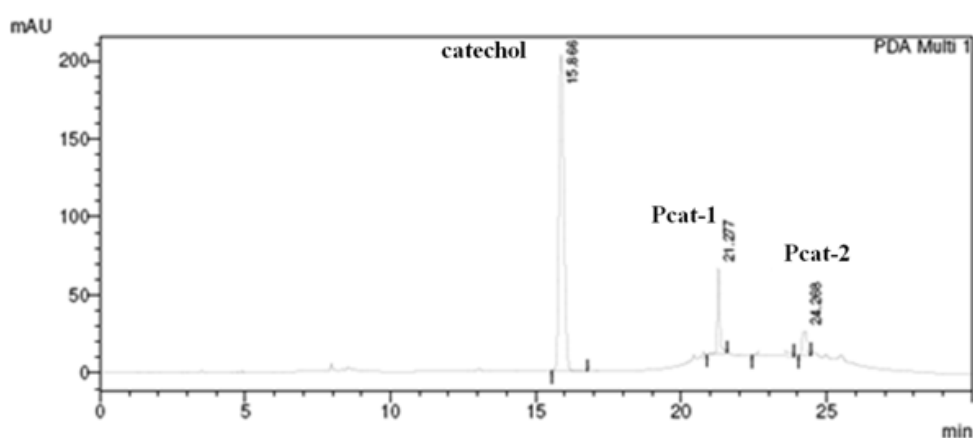
Figure 3.9 HPLC profile of 10 mM catechol oxidized by CATPO (3.63 U/µg) for 30 min at 60 °C

Table 3.6 Retention times and areas of the reaction products of catechol oxidized by CATPO (3.63 U/μg) for 30 min at 60 $^{\circ}$C

Peak	Ret. Time (min)	Area (%)
1 (catechol)	15.8	66
2 (Pcat-1)	21.2	20
4 (Pcat-2)	24.2	14

At the end of 30 min oxidation of catechol by CATPO at 60 $^{\circ}$C, again two major products were obtained, one at 21.2 min (Pcat-1), and the second one at 24.2 min (Pcat-2) (Figure 3.9 and Table 3.6). These two products are likely to be the same products observed at 10 min. Area percentage of catechol decreased from 83% to 66 % at 30 min, as expected. Area percentage of products P-cat-1 and P-cat-2 increased from 12 and 5 to 20 and 14 respectively.
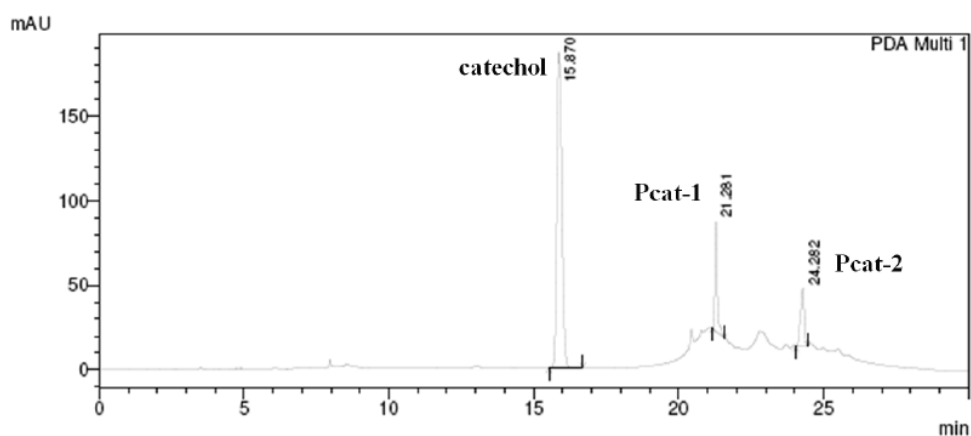
Figure 3.10 HPLC profile of 10 mM catechol oxidized by CATPO (3.63U/μg) for 1 h at 60 $^{\circ}$C

Table 3.7 Retention times and areas of the reaction products of catechol oxidized by CATPO (3.63U/µg) for 1 h at 60 ^{o}C

Peak	Ret. time	Area (%)
1 (catechol)	15.8	65
2 (Pcat-1)	21.2	25
3 (Pcat-2)	24.2	10

In the same way, two major fractions were observed at 21.2 (Pcat-1) and 24.2 min (Pcat-2) (Figure 3.10 and Table 3.7) from the oxidation of catechol by CATPO for 1 h at 60 ^{o}C. While the concentrations of Pcat-1 and Pcat-2 increased, catechol concentration decreased. The fact that the elution times of both products are higher than that of the catechol monomer suggests that these products have lower polarities than catechol.
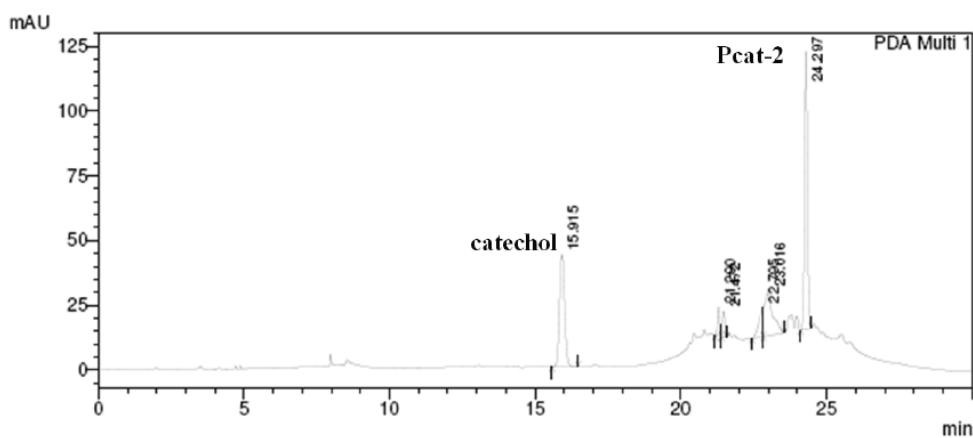
Figure 3.11 HPLC profile of 10 mM catechol oxidized by CATPO (3.63 U/µg) for 24 hs at 60 ^{o}C

67

Table 3.8 Retention times and areas of the reaction products catechol oxidized by CATPO (3.63 U/μg) for 24 hs reaction at 60 $^{\circ}$C

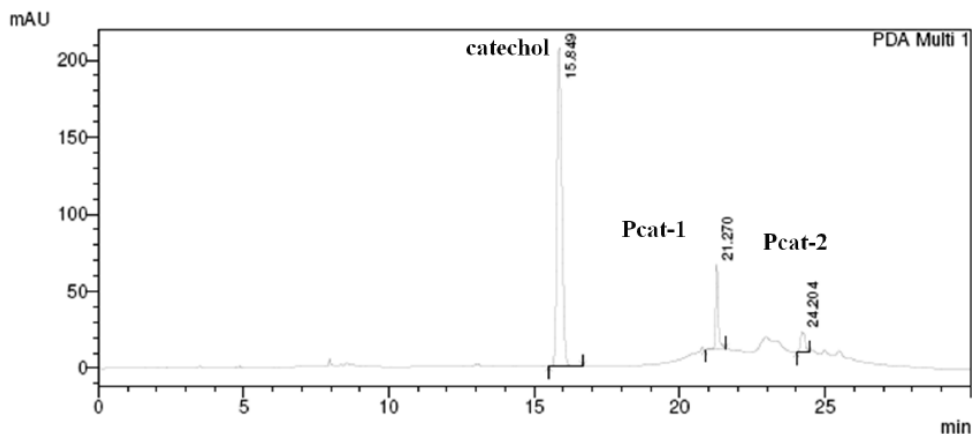| Peak	Ret. Time (min)	Area (%)
1 (catechol)	15.9	28
2 (Pcat-1)	21.2	3.4
3 (Pcat-3)	21.4	3
4 (Pcat-4)	22.7	6
5 (Pcat-5)	23.0	18.6
6 (Pcat-2)	24.2	40

After 24 hs, five major oxidation products were identified (Figure 3.11 and Table 3.8). Pcat-1 and Pcat-2 are the common products at 10 min, 30 min, 1 h and 24 hs. At the beginning of the reaction, the area percentage of the Pcat-1 increased 0% to 23% until 1 h, but then decreased to 3.4 % at 24 hs. Area percentage of Pcat-2 was 40% at 24 hs reaction, where it was 10 % at 1 h and 4% at 30 min reactions. After Pcat-2, no other products were observed on the chromatogram at any time of the reactions. This result indicates that Pcat-2 is the most stable product and has the lowest polarity and among the products.

Pcat-3, Pcat-4 and Pcat-5 were only seen at 24 hs reaction. The previous studies on auto-oxidation of phenolic compounds, as described in section 3.2.1.1, showed that, catechol undergoes auto-oxidation at 24 hs. Therefore, it is not certain that these products are the enzyme-catalyzed products.

3.3.1.2.2 Effects of Initial Catechol Concentrations on CATPO Catalyzed Oxidation Products of Catechol

For analysis of initial catechol concentration on the CATPO catalyzed oxidation of products 10^{-2} mM, 10^{-1} mM, 1mM, 10 mM and 100 mM catechol were used. At catechol concentration lower than 10 mM no product formation was observed. This could be due to the very low concentration of catechol and oxidation products

inadequate to observe on HPLC. On the other hand, no color change could be observed in the tubes contain catechol lower than 10 mM. At 10 mM and 100 mM concentration of catechol. two major products were detected by HPLC. UV-Vis spectra of the products exhibited the same absorption profiles of Pcat-1 and Pcat-2 (Appendix G). Accordingly, altering the substrate concentration did not show a significant effect on product formation.

3.3.1.2.3 Effects of Methanol Concentration on CATPO Catalyzed Oxidation Products of Catechol

Aqueous organic solutions (such as methanol) play an important role in enzymatic polymerization of poly-aromatics because the reactant monomer and the product polymer are usually poorly soluble in aqueous solvents such as water. In 0-10 % (v/v) methanol, catechol could not dissolve properly. The maximum activity was observed at 10-60 % (v/v) methanol. Two major product peaks were observed in 10-60 % (v/v) methanol. UV-Vis spectra of the products exhibited the same absorption profiles of Pcat-1 and Pcat-2 Altering the methanol concentration 10 % to 60 % did not show any innovation in the product formation.

3.3.1.2.4 Effects of Medium pH on CATPO Catalyzed Oxidation Products of Catechol

The highest activity was observed at pH 7 for both phenol oxidase and catalase activity. CATPO-phenol oxidase was most active between pH 7-8, retaining c. 80 % of its activity at pH 8 and preserved only c. 25% of its activity in the pH range of 6-7 (Sutay *et al.*,2007). Two major product peaks were observed at pH 7. UV spectrum of these products showed same absorption feature as Pcat-1 and Pcat-2. Pcat-1 also was detected at pH 6 and pH 8, where Pcat-2 was not. This could depend on the decrease of CATPO activity and low concentration of product Pcat-2. At pH 5 and pH 9, none of the product peaks could be observed (Appendix G).

3.3.1.2.5 Effect of Temperature on CATPO Catalyzed Oxidation Products of Catechol

Relative activities were over 70 % between 30-75 °C for catalase and between 55-75 °C for phenol oxidase having the maximum activity at 60 °C for both activities (Sutay *et al.*,2007). At 60 °C two major product peaks were observed by HPLC. Whereas at 50 ^{o}C and 70 ^{o}C only one product peak could be observed with a UV-Vis spectrum similar to Pcat-1 (Apppendix G). At 40 ^{o}C and 80 ^{o}C none of the product peaks were detected.

3.3.1.2.6 Effect of Enzyme Concentration on CATPO Catalyzed Oxidation Products of Catechol

1 μg, 10 μg and 100 μg enzyme solution in potassium phosphate buffer was analyzed. Pcat-1 and Pcat-2 were detected on HPLC for each of the reaction (Apppendix G).

3.3.1.3 UV-Vis Spectrum Profile of Oxidation Products of Catechol Catalyzed by CATPO

Ultraviolet-Visible spectroscopy refers to absorption spectroscopy or reflectance spectroscopy in the ultraviolet and visible spectral region between 200-800 nm. UV-Vis spectra uses light in the visible and adjacent ranges. UV-Vis spectroscopy could be used in the quantitative determination of solutions of transition metal ions, highly conjugated organic compounds, and biological macromolecules.

In our studies, UV/Vis spectrophotometer was used as a detector for HPLC. The presence of catechol gave a response assumed proportional to the concentration. For accurate results, the instruments' response to catechol in the unknown was compared with the response to a standard, similar to the use of calibration curves.

The wavelengths of absorption peaks are correlated with the types of bonds in a given molecule and are valuable in determining the functional groups within a

molecule. The nature of the solvent, the pH of the solution, temperature, high electrolyte concentrations, and the presence of interfering substances can influence the absorption spectrum. Experimental variations such as the slit width (effective bandwidth) of the spectrophotometer will also alter the spectrum.

Unsaturated aromatic ring compounds absorb light in the 200 to 800 nm region. Compared to isolated multiple bonds, conjugated double bonds (C=C) in the oxidation products showed enhanced absorptivity and to a shiftin λ max over a wider range of wavelength. An unsaturated aromatic ring in a compound shows maximum absorbance near 261 nm, whereas carbon atom double-bonded to an oxygen atom: C=O exhibits maximum absorbance near 290 nm.

According to the literature, catechol exhibits very strong light absorption near 275 nm (Duncan *et al.,* 2004) (Figure 3.12). Pcat-1 exhibits very strong light absorption at 266 and weaker absorption at 290 nm, whereas Pcat-2 at 253, 293 and 311 nm (Figure 3.13 and Figure 3.14 respectively). These data are the clues of the change on structure of catechol by oxidation. UV spectrum results cannot give detailed information about the functional groups of the analytes as the IR spectra. However, it is a convenient method to observe the difference between the chemistry and concentration of catechol and its products as well as to compare the products of CATPO and laccase and tyrosinase oxidations (section 3.4 and 3.5).
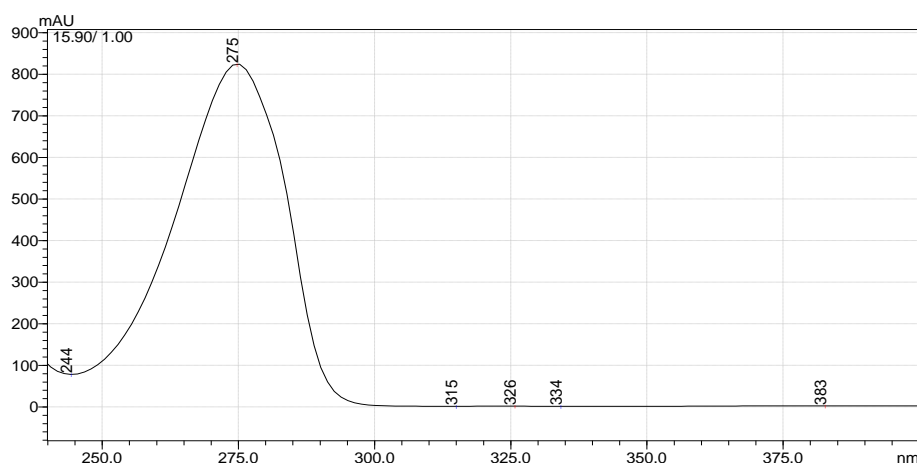
Figure 3.12 UV-Vis spectra of catechol (lambda max at 275 nm)

71
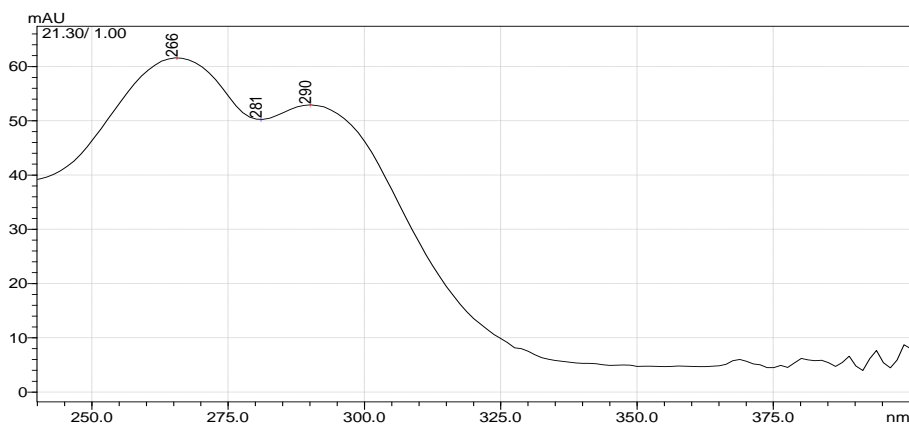
Figure 3.13 UV-Vis spectra of Pcat-1(lambda max at 266 nm and 290 nm)
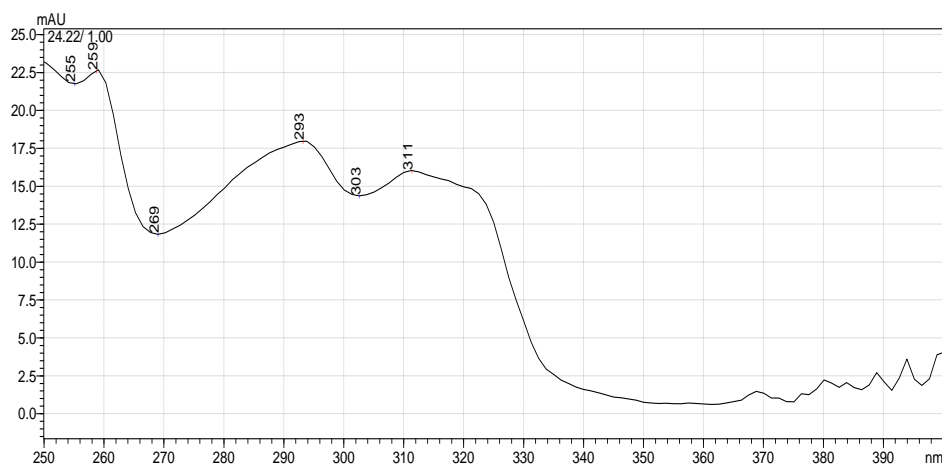
Figure 3.14 UV-Vis spectra of Pcat-2 (lambda max at 259 nm, 293 and 311 nm)

3.3.1.4 Analysis of the Oxidation Products with ESI/LC-MS

Mass spectrometers work by ionizing molecules and then sorting and identifying the ions according to their mass-to-charge (*m/z*) ratios. The LC-MS system used in this study is equipped with an Electrospray Ionization (ESI) source, which is used to produce ions. In contrast to the positive mode, under the negative mode, the phenolic compounds and their oxidation products could be ionized, due to the proton affinity of the samples. Therefore, the source was operated under the negative electrospray mode. The reaction mixture of catechol that was oxidized for 1 h at 60 $^{\circ}$C, was used in ESI-LC-MS analysis.
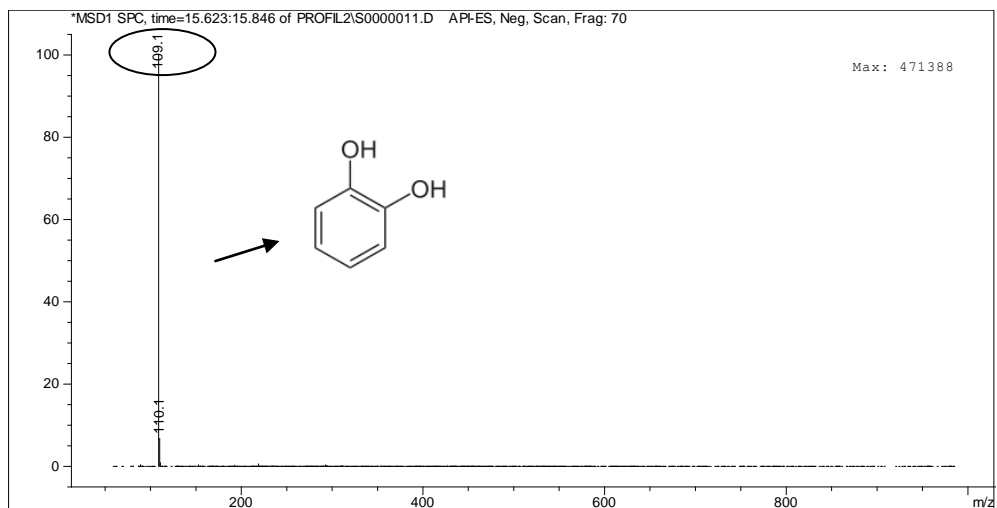
Figure 3.15 Mass spectra and molecular structure of un-reacted catechol RT: 15.8 min (base peak m/z ratio: 109)
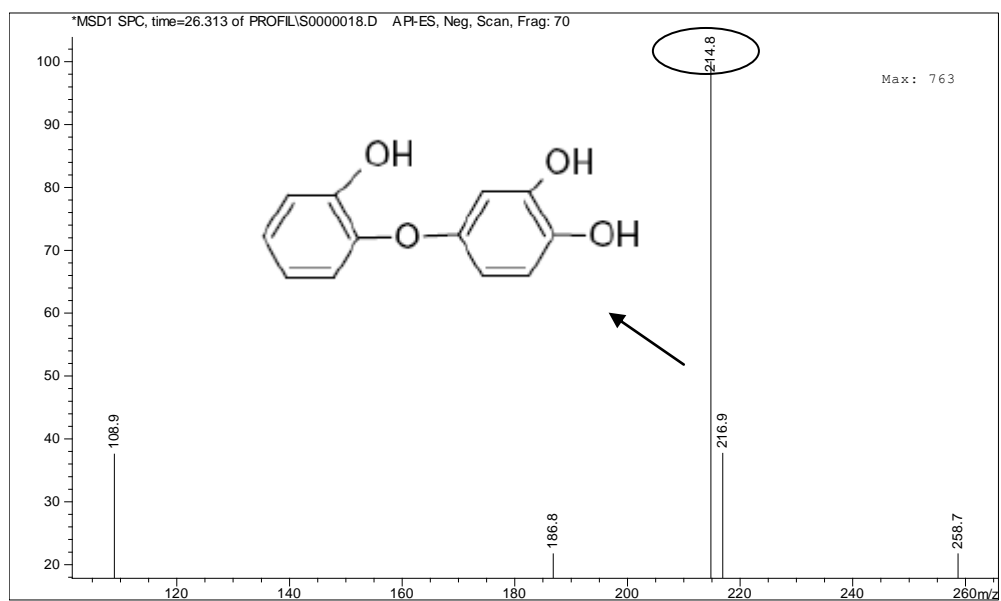
Figure 3.16 Mass spectra and suggested molecular structure of oxidation products at RT: 21.2 min (Pcat-1) (the base peak m/z ratio: 214.9)
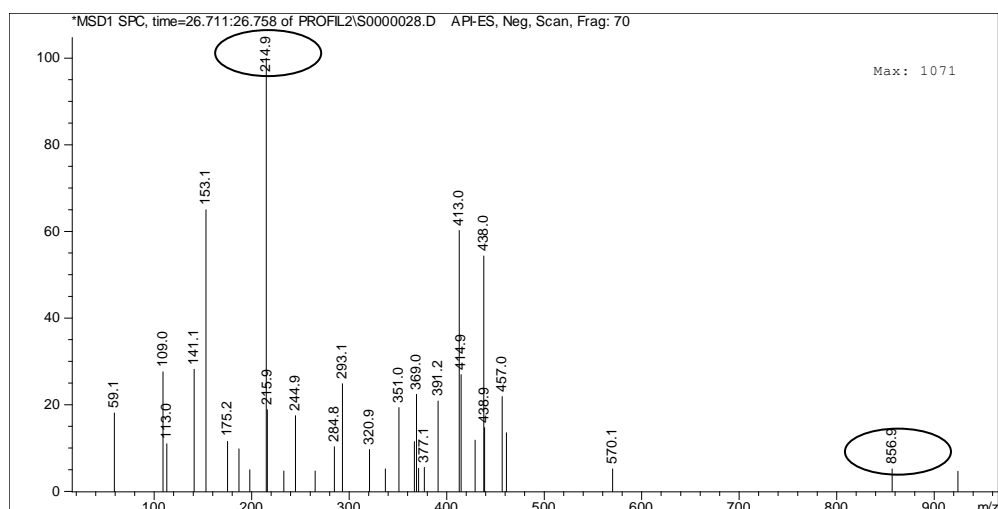
Figure 3.17 Mass spectra of oxidation product at RT: 24.2 min (Pcat-2) (the base peak m/z ratio: 214.9, the main peak m/z ratio: 856.9)

The peak with the retention time 15.8 min is un-reacted catechol (m/z = 109) (Figure 3.15). The LC-MS result verifies the HPLC observation and shows that there is still un-reacted catechol in the reaction mixture. The ESI/LC-MS spectra of major product fragments confirm the formation of oxidation products from catechol after 1 h reaction with CATPO. The peak with retention time 21.2 min (Pcat-1) is likely to be mainly a C-O-C dimer of catechol ([M-H]$^-$ with m/z 214.9) (Figure 3.16). Furthermore, ESI-MS spectra indicated the presence of oligomers with larger molecular mass ([M-H]$^-$ with m/z 856.9 (Pcat-2) (Figure 3.17). Fragmentation of the oligomers shows a similar dimer profile with a 214.9 molecular mass.

In the study of Smejkalova *et al*., (2006), oxidative polymerization of catechol was demonstrated with synthetic water-soluble iron-porphyrin used as an alternative to bio-labile natural peroxidase. The occurrence of both C-C and C-O-C coupling mechanisms were demonstrated separately. Three major product fractions (A, B and C) were detected during the HPLC analysis of Smejkalova *et al.,* (2006). These products had lower polarities and higher molecular weights than the catechol monomer, according to their retention times during analysis. The MS analysis indicated that, A, B and C had different retention times but the same molecular mass, showing that all the three products are catechol dimers with C-C coupling. In another study of Smejkalova *et al*. (2006), the occurrence of C-O-C bonding between

catechols was detected by NMR in the same system. Accordingly, it was suggested that free radicals of dehydrogenated catechol may occur in different resonance states (Figure 3.18) and that coupling reactions between the resonance forms (1+1), (1+2), (1+3), and (1+4) would result in C-O-C bonding (Figure 3.20) and formation of oxyphenylene units, while C-C coupling (Figure 3.19) and formation of phenylene units may be observed for the reactions between (2+2), (2+3), (2+4),(3+3), (3+4), and (4+4) (Smejkalova *et al.*, 2006).
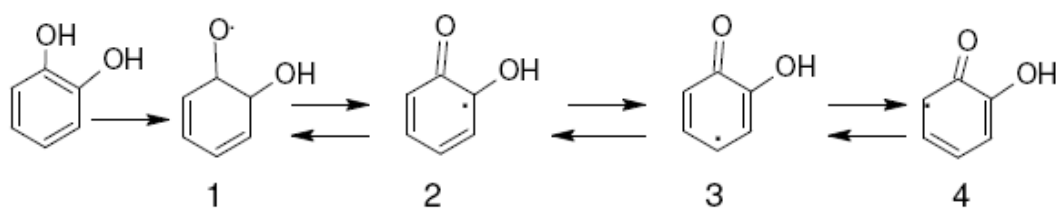
Figure 3.18 Resonance Structures 1-4 of Intermediate Radicals Generated during Iron-Porphyrin-Catalyzed Oxidation of Catechol (Smejkalova *et al.*, 2006)
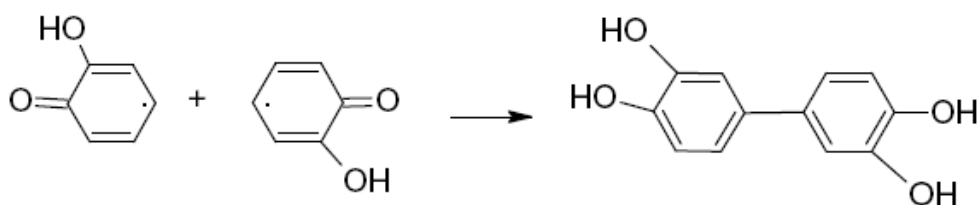
Figure 3.19 Suggested coupling reactions between some of the catechoyl radicals leading to the formation of C-C coupled dimers (Smejkalova *et al.*, 2006)
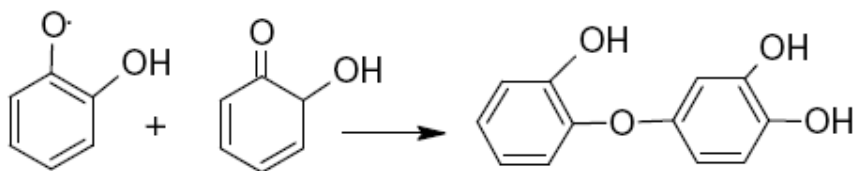
Figure 3.20 Suggested coupling reactions between some of the catechoyl radicals leading to the formation of C-O-C coupled dimers (Smejkalova *et al.*, 2006).

In another study, oxidative polymerization of catechol by horseradish peroxidase contain a heme cofactor in their active sites, was studied and the structure of the catechol polymers were analyzed by IR spectroscopy (Dubey *et al.*, 1998). According to the results, the polymer structure was suggested to be composed of a mixture of phenylene and oxyphenylene units, resulting in a complex polymer (Figure 3.21).
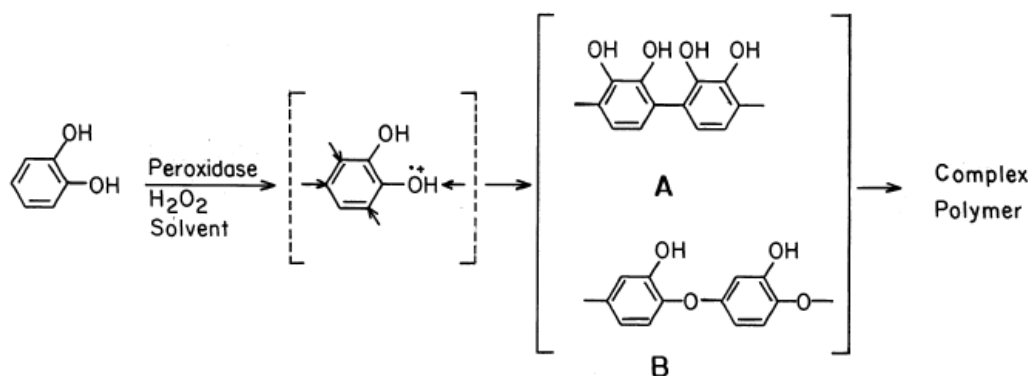
Figure 3.21 The proposed chemical structure of poly(catechol) catalyzed by peroxidase (Dubey *et al.,* 1998)

Enzymatic polymerization of catechol was also analyzed by Aktaş *et al.* (2003). In this study, polymerization of catechol was performed by using *Trametes versicolor* laccase. The molecular structure of the catechol polymers were determined by FT-IR. It was found that catechol units are linked together via phenyl-ether bonds (Figure 3.22)
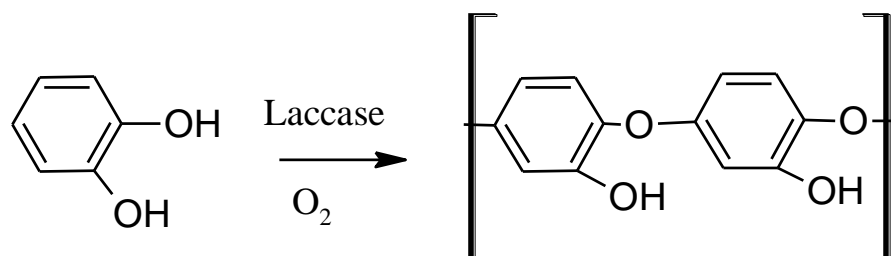
Figure 3.22 The proposed chemical structure of poly(catechol) catalyzed by laccase (Aktaş *et al.,* 2003)

In our study, as mentioned, two major products were observed (Pcat-1 and Pcat-2). LC-MS analysis of products Pcat-1 and Pcat-2 have indicated that, Pcat-1 is a dimer and Pcat-2 is an oligomer of catechol. This indicates that only one type of a dimer could be observed at the end of the 1 h oxidative polymerization of catechol by CATPO.

The data coming from the IR spectrum of CATPO catalyzed polymerization of catechol did not clearly indicate the formation of C-O-C phenyl ether bonds. However, the two broad peaks centered at 3450 cm^{-1} and 3325 cm^{-1} is due to phenolic O−H bonds on catechol are not clear on polycatechol spectrum due to the utilization of OH groups during polymerization. The FT-IR absorption bands of the product structure were limited compared to the catechol absorption bands. This is likely to be due to the more rigid structure of the product, compared to that of the catechol molecule itself (Aktas *et al*., 2003). Furthermore, the amount of catechol and product used in the preparation of the samples were not exactly the same, and this may have affected the results.

According to the HPLC, LC-MS and IR results, the oxidation of catechol by CATPO after 1 h reaction may be suggested to advance through the coupling reactions between the resonance forms (1+1), (1+2), (1+3), and (1+4), resulting in C-O-C bonding and the formation of oxy-phenylene units. The oxidation patterns of the other phenolic compounds and the data that came out of the oxidation of catechol by laccase also support this hypothesis.
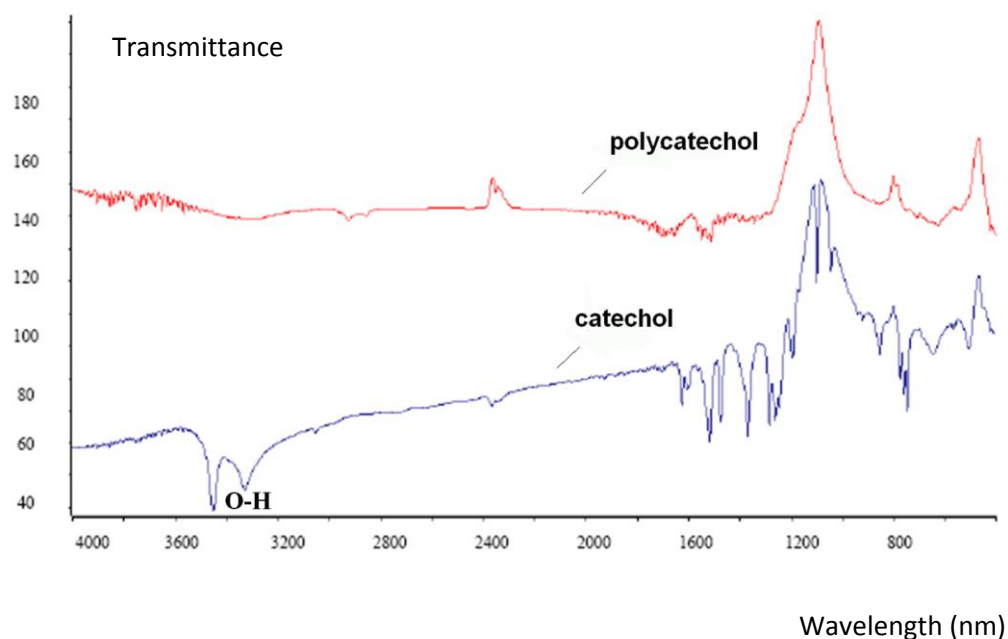
Figure 3.23 FT-IR spectra of catechol and polycatechol

3.3.2 Oxidation of Chlorogenic Acid by CATPO

3.3.2.1 Analysis of the Standard and the Auto-oxidation of Chlorogenic Acid

Different concentrations (5, 10, 20 and 40 mM) of chlorogenic acid solutions in methanol were prepared, injected and run on RP-HPLC, both to see their retention times and areas. Due to the retention times and areas of the chlorogenic acid, concentration curve was drawn (Appendix F). Only 10 mM chlorogenic acid chromatogram is shown in Figure 3.24-a to see the retention time of the phenolic compound. The chlorogenic acid peak appeared at 21.0 ± 0.1 min To analyze auto-oxidation, 10 mM chlorogenic acid in methanol-phosphate acid buffer was incubated for at 60 C^o for 1 h (Figure 3.24-b). Retention times and area values are shown on Table 3.9. Auto-oxidation until 1 h incubation was not observed.

(a)

(b)
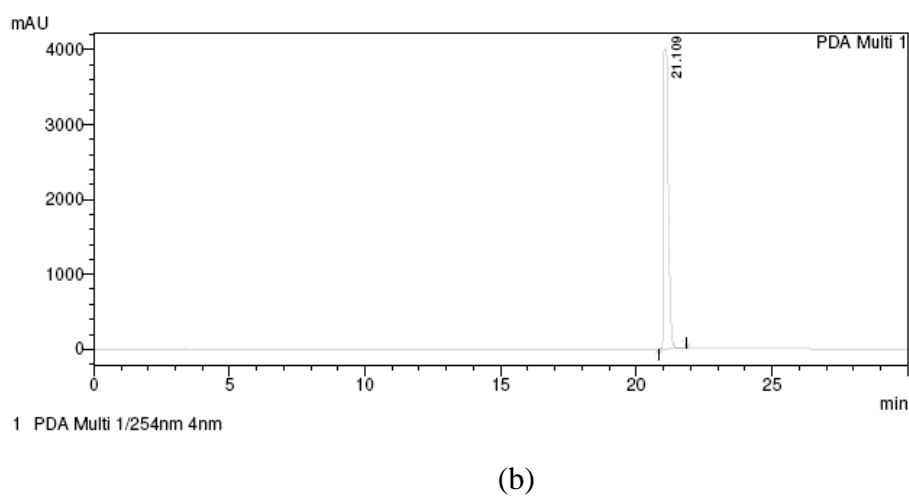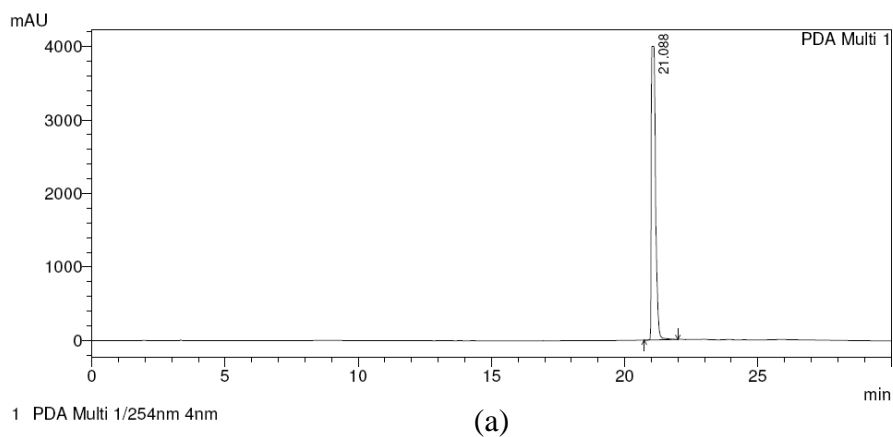
Figure 3.24 (a) 10 mM chlorogenic acid (b) Auto-oxidation assay

Table 3.9 Retention times and areas of Figure 3.18- and b

Figure	Retention Time	Area %	Concentration
a	21.08	100	10 mM
b	21.09	100	10 mM

3.3.2.2 Analysis of Oxidation Products of Chlorogenic Acid

The reaction mixture used for the oxidation of chlorogenic acid by CATPO was performed in methanol-potassium phosphate buffer as described in section 2.6.2. Reaction mixtures were incubated at 60°C for 1 h. Reactions were terminated with

acetic acid. Reaction products were analyzed by HPLC and stored at -20 ^{o}C until LC-MS analysis.
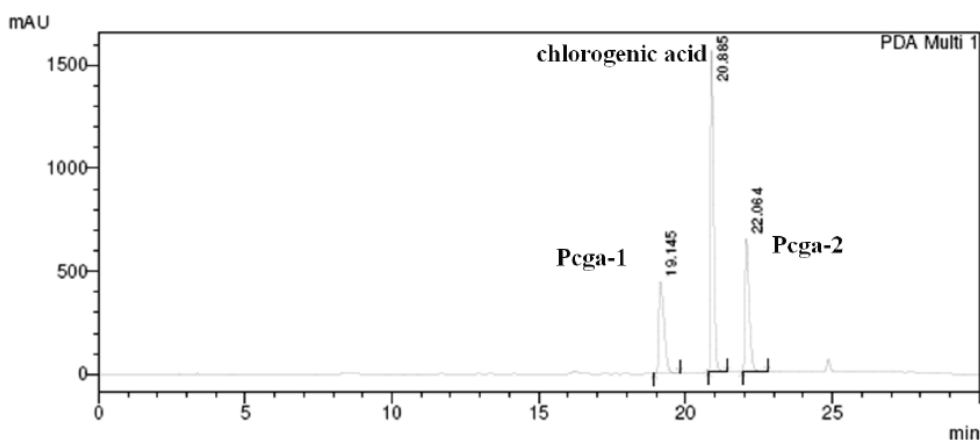
Figure 3.25 HPLC profile of 10 mM chlorogenic acid oxidized by CATPO (3.63 U/μg) for 1 h at 60 ^{o}C

Two major product fractions were observed (Figure 3.25) at 19.1 min (Pcga-1) and at 22.0 min (Pcga-2) (Table 3.10) from the oxidation of chlorogenic acid by CATPO for 1 h at 60 ^{o}C. Pcga-1 elution time suggested that this product has higher polarity than chlorogenic acid. On the other hand, Pcga-2 has lower polarity and than the chlorogenic acid.

Table 3.10 Retention times and areas of the reaction products of chlorogenic acid oxidized by CATPO for 1 h at 60 ^{o}C

Peak	Retention Time	Area %
1 (Pcga-1)	19.1	23.9
2 (chlorogenic acid)	20.8	48.5
3 (Pcga-2)	22.0	27.6

3.3.2.3 UV-Vis Spectrum Profile of Oxidation Products of Chlorogenic Acid Catalyzed by CATPO

Preliminary information on oxidation products was provided by UV-Vis spectra recorded during elution. Chlorogenic acid exhibits very strong light absorption near 290 and 326 nm as standards in literature (Figure 3.26) (Osman *et al.,* 2009). Pcga-1 exhibits very strong light absorption at 325 and weak absorption at 290 nm (Figure 3.27). Also, Pcga-2 exhibits very strong light absorption at 328 nm and weak absorption at 290 nm (Figure 3.28).
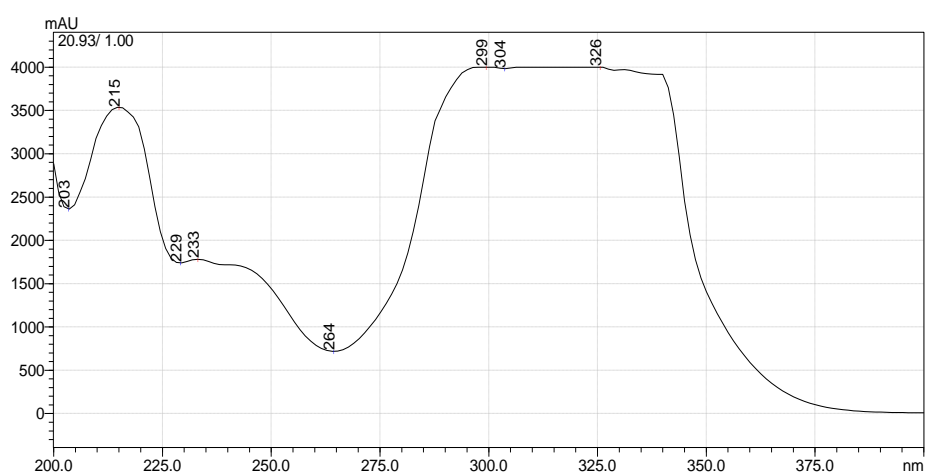
Figure 3.26 UV-Vis spectra of chlorogenic acid (lambda max. at 299 and 326 nm)
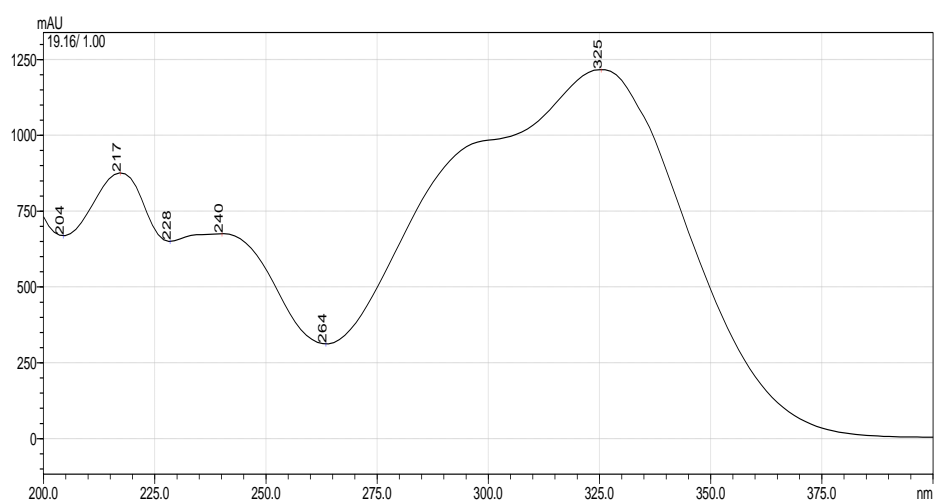
Figure 3.27 UV-Vis spectra of Pcga-1 (lambda max. at 325 nm.)
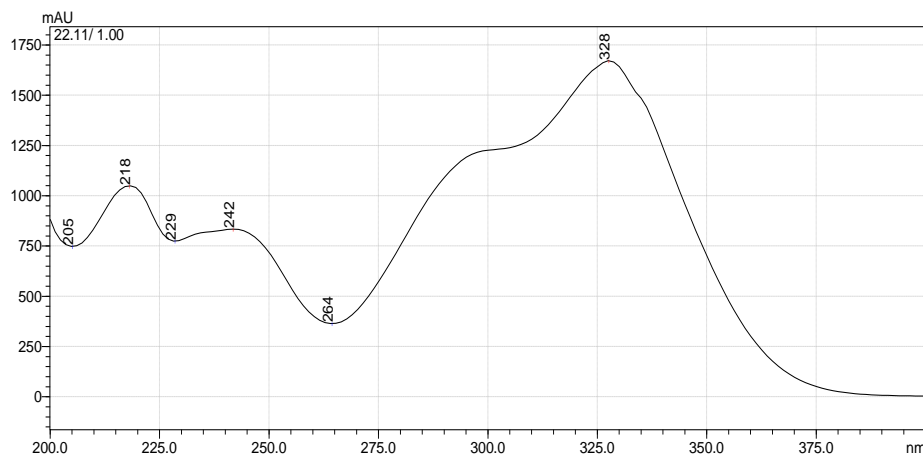
Figure 3.28 UV-Vis spectra of Pcga-2 (lambda max. at 328 nm)

3.3.2.4 Analysis of Oxidation Products with ESI/LC-MS

The reaction mixture incubated 1 h was run on ESI/LC-MS analyzer. The source was operated in negative electro-spray mode. After 1 h, reaction 2 major product peaks were identified and mass/charge ratios were found out.

Peak at retention time 19.1 min mass (Pcga-1) spectra gave m/z 353 which could depends on the stable radical of chlorogenic acid (Figure 3.30). The oxidation of *o*-diphenols such as chlorogenic acid, by polyphenol oxidases is known to proceed via the formation of *o*-quinones. Here, chlorogenic acid oxidation by CATPO may afford one types of dimer. Based on the evidence provided by the liquid chromatography-mass spectrometry (LC-MS) studies, dimerization of the chlorogenic acid was seen. However, this dimer might form through an O-O bond (Figure 3.29), although the possibility of C-C and C-O bonds cannot be ruled out. There is no any fragmentation product on the chromatogram during the MS analysis, so this make difficult to understand the bond between the monomers. The probable structures belongs to dimer of the chlorogenic acid was drawn appropriate to the literature (Osman *et al.*, 2009).

Peak at retention time 20.8 min show the un-oxidized chlorogenic acid monomer (m/z 354) (Figure 3.30). Peak 3 at retention time 22.0 min (Pcga-2) was identified as chlorogenic acid dimer (m/z 707) and sodium adduct (m/z 729) [M-H+Na]⁻ (Figure 3.32).
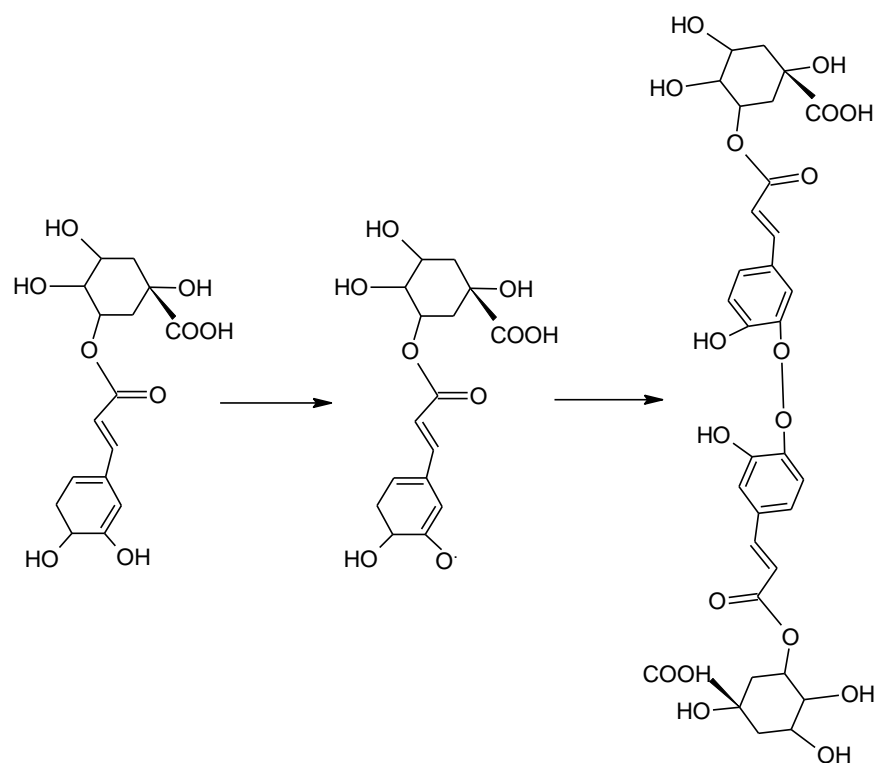
Figure 3.29 Putative, generalized oxidation pathway of chlorogenic acid leading to the formation of dimers (Osman *et al.,* 2009)
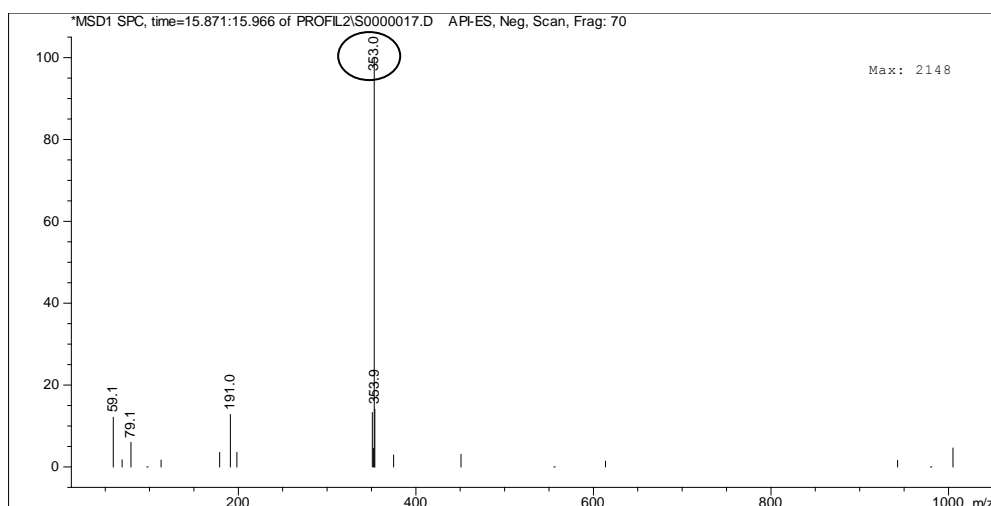
Figure 3.30 Mass spectra and molecular structure of chlorogenic acid keto-enol tautomerism RT: 19.1 (Pcga-1) (the base peak m/z ratio: 353)
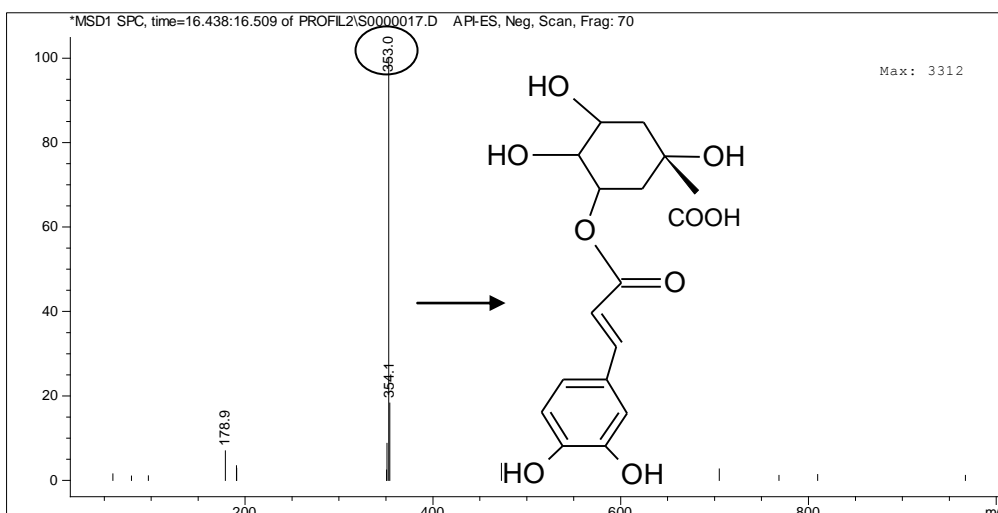
Figure 3.31 Mass spectra and molecular structure of un-reacted chlorogenic acid monomer at RT: 20.8 (the base peak m/z ratio: 353)
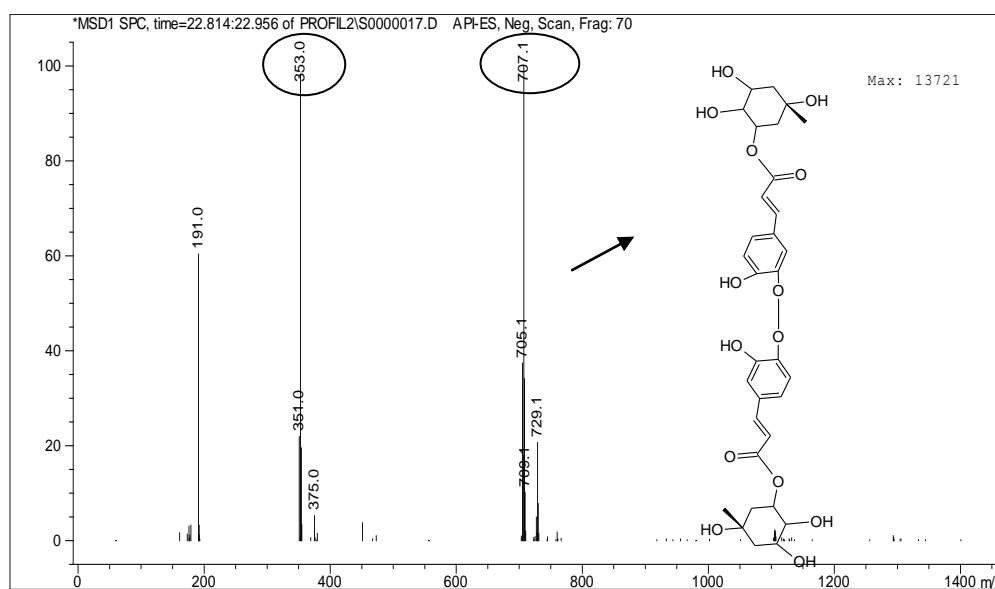
Figure 3.32 Mass spectra and suggested molecular structure of products at RT: 22.0 (Pcga-2) (the base peak m/z ratio: 707, the main peak m/z ratio: 353)

84

3.3.3 Oxidation of Catechin by CATPO

3.3.3.1 Analysis of the Standard and the Auto-oxidation of Catechin

As a standard, different concentrations (5, 10, 20 and 40 mM) of catechin were prepared in methanol, injected and run on RP-HPLC, both to see their retention times and areas. According to the retention times and areas of the catechin, concentration curve was drawn (Appendix F). Only the 10 mM catechin chromatogram is shown in Figure 3.33-a. Next, 10 mM catechin in methanol-potassium phosphate buffer was incubated at 60 C^o for 1 h to analyse auto-oxidation (Figure 3.33-b and Table 3.11), however, auto-oxidation was not observed.
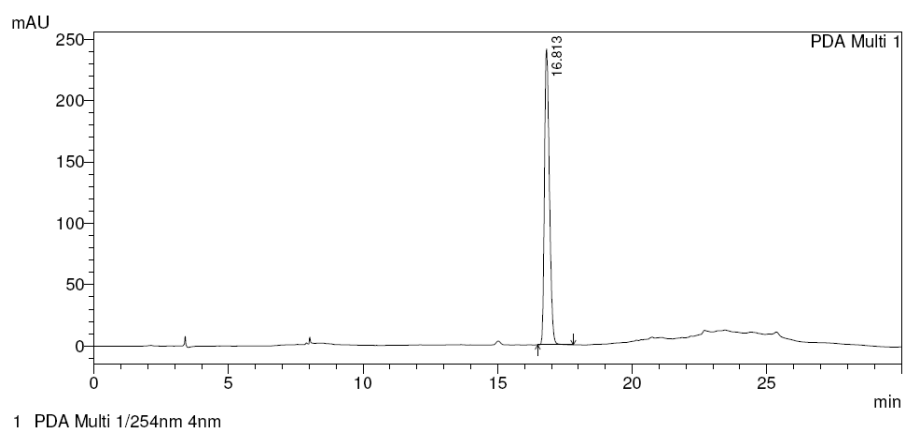
(a)
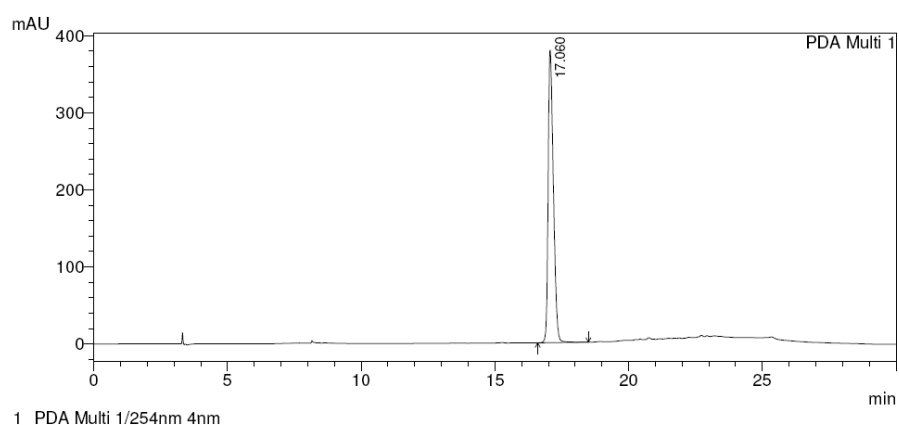
(b)

Figure 3.33 (a) 10 mM catechin (b) Auto-oxidation assay at 60°C and 1 h

Table 3.11 Retention times and areas of Figure 3.33- a and b

Peak	Retention time	Area %	Concentration
1	16.8	100	10 mM
2	17.0	100	10 mM

3.3.3.2 Analysis of the Oxidation Products of Catechin

The reaction mixture used for the oxidation of 10 mM (+)-catechin by CATPO contained methanol-potassium phosphate buffer, as described in section 2.6.2. Reaction mixtures were incubated at 60°C for 1 h and the reactions were terminated with acetic acid (50 mM). Products were analyzed by HPLC and stored at -20 °C until LC-MS analysis.

Four major product fractions were observed during the oxidation of catechin by CATPO (Figure 3.34). The incubation of CATPO with (+)-catechin gave rise to products of which one eluted earlier and others latter than the parent one. The hydrophilic product differs from hydrophobic ones in polarity.
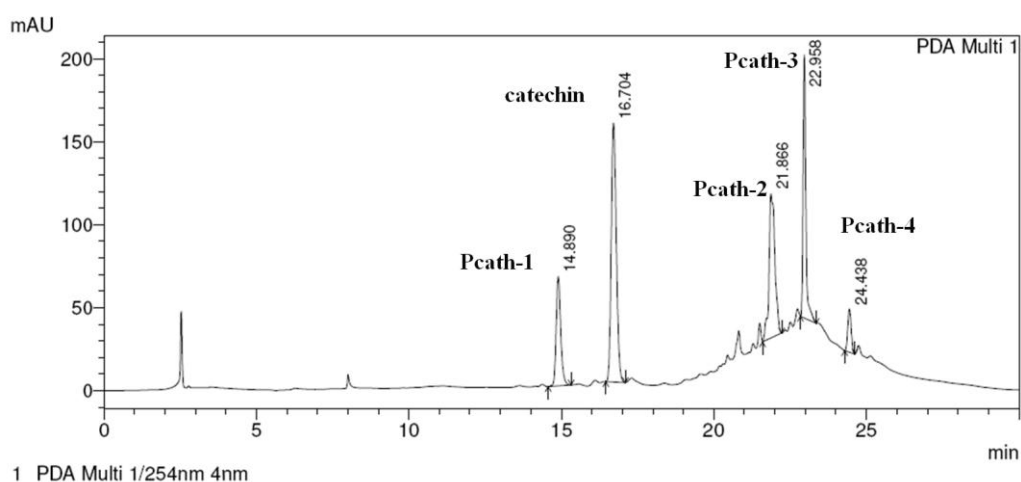
Figure 3.34 HPLC profile of 10 mM catechin oxidized by CATPO (3.63 U/μg) for 1 h at 60 °C

Table 3.12 Retention times and areas of the reaction products of catechin oxidized by CATPO for 1 h at 60 $^{\circ}$C

Peak	Retention time	Area %
1 (Pcath-1)	14.9	14.1
2 (catechin)	16.7	37.1
3 (Pcath-2)	21.8	24.2
4 (Pcath-3)	21. 9	20.2
5 (Pcath-4)	24.4	4.1

3.3.3.3 UV-Vis Spectrum Profile of Oxidation Products of Catechin Catalyzed by CATPO

Before LC-MS analysis preliminary information on oxidation products was provided by UV-is spectra recorded during elution. Catechin exhibits very strong light absorption near 279 nm. (Figure 3.35). The hydrophilic product differs from hydrophobic ones not only in polarity but also in its UV-Vis absorption spectra. Pcath-1 exhibited very strong light absorption at 279 nm (Figure 3.36) and Pcath-2, Pcath-3 and Pcath-4 exhibited very strong light absorbance around 400 nm (Figure 3.37). Similarities were observed in the spectral features of Pcath-2, Pcath-3 and Pcath-4, suggesting the presence of similar chromophores and/or structural analogies. Spectra relevant to compounds Pcath-1 showed different UV-Vis absorbance than the other, suggesting the structural differences. This difference could depend on the two type of dimers formation during oxidation of catechin as mentioned in section 3.3.3.4.
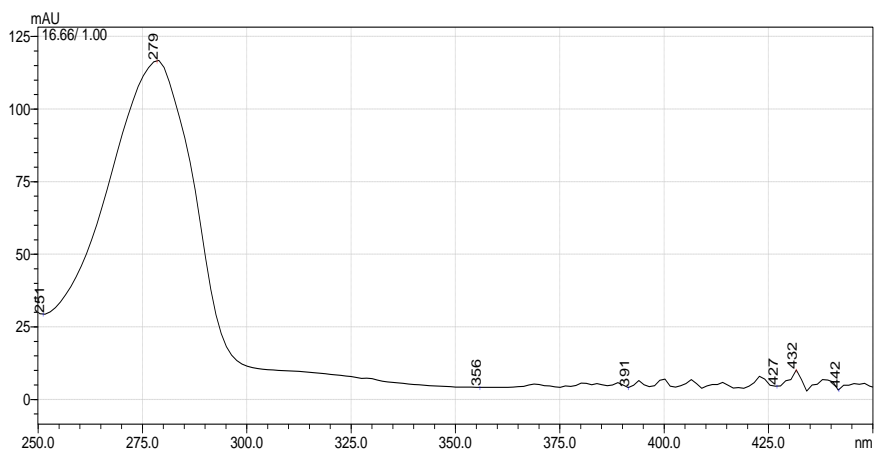
Figure 3.35 UV-Vis spectra of catechin (lambda max. at 279 nm)
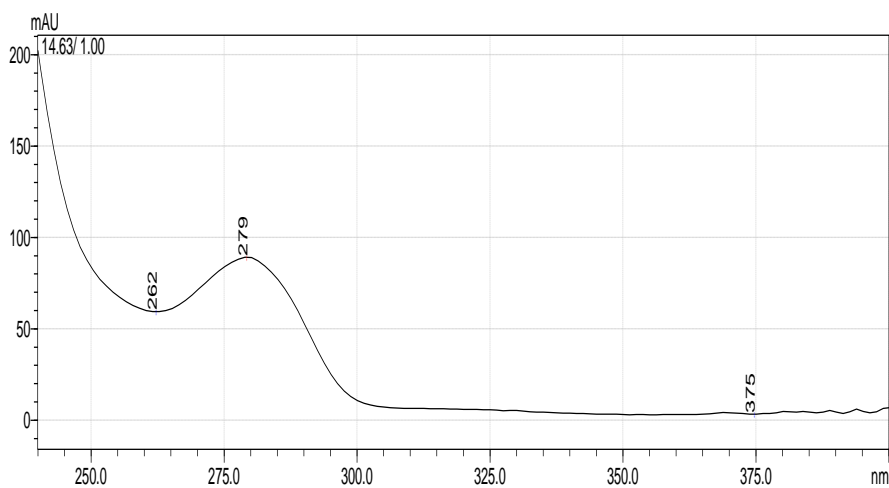
Figure 3.36 UV-Vis spectra of Pcath-1 (lambda max. at 279 nm)
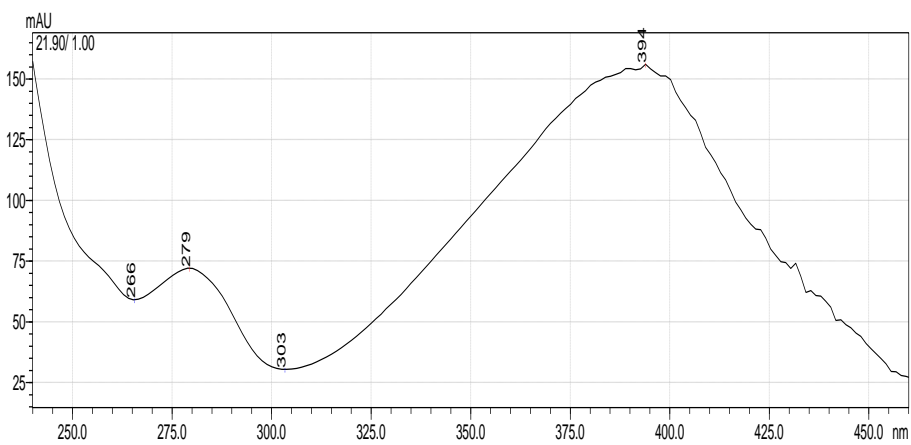
Figure 3.37 UV-Vis spectra of Pcath-2, Pcath-3 and Pcath-4 (lambda max. around 400 nm)

3.3.3.4 Analysis of the Oxidation Products of Catechin with ESI/LC-MS

The reaction mixture incubated 1 h was run on ESI/LC-MS analyzer. The source was operated in negative electro-spray mode. After 1 h, reaction 4 major product peaks (Pcath-1, Pcath-2, Pcath-3 and Pcath-4) were identified and mass/charge ratios were found out.

In the literature, two types of catechin dimers are characterized from the oxidation of catechin by laccase or other enzymatic systems. These are type A and type B dimers. Two mechanisms have been proposed for the formation of these type A and type B dimers: (a) nucleophilic addition of A-ring of a catechin to the B-ring of its oxidation product (the quinone) and (b) coupling of catechin radicals (Osman *et al.,* 2007).

The nucleophilic addition prevails at the higher pH on the other hand radical mechanism mainly occurs at values of pH below 4. In the latter case where CATPO optimum pH is 7, the yellow dimers of catechin are major products and this type of dimerization usually occurs between C8 of A-ring and C6' of the B-ring of an oxidized catechin unit. Studies by NMR done by researchers established the presence of this C8-C6' interflavin bond in the enzyme-catalyzed yellow dimers (Osman *et al.,* 2007). The yellow pigment color at pH 7 value suggests that the CATPO-catalyzed polymerization reaction proceeds principally by nucleophilic but not by radical mechanism. First, catechin is oxidized to semiquinone and *o*-quinone by enzymatic manner. Then, *o*-quinone reduced to hydrophilic dimer (type B dimer). Type B dimer enzimatically oxidized to the hydrophobic dimers (Figure 3.38). The conversion of dehydrocatechin B to type A (hydrophobic) is an oxidative intramolecular reaction (Figure 3.39). Once formed, the hydrophobic dimers are further oxidized by the enzyme to an o-quinone, which, most likely, condenses with catechin to form the reduced trimer and tetramer (Osman *et al.,* 2007).

Based on the ESI/LC-MS, hydrophilic dimer (type-B) (Figure 3.41), hydrophobic dimer (type-A) (Figure 3.42) and oligomers (trimer, tetramer and their oxidized forms froms) were detected (Figure 3.43 and Figure 3.44) according to their polarity on HPLC and mass/ratio on LC-MS.
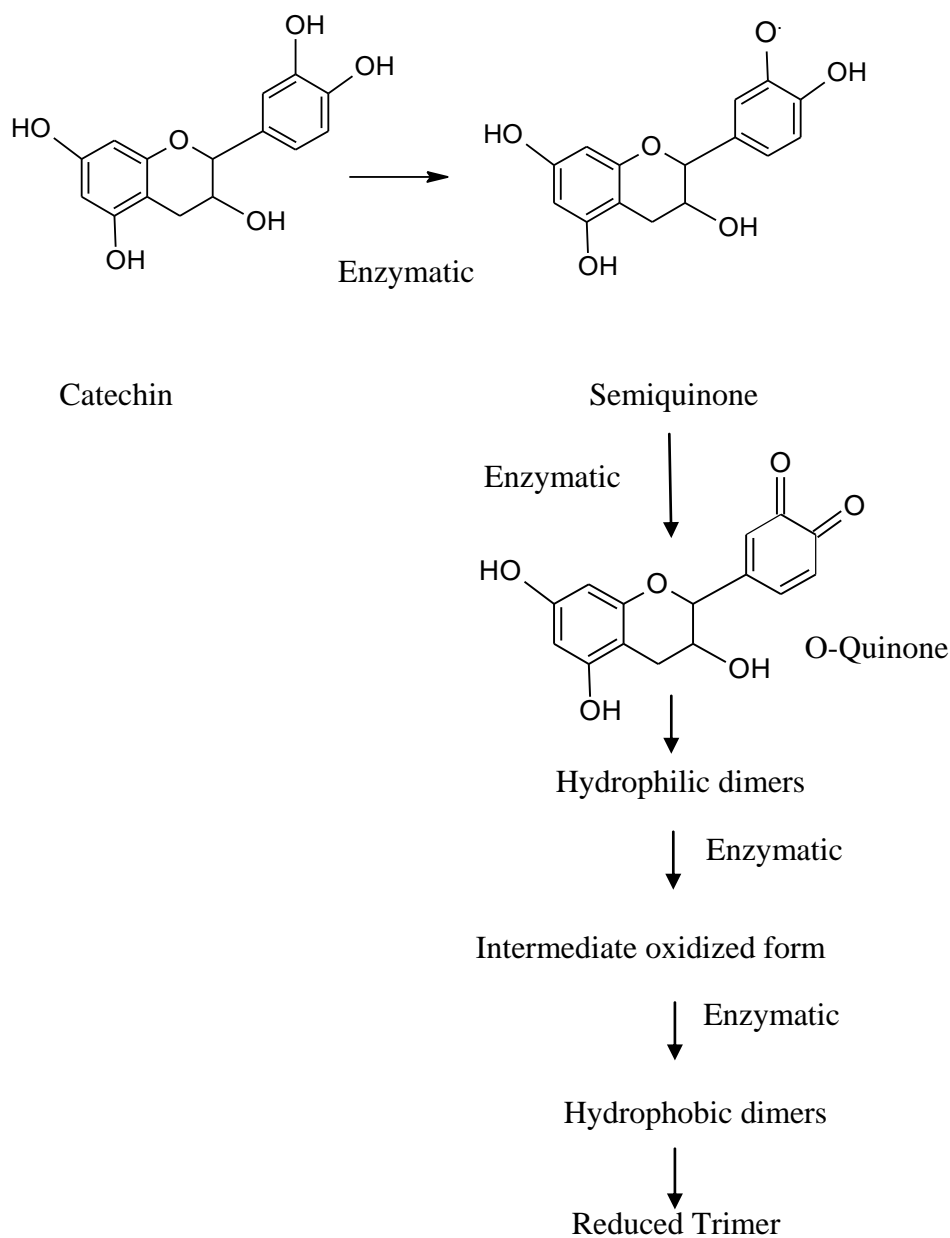
Figure 3.38 Figure illustrating the oxidation product formation pathway from catechin by enzimatically (Osman *et al.* 2007)
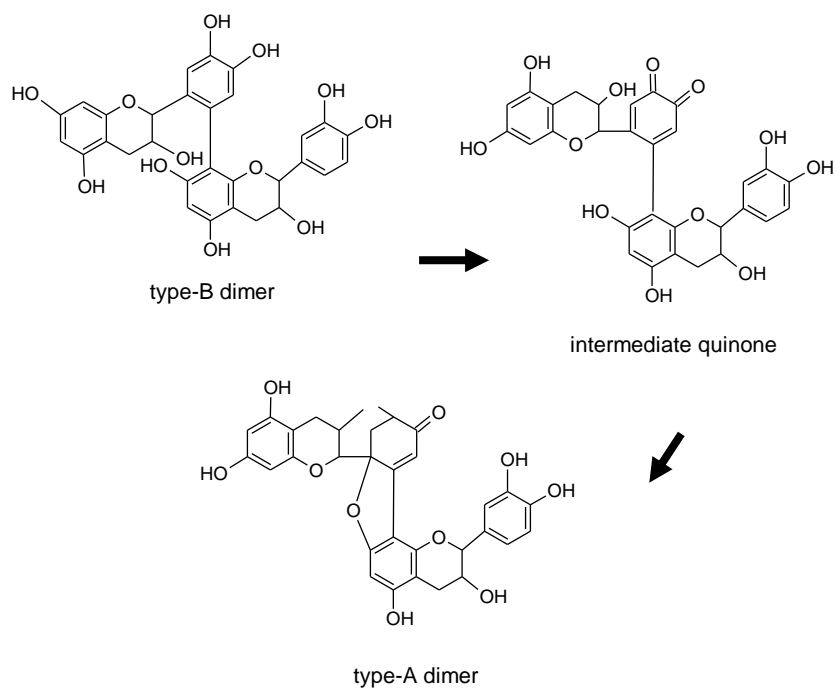
**Figure 3.39** Scheme illustrating the conversion of type-B dimer to type A-dimer (Osman *et al.,* 2007)
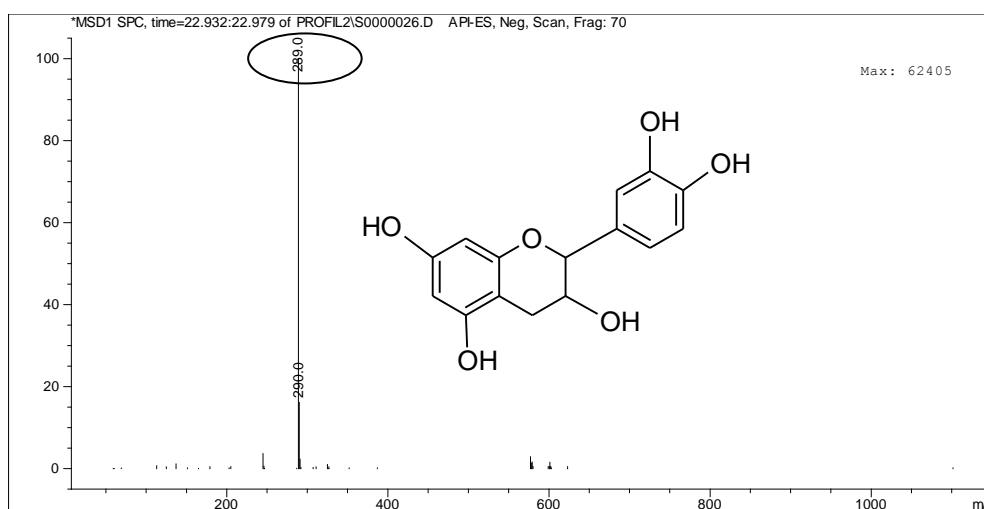
Figure 3.40 Mass spectra and molecular structure of un-reacted catechin monomer at RT: 16.8 (the base peak m/z ratio: 289)
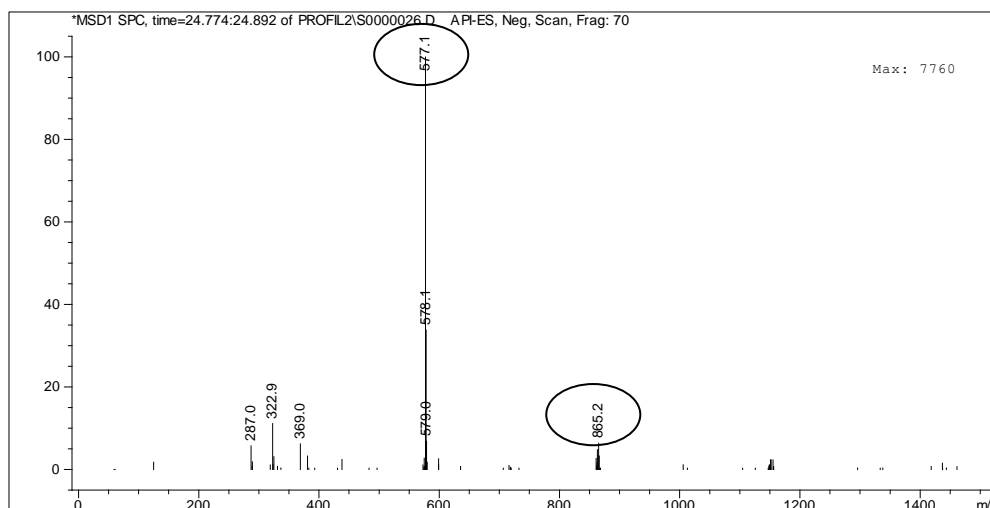
Figure 3.41 Mass spectra of hydrophilic dimer at RT: 14.9 (Pcath-1) (the base peak m/z ratio: 577) and trimer (m/z ratio: 865)
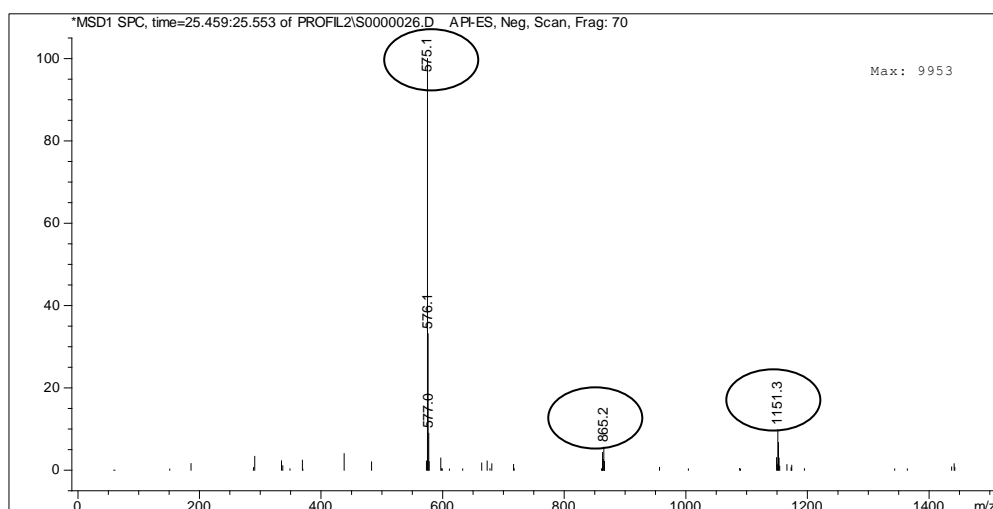
Figure 3.42 Mass spectra of hydrophobic dimer at RT: 21.8 (Pcath-2) (the base peak m/z ratio: 575) and trimer (m/z ratio: 865) and tetramer (m/z ratio: 1151)
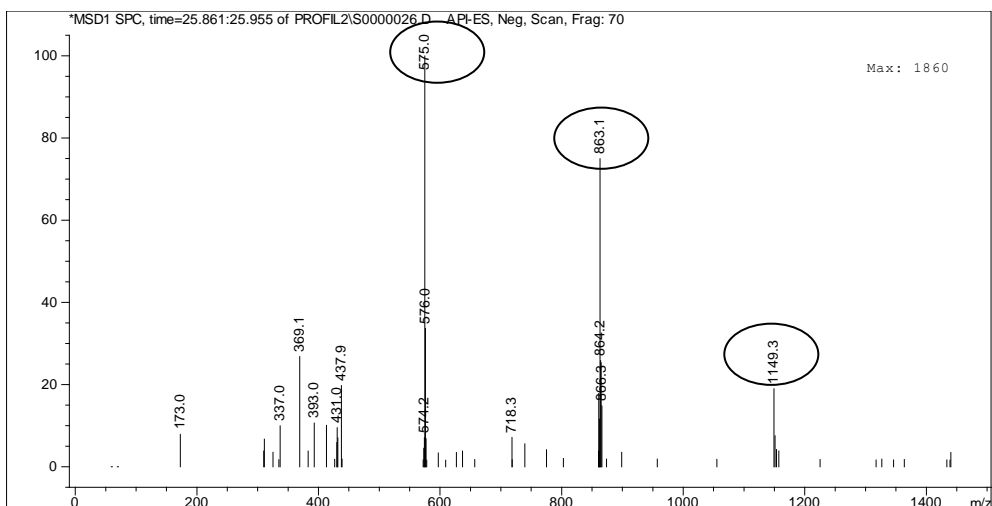
Figure 3.43 Mass spectra of hydrophobic dimer at RT: 21.9 (m/z 575) (Pcath-3); which most likely, condenses with catechin to form the reduced trimer (m/z 863) and tetramer (m/z 1149)
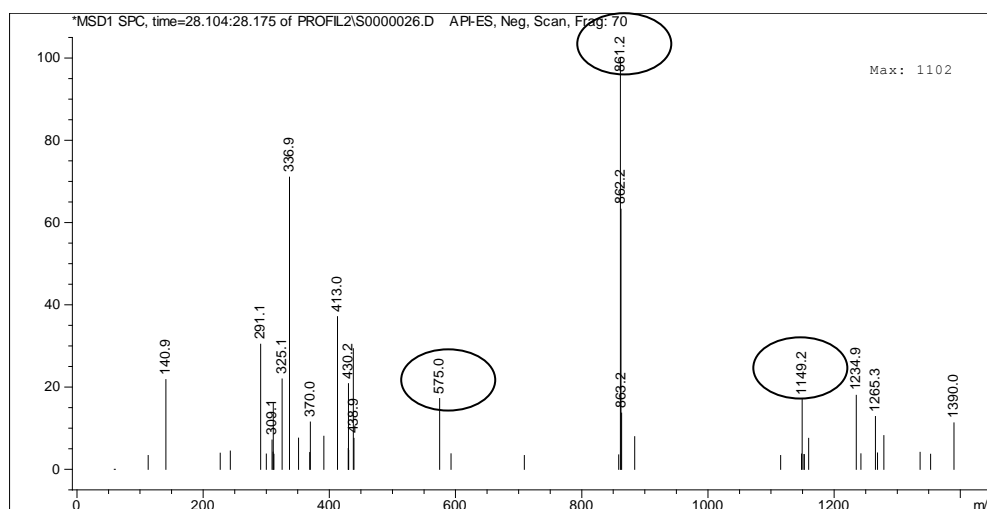
Figure 3.44 Mass spectra of the oxidized trimer RT: 24.4 (m/z 861) and tetramer (m/z 1149) (Pcath-4)

3.3.4 Oxidation of Caffeic Acid by CATPO

3.3.4.1 Analysis of the Standards and the Auto-oxidation of Caffeic Acid

As a standard, different concentrations (5, 10, 20 and 40 mM) of caffeic acid solutions in methanol were prepared, injected and run on RP-HPLC, both to see their

retention times and areas. Due to the retention times and areas of the caffeic acid, concentration curve was drawn (Appendix F). Only 10 mM caffeic acid chromatogram is shown in Figure 3.45-a to see the retention time of the phenolic compound. Also, to analyze if there can be an auto-oxidation at 1 h incubation, 10 mM caffeic acid in methanol-potassium phosphate buffer was incubated at 60 C^{o} for 1 h (Figure 3.45-b). Auto-oxidation was not observed during 1 h incubation.
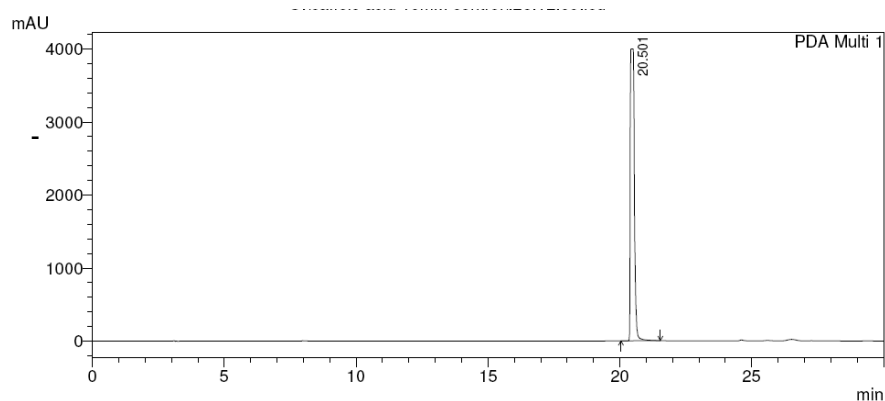
(a)
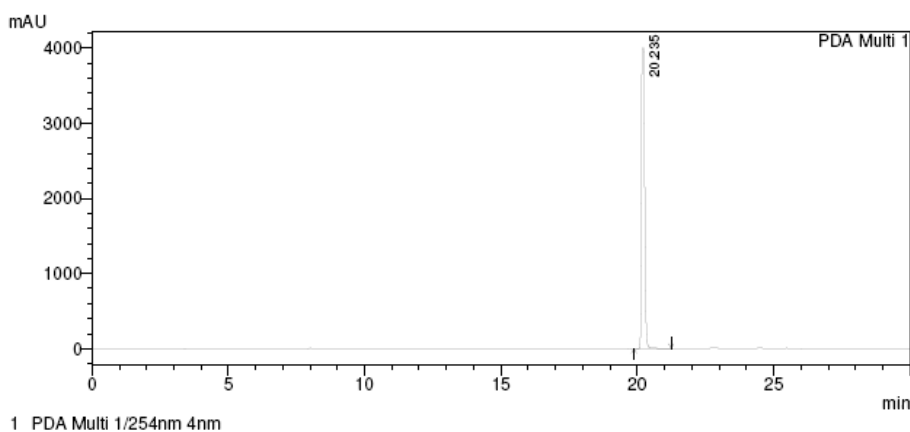
(b)

Figure 3.45 (a) 10 mM caffeic acid (b) Auto-oxidation assay at 60 ^{o}C for 1 h

Table 3.13 Retention times and area percentage of Figure 3.45 a and b

Peak	Retention time	Area %	Concentration
1	20.501	100	10 mM
2	20.235	100	10 mM

94

3.3.4.2 Analysis of the Oxidation Products of Caffeic Acid

The reaction for the oxidation of caffeic acid by CATPO was performed in methanol-potassium phosphate buffer, as described in section 2.6.2. Reaction mixtures were incubated at 60°C for 1 h and the reactions were terminated with acetic acid. Products were analyzed by HPLC and stored at -20 $^{\circ}$C until LC-MS analysis.

Two major product peaks were obtained from the oxidation of caffeic acid by CATPO (Figure 3.46). Elution of the oxidation products, after caffeic acid, indicated that all of them are less polar than caffeic acid itself.
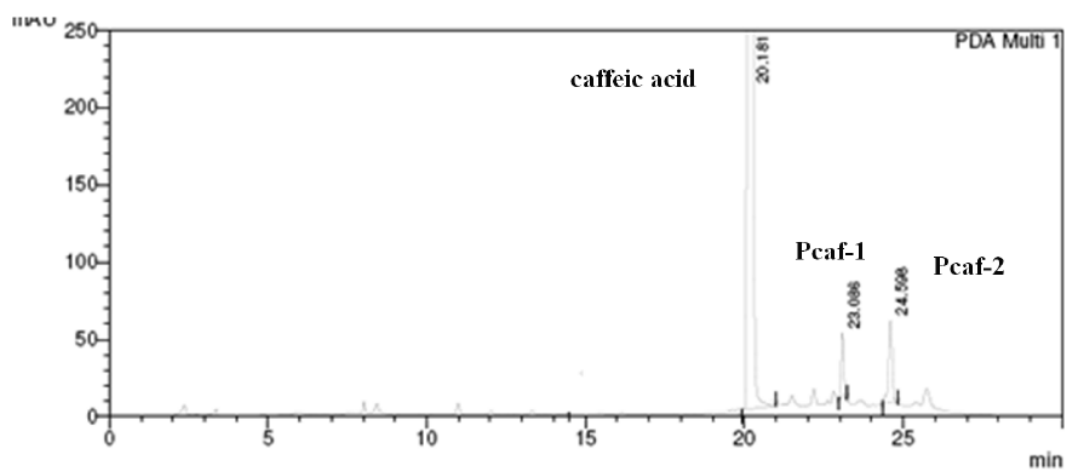
Figure 3.46 HPLC profile of 10 mM caffeic acid oxidized by CATPO (3.63 U/µg) for 1 h at 60 $^{\circ}$C

Table 3.14 Retention times and areas of the reaction products of caffeic acid oxidized by CATPO for 1 h at 60 $^{\circ}$C

Peak	Retention time	Area %
1 (caffeic acid)	20.1	72
2 (Pcaf-1)	23.0	14
3 (Pcaf-2)	24.5	16

3.3.4.3 UV-Vis Spectrum Profile of Oxidation Products of Caffeic Acid

Caffeic acid exhibits very strong light absorption near 297 and 324 nm (Pati *et al.,* 2006) (Figure 3.47).

Pcaf-1 and Pcaf-2 exhibited a spectrum similar to that of caffeicins (see section 3.3.4.4) with a different ratio between the absorbance at 288 and 319 nm, with respect to caffeic acid itself, suggesting a partial loss of the side-chain conjugation during oxidation (Figure 3.48).
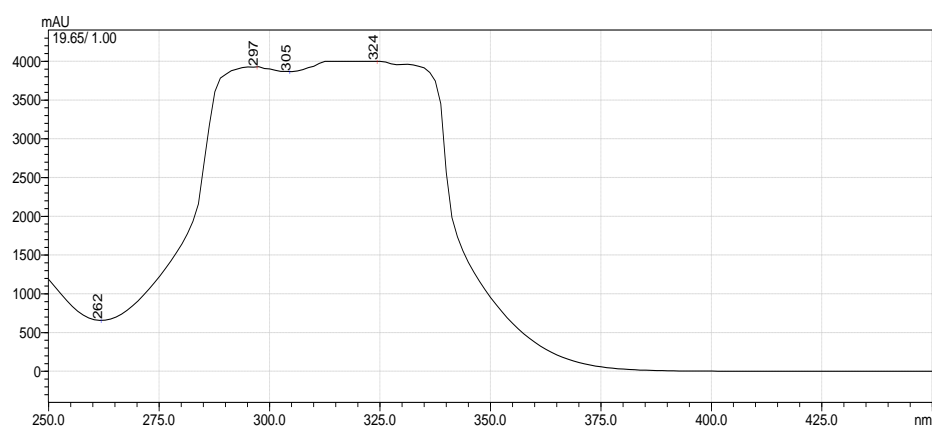
Figure 3.47 UV-Vis spectra of caffeic acid (lambda max. at 297 and 324)
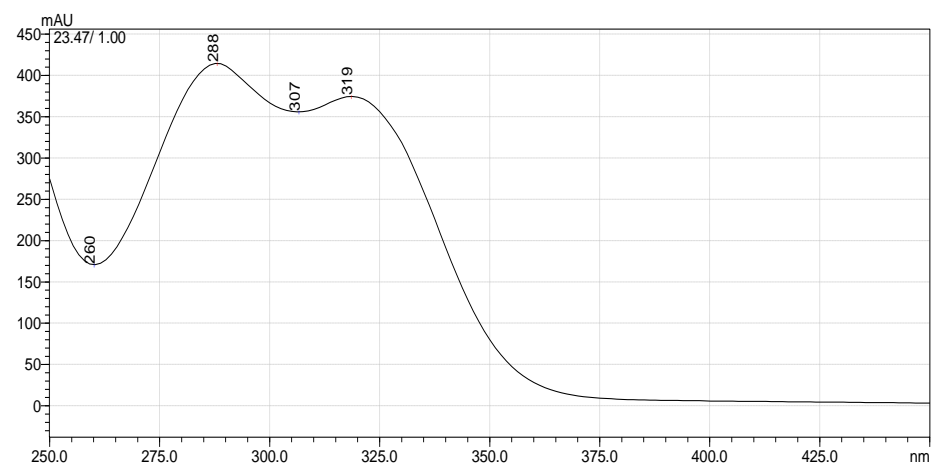
Figure 3.48 UV-Vis spectra of Pcaf-1 and Pcaf-2 (lambda max. at 288 and 319)

3.3.4.4 Analysis of the Oxidation Products of Caffeic Acid with ESI/LC-MS

In literature different types of dimer structures are defined (Pati *et al*., 2006) (Figure 3.49)

    a- 'Michael 1-4 type nucleophilic reaction in which the addition of a hydroquinone phenolic ring on a o-quinoneis occurred by leading of carbon-carbon linkage ('type a' structure)'

    b- 'After quinone rearrangement to quinone methide, nucleophilic addition of hydroquinone double-bond is occurred by leading to several couplings with the formation of ciclolignans derivatives ('type b' structure)'.

    c- 'Reverse disproportionation between quinone and hydroquinone provide generation of semiquinones radicals, which can then randomly couple and form different dimers through C-C ('type a' structure), ether ('type c' structure), C_α-C_α ('type b' structure), C_α-O ('type d' structure) coupling'.

    d- 'Polymerization involving side-chain hydroquinone double-bond and one or two hydroxyl groups of caffeic acid generating structures named caffeicins ('type d structure')'.

The mass spectra of caffeic acid oxidation products showed that after 1 h reaction Pcaf-1 is a caffeic acid dimer with m/z 312 (Figure 3.51) and Pcaf-2 is a caffeic acid tetramer with m/z: 715 (Figure 3.52). Pcaf-2 is also showed peaks at m/z ratio of 133, 179, 269, 313, and 359 (Figure 3.52), probably corresponding to the degradation of the tetramer and then dimer and losses of CO_2 and H^+. Peak m/z 133 probably corresponds to losses of the CO_2. Similarly, peak m/z 313 is likely to correspond to CO_2 losses of a dimer during LC-MS. Among all the possible caffeic acid dimers described in the literature, only caffeicin-like ones (type d structure Figure 3.49) can explain the observed fragments. Fragmentation is illustrated as Figure 3.53.
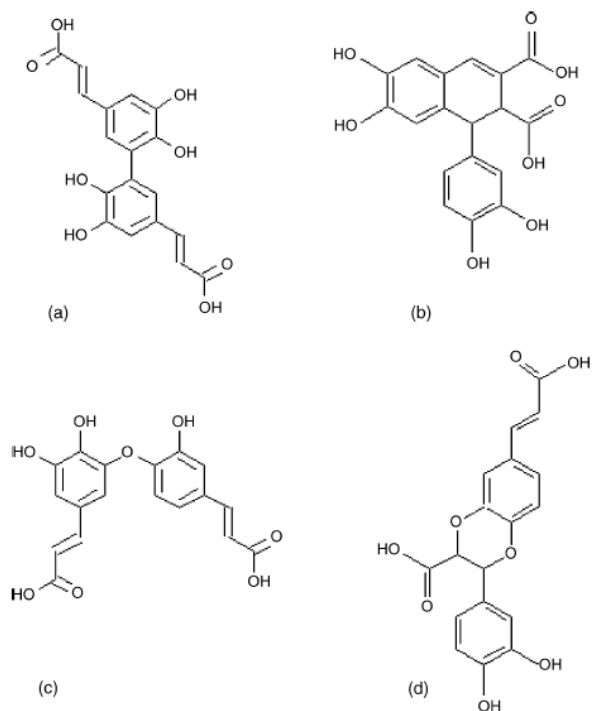
Figure 3.49 Representative structures for caffeic acid dimers proposed in the literature (Pati *et al*., 2006)
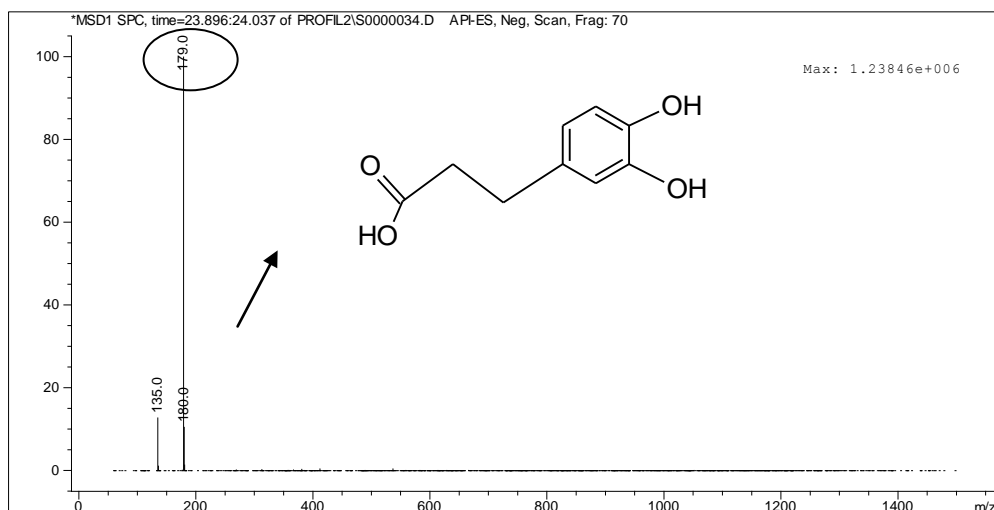
Figure 3.50 Mass spectra and molecular structure of un-oxidized caffeic acid at RT: 20.3 (the base peak m/z ratio: 179)
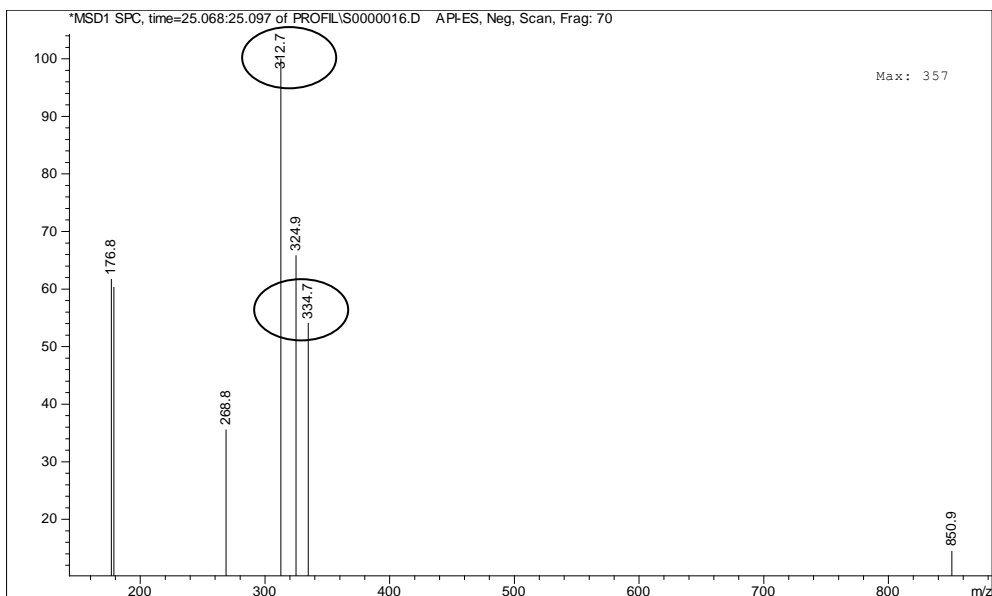
Figure 3.51 Mass spectra of products at RT: 23.0 (Pcaf-1) (caffeic acid dimer with 334 m/z ratio and formic acid lost fragment as the base peak m/z ratio: 312)
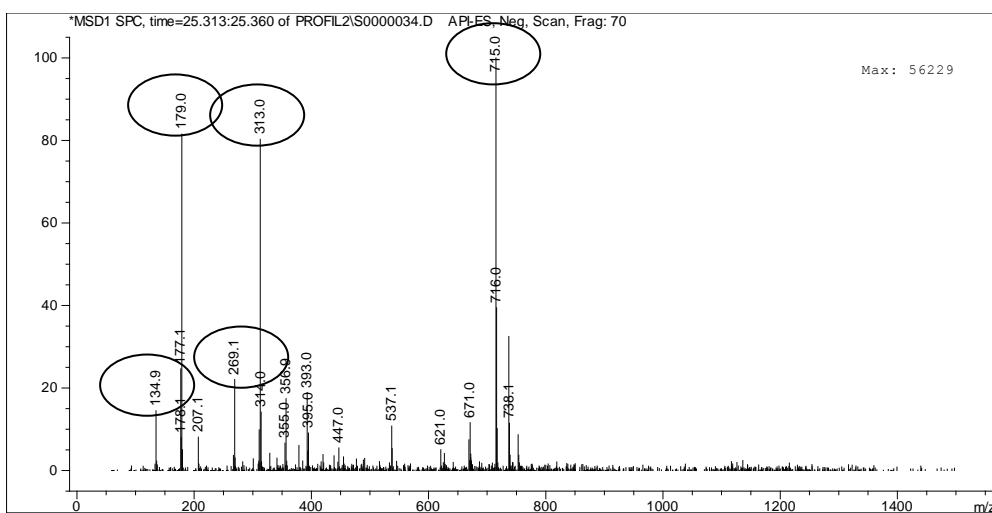
Figure 3.52 Mass spectra of products at RT: 24.5 (Pcaf-2) (the base peak m/z ratio: 715- tetramer of caffeic acid and the main fragments formed during ionization, m/z ratio: 134, 179, 269, and 313)
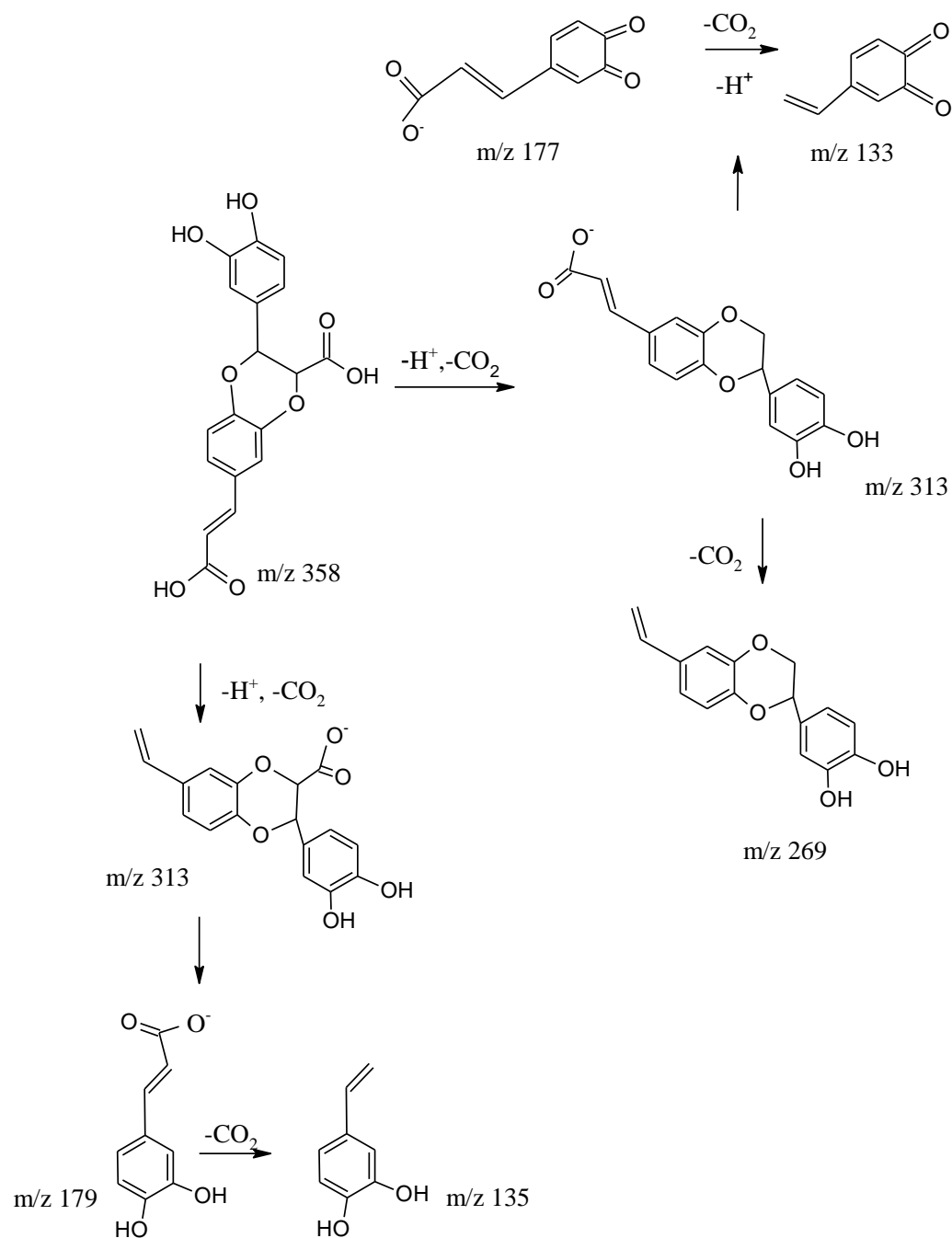
Figure 3.53 Fragmentation scheme hypothesized for structures corresponding to caffeicin-like dimers of caffeic acid (Pati *et al.*, 2006)

3.4 Oxidation of Phenolic Compounds by Laccase from *T. versicolor*

Laccase and tyrosinase/catechol oxidases are the two major groups of phenol oxidases. All these enzymes are copper-containing oxidases. Thus, the mechanism of

oxidation is likely to be different from CATPO, which contains heme at its catalase active site, and no copper atoms. Nevertheless, it was of interest to compare the products of phenol oxidation by these two different classes of phenolases, in order to compare the oxidation/polymerization capacities of these oxidases and that of CATPO, at least for those compounds where oxidation was observed by CATPO, namely catechol, chlorogenic acid, catechin and caffeic acid. In this respect, laccase from *Trametes versicolor* and tyrosinase from *Agaricus bisporus* were used, in this study, for the sake of comparison.

According to the literature, laccase is capable of oxidizing chlorogenic acid, catechol, hydroquinone, and catechin (Duran *et al.,* 2002, Osman *et al.,* 2007). In our study, oxidation products of catechol, caffeic acid and catechin were observed, however, chlorogenic acid was not oxidized.

The reaction for the oxidations of catechol, chlorogenic acid, catechin and caffeic acid by laccase, were performed in methanol- potassium citrate buffer as described in section 2.8.1. Reaction mixtures were incubated at 25°C for 1 h. Reactions were terminated with acetic acid and products were analyzed by HPLC and stored at -20 °C until LC-MS analysis.

3.4.1 Oxidation of Catechol by Laccase from *T. versicolor*

Three major fractions were observed at 21.9 (PLcat-1), 23.1 min (PLcat-2) and at 24.7 min (PLcat-3) from the oxidation of catechol by laccase for 1 h at 25 °C (Figure 3.54 and Table 3.15). The fact that the elution times of all products are latter than that of the catechol monomer suggests that these products have lower polarities than catechol. Catechol concentration decreased to 50.2 % at 1 h reaction by laccase.
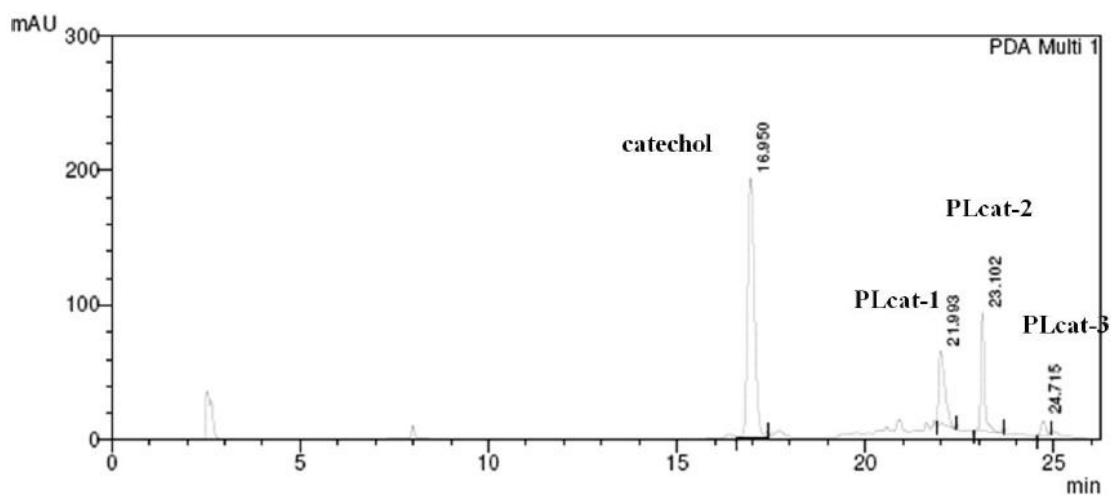
Figure 3.54 HPLC profile of 10 mM catechol oxidized by laccase (23.1 U/mg) for 1 h at 25°C

Table 3.15 Retention times and areas of the reaction products of catechol oxidized by laccase for 1 h at 25 $^{\circ}$C

Peak	Retention time	Area %
1 (catechol)	16.9	50.2
2 (PLcat-1)	21.9	22.2
3 (PLcat-2)	23.1	15.6
4 (PLcat-3)	24.7	7
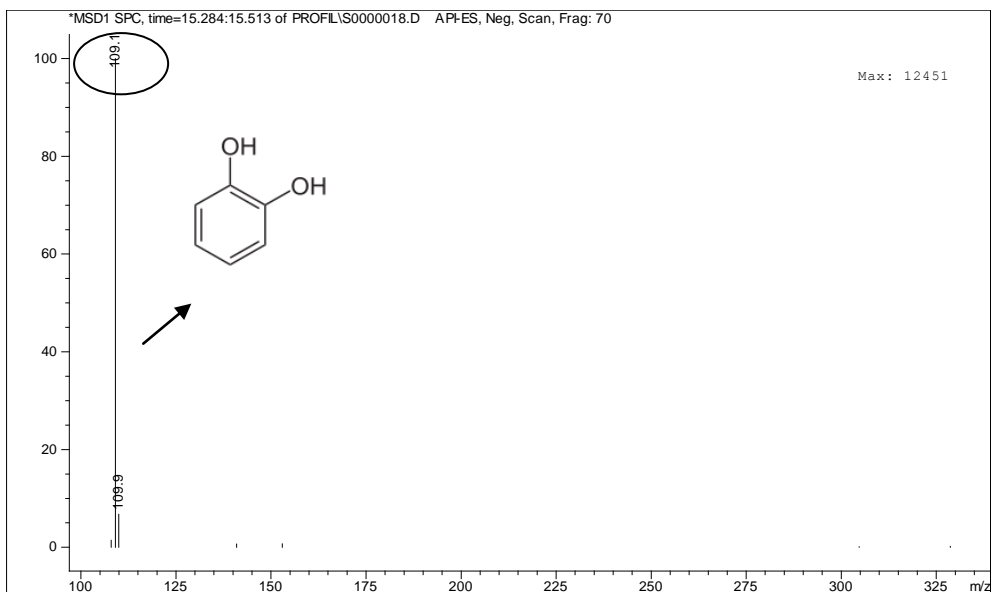
Figure 3 55 Mass spectra and molecular structure of un-oxidized catechol at RT: 16.9 (the base peak m/z ratios: 109)
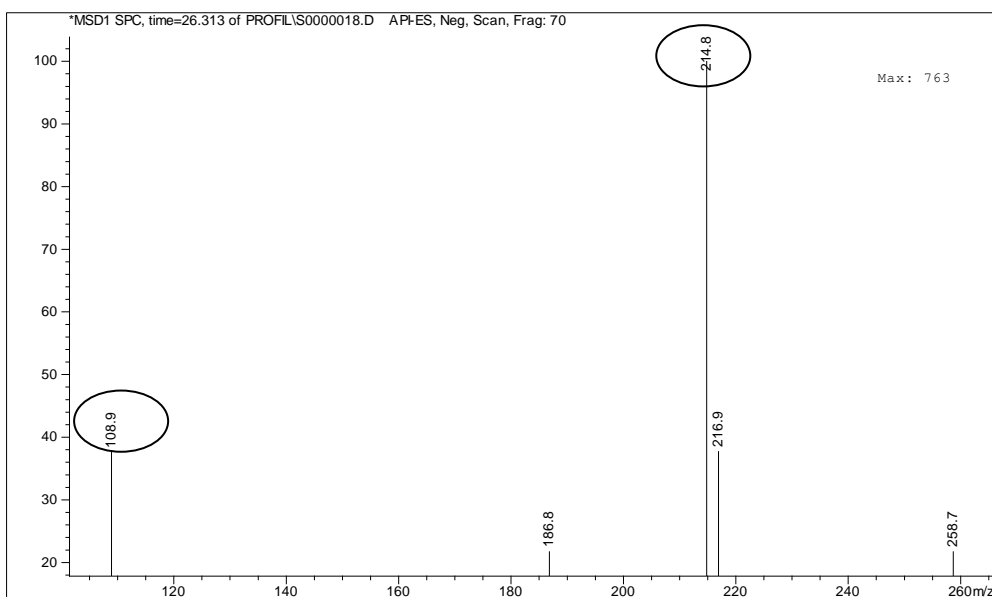
Figure 3.56 Mass spectra catechol dimer at RT: 21.9 min (PLcat-1) (the base peak is the dimer of catechol with 214.9 m/z ratios)
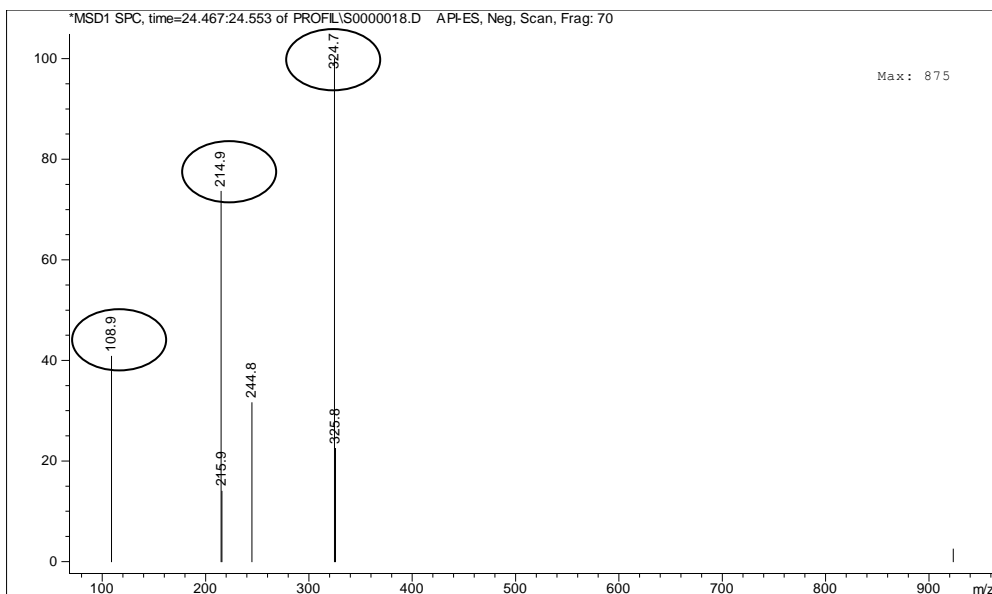
Figure 3.57 Mass spectra of catechol trimer at RT: 23.1 min (PLcat-2) (the base peak is the tetramer of catechol with 324.7 m/z ratios)
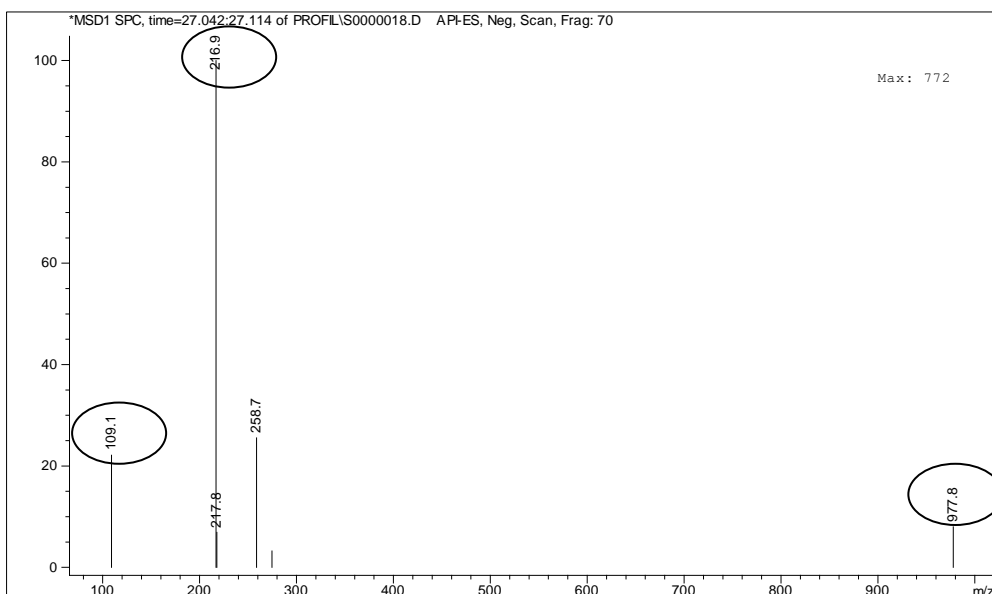
Figure 3.58 Mass spectra catechol oligomer at RT: 24. 7 min (PLcat-3) (the main peak m/z ratios: 977.8- oligomer of catechol and base fragment peak m/z ratios: 216.9-dimer of catechol)

The peak with the retention time 16.9 min is un-reacted catechol (m/z = 109) (Figure 3.55). The LC-MS result verifies the HPLC observation and shows that there is still

un-reacted catechol in the reaction mixture. The ESI/LC-MS spectra of major product fragments confirm the formation of oxidation products from catechol after 1 h reaction with CATPO. The peak with retention time 21.9 min (PLcat-1) is likely to be mainly a C-O-C dimer of catechol ([M-H]$^-$ with m/z 214.9) (Figure 3.56) Furthermore, the peak with retention time 23.2 min (PLcat-2) is likely to be a trimer of catechol ([M-H]$^-$ with m/z 324.7) (Figure 3.57). ESI-MS spectra indicated the presence of oligomers with larger molecular mass ([M-H]$^-$ with m/z 977.8 (PLcat-3) (Figure 3.58).

The similar retention times, UV-Vis spectra and m/z ratios of PLcat-1 with m/z 214.9 and Pcat-1 with m/z 214.9 suggest the same type of dimerization of catechol both by CATPO and laccase from *T. versicolor*. PLcat-2 which is likely to be a trimer of a catechol, with a retention times of 23.1 min. was not observed at 1 h reaction of catechol, oxidized by CATPO. m/z ratio of PLcat-3 (m/z 977.8) indicates the formation of catechol oligomers.

3.4.1.1 UV-Vis Spectrum Profile of Oxidation Products of Catechol Catalyzed by Laccase

Catechol exhibits very strong light absorption near 274 nm (Figure 3.59). As mentioned before, UV-Vis spectrum absorption results cannot give detailed information about the functional groups of the analytes. However, it is a convenient method to observe the difference of the products and concentration variation between catechol and products. PLcat-1 exhibits strong absorptions at 266 and 290 nm (Figure 3.60), which is the same as the UV-Vis spectrum profile of Pcat-1. As mentioned before, the same retention time profile on HPLC, molecular mass ratio on ESI/LC-MS and UV-Vis spectra of Pcat-1 and PLcat-1 indicate that the molecular structure of these two dimers could be same. PLcat-2 exhibited strong absorption at 253 and 284 nm and PLcat-3 at 293 nm and 311 nm (Figure 3.61 and Figure 3.62 respectively).
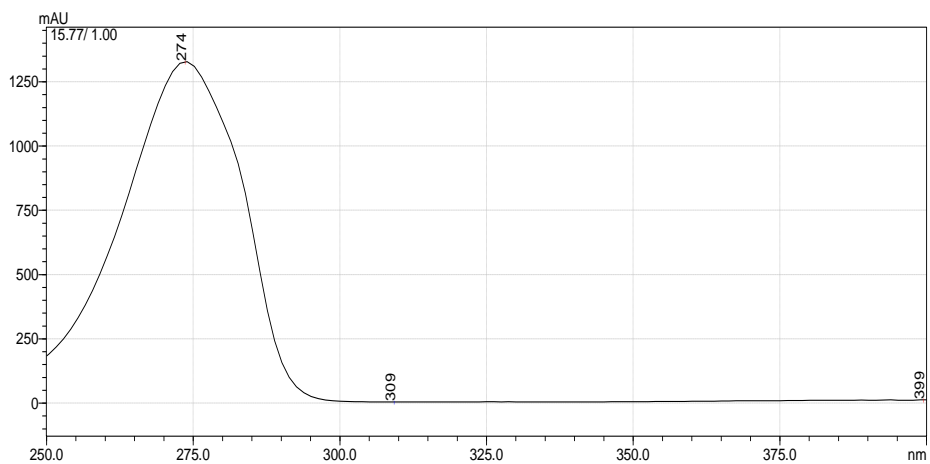
Figure 3.59 UV-Vis spectra of catechol (lambda max. at 274 nm)
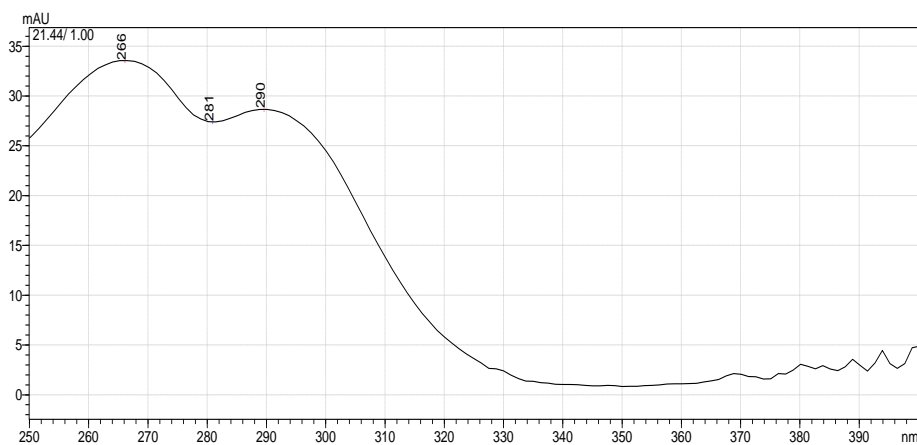
Figure 3.60 UV-Vis spectra of PLcat-1(lambda max. at 266 nm and 290 nm)
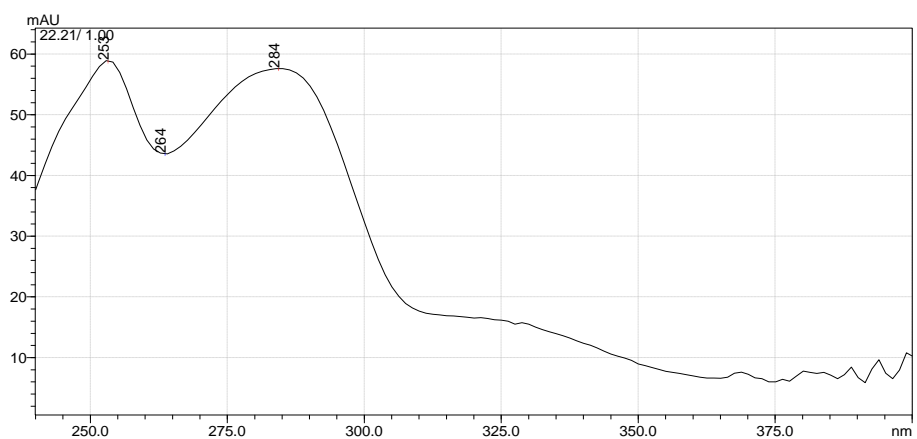
Figure 3.61 UV-Vis spectra of PLcat-2 (lambda max. at 253 and 284 nm)
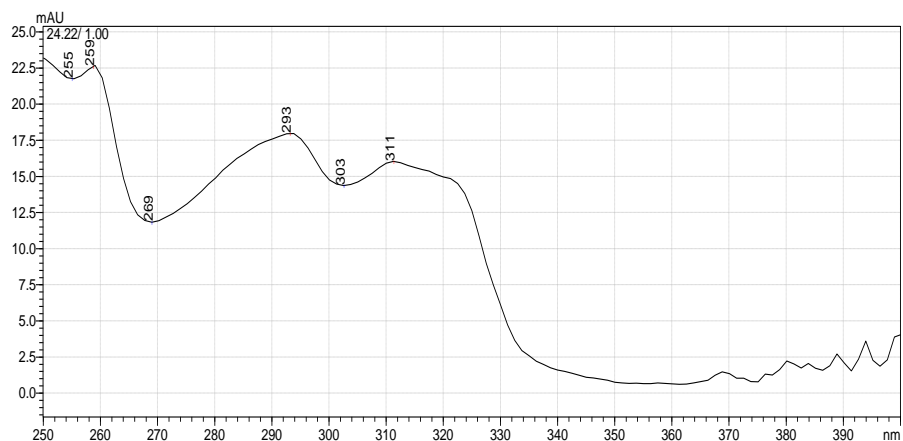
Figure 3.62 UV-Vis spectra of PLcat-3 (lambda max. at 293 nm and 311 nm)

3.4.2 Oxidation of Catechin by Laccase

Four major product fractions were observed during the oxidation of catechin by laccase (Figure 3.63).
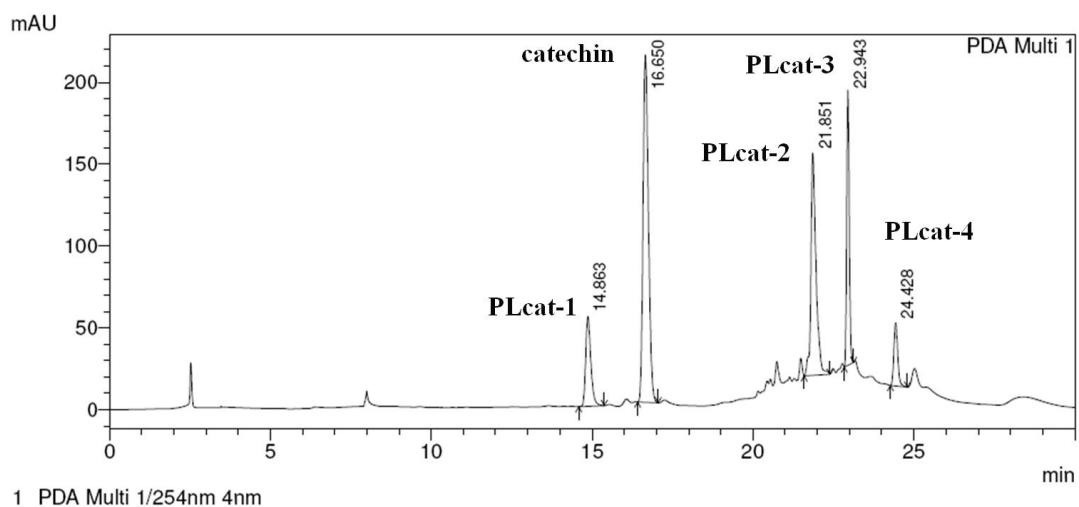
Figure 3.63 HPLC profile of 10 mM catechin oxidized by Laccase (23.1 U/mg) for 1 h at 25 $^\circ$C

Table 3.16 Retention times and areas of the reaction products of catechin oxidized by laccase for 1 h at 25 °C

Peak	Retention time	Area %
1 (PLcath-1)	14.8	10.4
2 (catechin)	16.5	42.2
3 (PLcath-2)	21.8	25.5
4 (PLcath-3)	22.9	16.0
5 (PLcath-4)	24.4	5.5
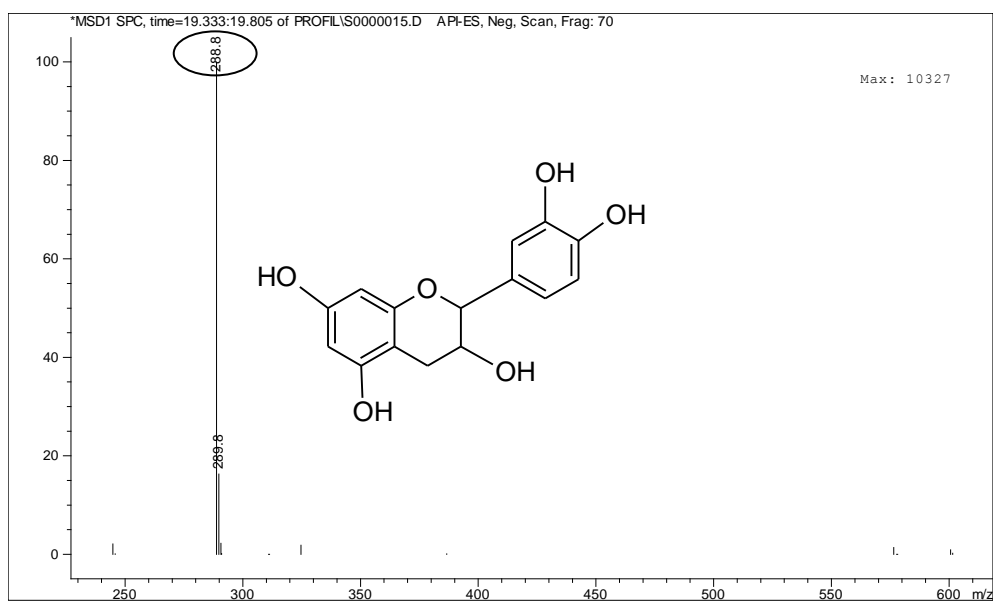
Figure 3.64 Mass spectra and molecular structure of un-oxidized catechin at RT: 16.5 (the base peak m/z ratio: 289)
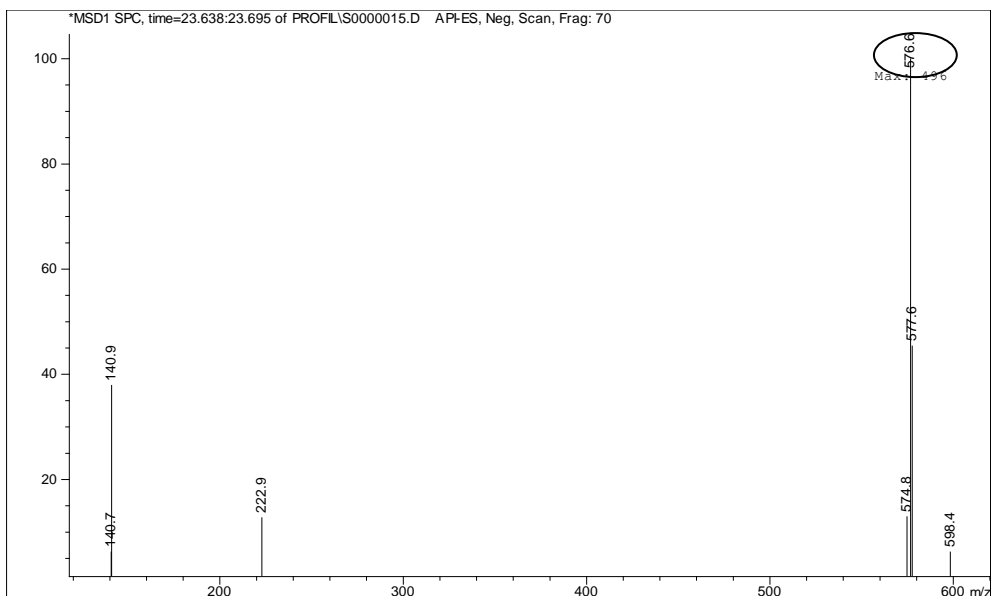
Figure 3.65 Mass spectra of hydrophilic dimer at RT: 14.8 (PLcath-1) (the base peak m/z ratio: 576.6)
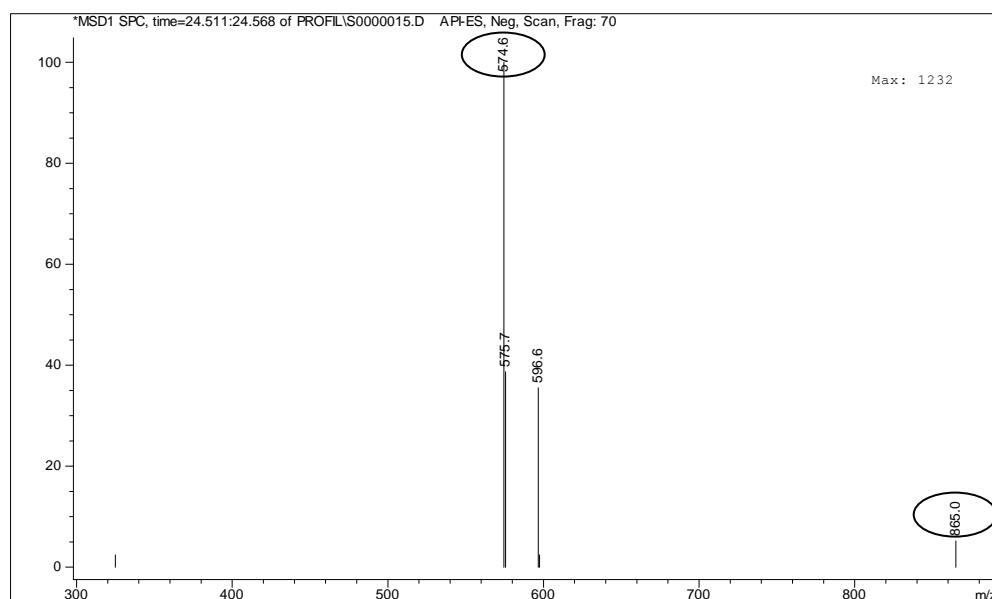
Figure 3.66 Mass spectra of a hydophobic dimer at RT: 21.8 (m/z 574.6) which most likely, condenses with catechin to form the reduced trimer-PLcath-2 with m/z 865
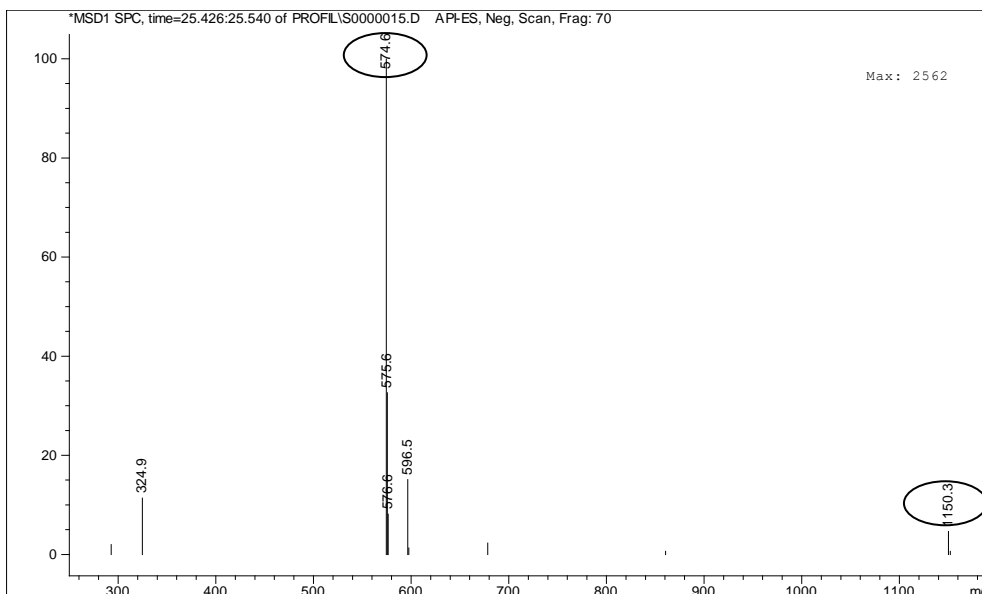
Figure 3.67 Mass spectra of a hydrophobic dimer at RT: 22.9 (m/z 574.6) which most likely, condenses with catechin to form the reduced tetramer-PLcat-3 (m/z 1150)

Similar to the CATPO- catalyzed reaction; the m/z ratios showed that, first catechin was oxidized to semiquinone and *o*-quinone then, *o*-quinone is reduced to a hydrophilic dimer (type B dimer) (MW=576.6 Da) (Figure 3.65). Type B dimer is enzimatically oxidized to the hydrophobic dimers (MW=575 Da) (Figure 3.66). Once formed, the hydrophobic dimers were further oxidized by the enzyme to an o-quinone (MW=574 Da) which, most likely, condensed with catechin to form the reduced trimer (MW=864 Da) (Figure 3.66) and then, tetramer (Figure 3.67).

3.4.2.1 UV-Vis Spectrum Profile of Oxidation Products of Catechin Catalyzed by Laccase

Catechin exhibits very strong light absorption near 279 (Figure 3.68). PLcath-1 exhibits very strong light absorption at 279 nm as Pcath-1 (Figure 3.69). PLcath-2 and PLcath-3 exhibits very strong light absorption around 401 nm similar to Pcath-2, Pcath-3 and Pcath-4 (Figure 3.70). These UV-Vis spectrum profiles very similar to data coming from oxidative products of catechin catalyzed by CATPO also support the LC-MS results.
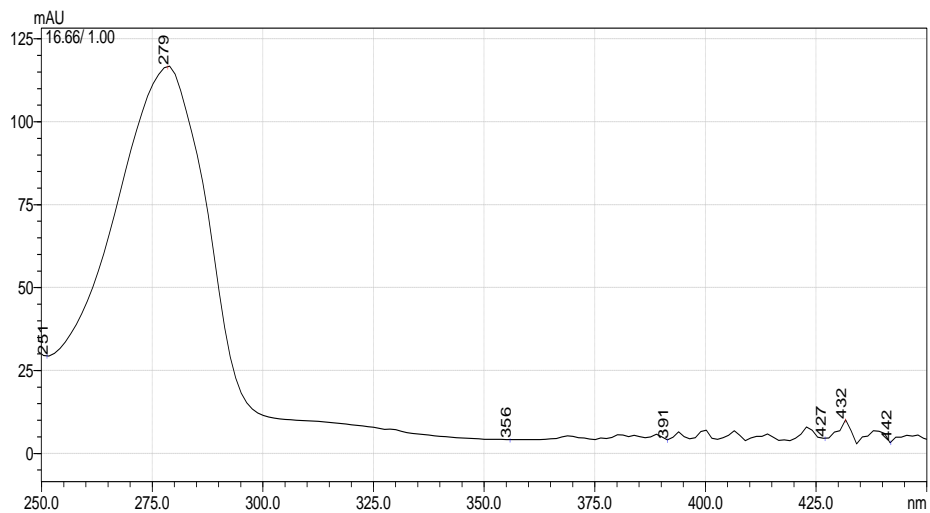
Figure 3.68 UV-Vis spectra of catechin (lambda max. at 279 nm
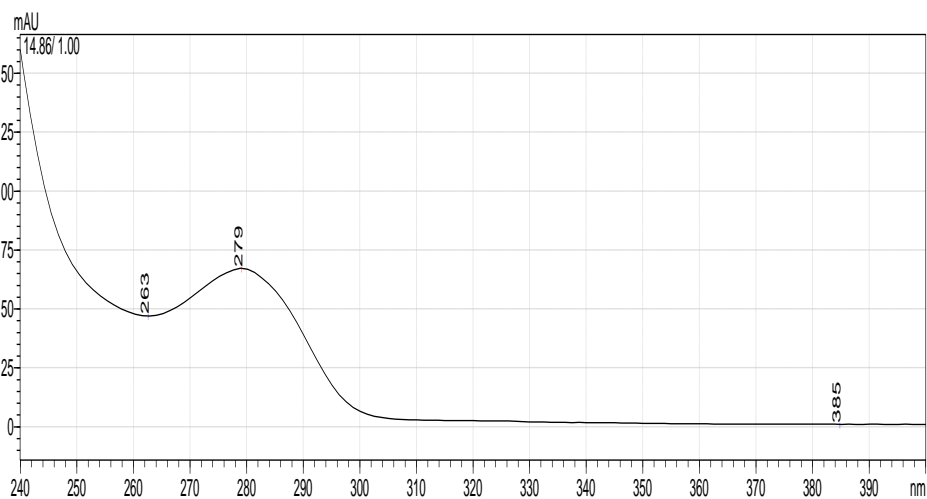
Figure 3 69 UV-Vis spectra of PLcath-1 (lambda max. at 279 nm)
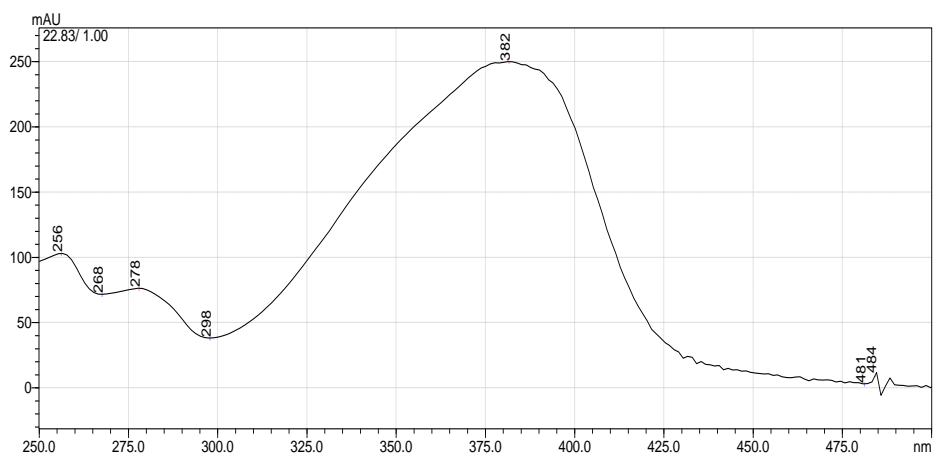
Figure 3.70 UV-Vis spectra of PLcath-2 and PLcath-3 (lambda max. at 382 nm)

3.4.3. Oxidation of Caffeic Acid by Laccase

Three major product peaks were obtained from the oxidation of caffeic acid by laccase are shown in Figure 3.71. Elution of the oxidation products, after caffeic acid, indicated that all of them are less polar than caffeic acid itself. PLcaf-2 and PLcaf-3 showed similar elution times with Pcaf-1 and Pcaf-2. On the other hand, PLcat-1 fragment has only seen on the chromatograms of the oxidation products catalyzed by laccase.
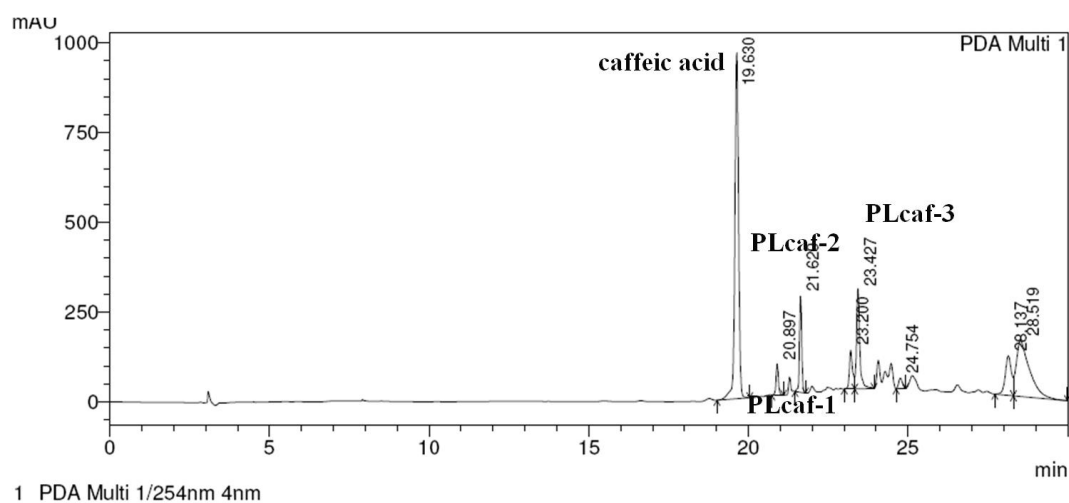
Figure 3.71 HPLC profile of 10 mM caffeic acid oxidized by laccase (23.1 U/mg) for 1 h at 25 °C

Table 3.17 Retention times and areas of the reaction products of caffeic acid oxidized by CATPO for 1 h at 25 °

Peak	Retention time	Area %
1 (caffeic acid)	19.6	70.21
2 (PLcaf-1)	20.8	2.8
3 (PLcaf-2)	21.6	11.01
4 (PLcaf-3)	23.4	15.76

As mentioned before, the mass spectra of the oxidation products of caffeic acid showed two major products Pcaf-1 and Pcaf-2. Pcaf-2 could be a tetramer of caffeic acid with m/z: 715 (Figure 3.52). Pcaf-2 showed fragments with m/z ratio of 133, 179, 269, 313, and 359, probably corresponding to the degradation fragments of caffeic acid tetramer (C-O coupled) and formed by losses of CO_2 and H^+. Pcaf-1 with m/z 313 is a likely to correspond to CO_2 losses of a caffeic acid dimer (C-O coupled) during mass spectroscopy (Figure 3.51). Among all the possible caffeic acid dimers (type a, type b, type c and type d) described in the literature, only caffeicin-like (type-d) ones can explain the observed fragments during mass spectroscopy of caffeic acid products oxidized by CATPO.

PLcaf-2 gave the base peak m/z ratio is 312, and the main peak m/z ratio 1157, which could be a caffeic acid tetramer (Figure 3.75). PLcaf-3 showed that, the base peak has m/z ratio of 312, and the main peak m/z 736 indicated the formation of caffeic acid dimer (Figre 3.76).

PLcaf-1 was unique to laccase. ESI/LC-MS analysis indicated that, PLcaf-1 has m/z ratio of the base peak 714 (tetramer of caffeic acid) and m/z ratio of the fragments 366 (dimer of caffeic acid), 269, 159, 141 (fragments occur from dimer of caffeic acid) (Figure 3.74). The fragments that have m/z ratio of 269, 159 and 141 were not observed after mass spectroscopy of caffeic acid oxidation products by CATPO. The MS spectra relevant to m/z 269, referred to product PLcaf-1 provided useful structural information. Peaks at m/z 159 and 141 could be observed for PLcaf-1 and this can be explained starting from a C-C type dimer structure occured through hydrogen transfers and then double-bond displacements for a C-C dimer (Pati *et al.,* 2006). This could be the C6-C6 type dimer as an example (Figure 3.72). Furthermore, linkages involving carbon positions at 2, 5, 6 can preserve the benzene ring conjugation. This generates six possible dimeric structures. Among these, the three ones involving position 2 (C2-C2, C2-C5, C2-C6) appear to be less likely because of steric hindrance (Pati *et al*., 2006).
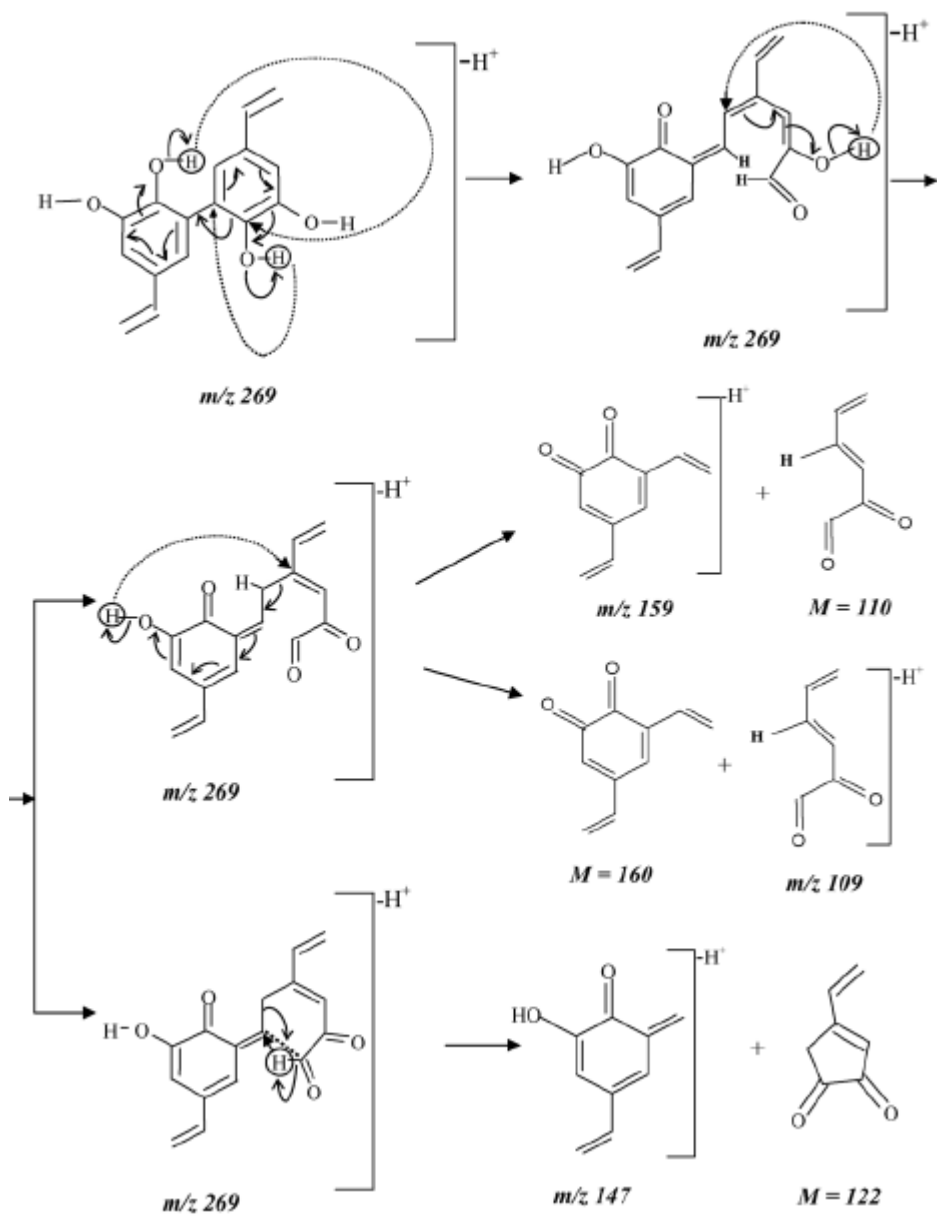
Figure 3.72 Fragmentation scheme of the fragment with m/z 269, corresponding to a C6-C6 type dimer arising from coupling of caffeic acid (Pati *et al.,* 2006)
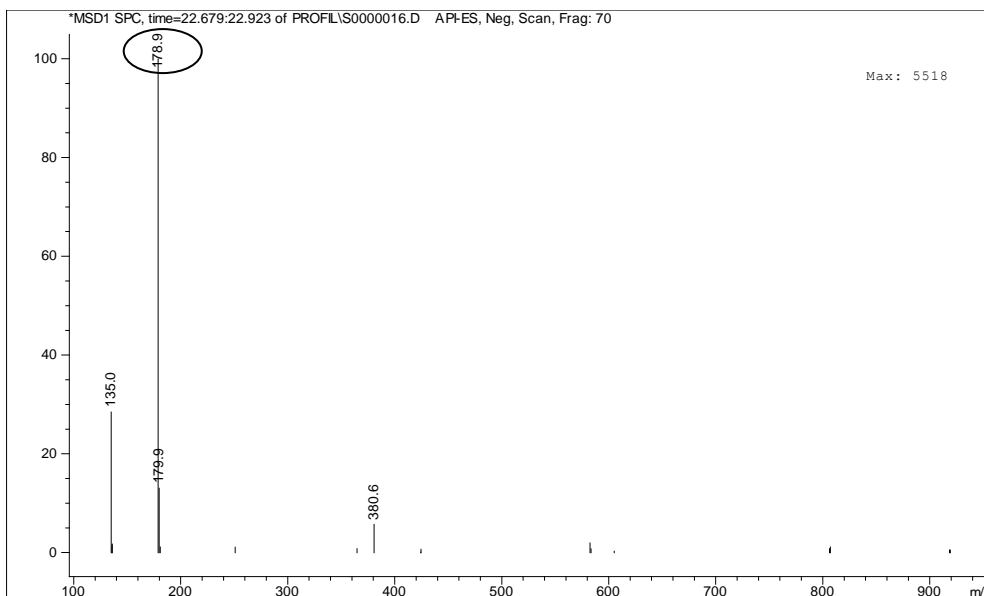
Figure 3.73 Mass spectra of un-oxidized caffeic acid at RT: 20.3 (the base peak m/z ratio: 179)
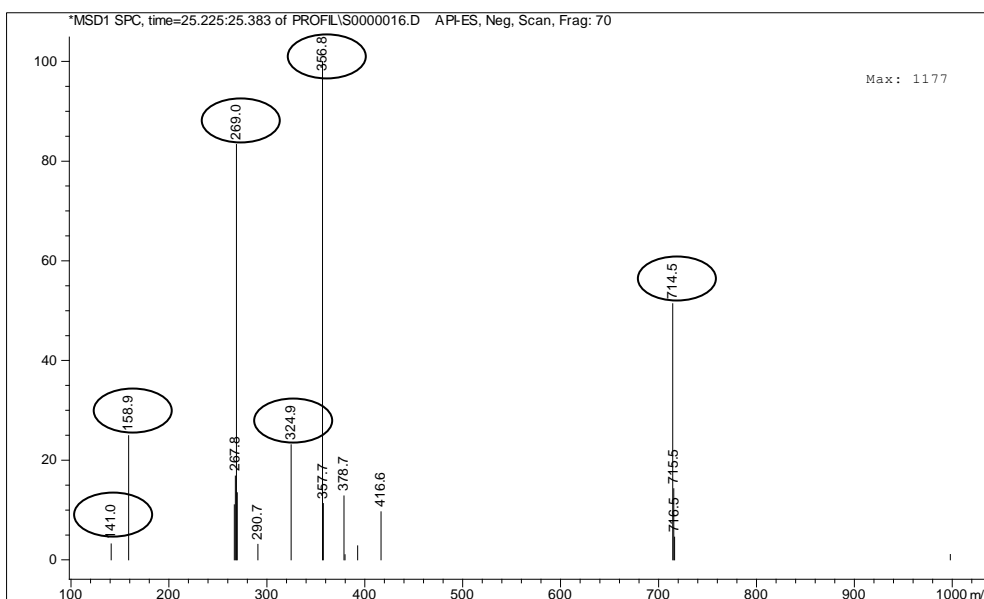
Figure 3.74 Mass spectra of products at RT: 20.8 (PLcaf-1) (the main peak m/z ratio 714.5- tetramer of caffeic acid, the base peak m/z ratio: 356-dimer of caffeic acid, the fragments m/z ratio: 269, 159, 141
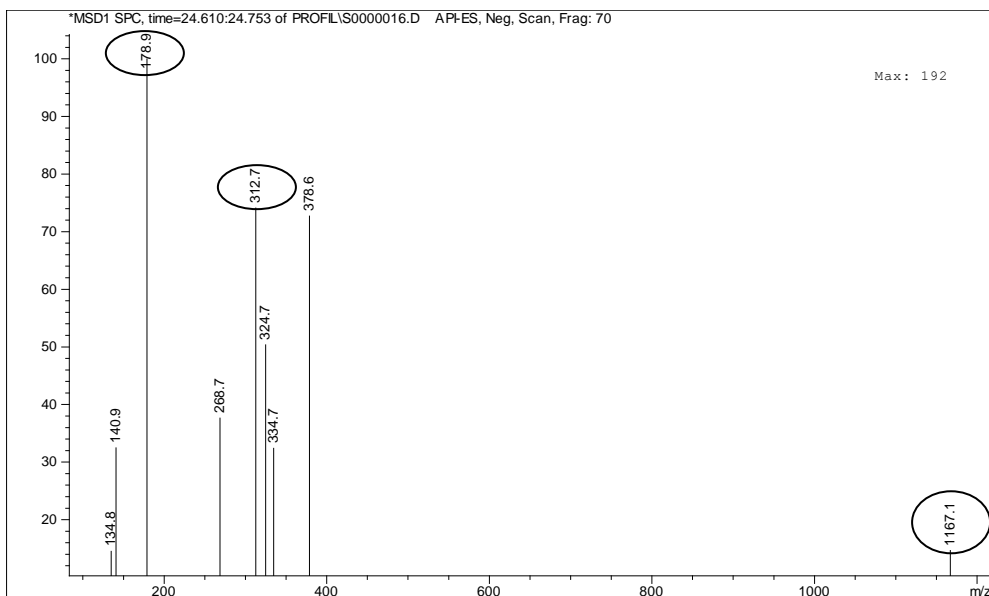
Figure 3.75 Mass spectra of products at RT: 21.6 (PLcaf-2) (the base peak m/z ratio: 178, the main peak m/z: 1167, the fragments m/z ratio: 312, 134, 179
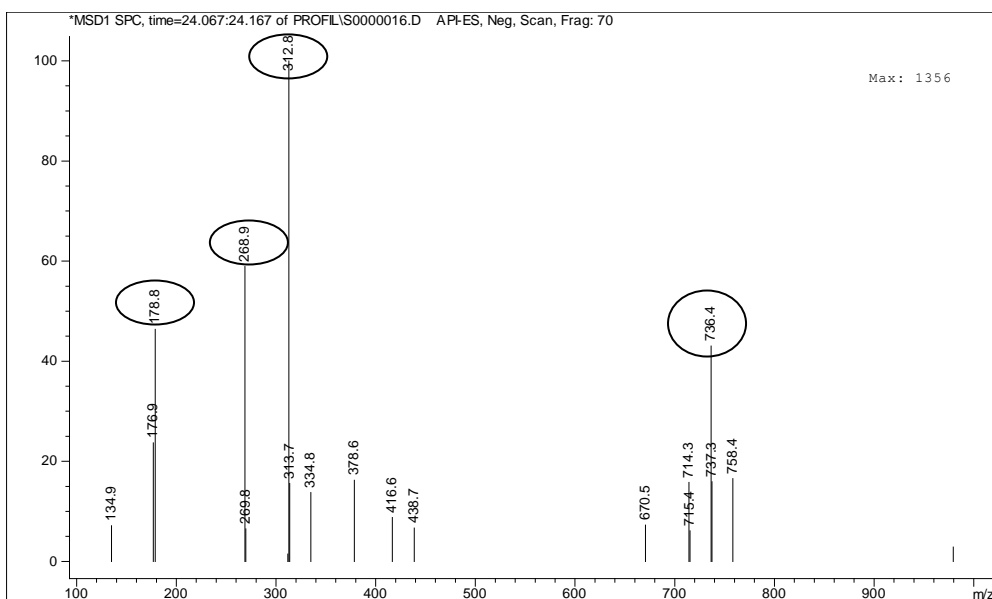
Figure 3.76 Mass spectra of products at RT: 23.4 (PLcaf-3) (the base peak m/z ratios: 312, the main peak m/z ratio 736 and fragments m/z ratios: 269 and 178)

3.4.3.1 UV-Vis Spectrum Profile of Oxidation Products of Caffeic Acid Catalyzed by Laccase

Caffeic acid exhibits very strong light absorption near 297 and 324 nm (Figure 3.77). Spectra relevant to compounds PLcaf-2 and PLcaf-3 (Figure 3.79) exhibited the same UV-Vis spectra with Pcaf-1 and Pcaf-2. PLcaf-2 and PLcaf-3, exhibited spectra similar to those of caffeicins type caffeic acid dimer, with a different ratio between the absorbance at 288 and 319 nm suggesting that during oxidation of caffeic acid there is a partial loss of the side-chain conjugation. On the other hand, spectra relevant to the PLcaf-1 (Figure 3.78) exhibited lambda max. at 324 nm similar to that unreacted caffeic acid, suggesting that the side chain conjugation of the molecule is still present. They could be then related to caffeic acid type a like dimer formation arising from Michael 1,4 addition between the caffeic acid quinone and another caffeic acid molecule. This process does not involve the side chain conjugation.
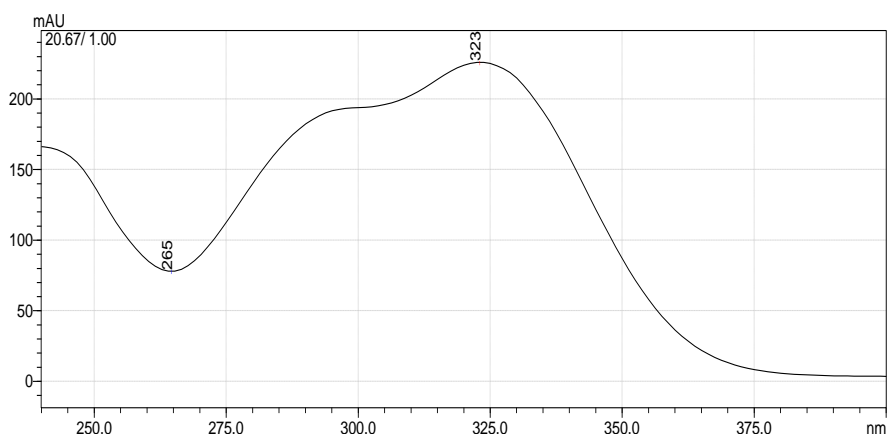
Figure 3.77 UV-Vis spectra of caffeic acid (lambda max. at 297 and 324)
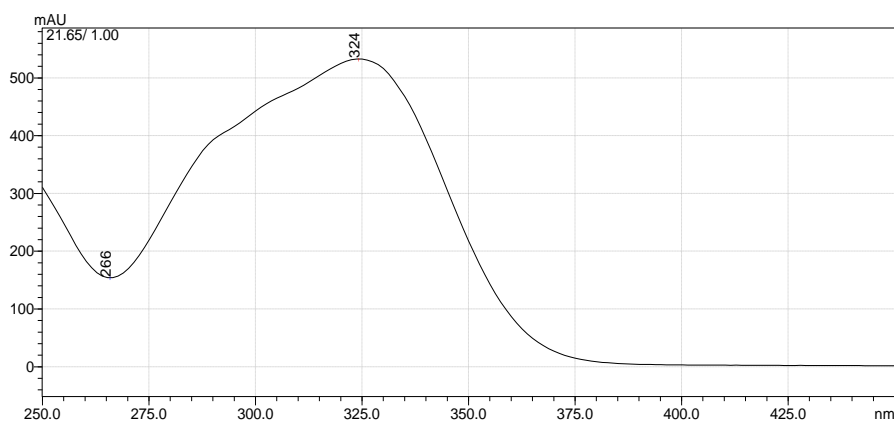
Figure 3.78 UV-Vis spectra of PLcaf-1 (lambda max. at 324)

117
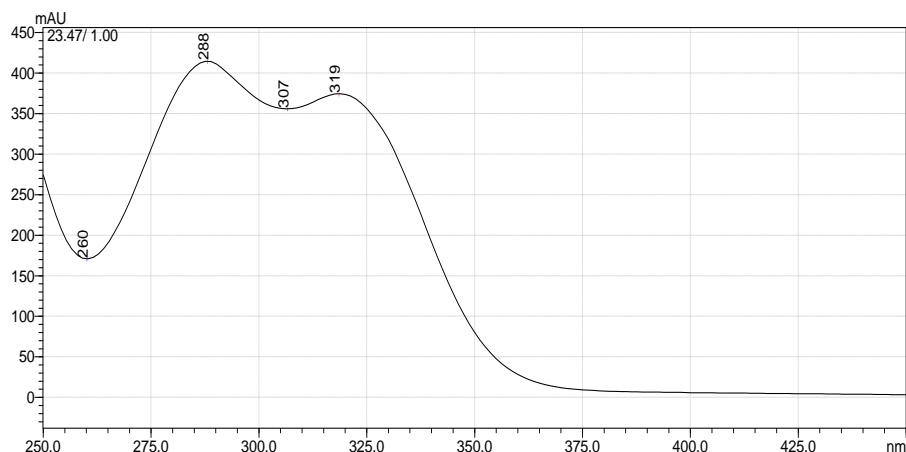
Figure 3.79 UV-Vis spectra of PLcaf-2 and PLcaf-3 (lambda max. at 288 and 319)

3.5 Oxidation of Phenolic Compounds by Tyrosinase from *Agaricus bisporus*

According to the literature, tyrosinase is capable caffeic acid, catechin and aromatic compounds. (Duran *et al.,* 2002, Munoz *et al.,* 2008, Pati *et al*., 2006). In our study, oxidation products of catechol and catechin but not chlorogenic acid and caffeic acid, were detected by the tyrosinase of *A. bisporus*.

The reaction for the oxidation of catechol, caffeic acid, chlorogenic acid and catechin by tyrosinase, was performed in methanol- potassium-phosphate buffer as described in section 2.8.2. Reaction mixtures were incubated at 25°C for 1 h. Reactions were terminated with acetic acid and products were analyzed by HPLC and stored at -20 °C until LC-MS analysis

3.5.1 Oxidation of Catechol by Tyrosinase

One major product peak was obtained from the oxidation of catechol by tyrosinase (Figure 3.80). Elution of the oxidation products, after catechol indicated oxidation product was less polar than catechol.

.
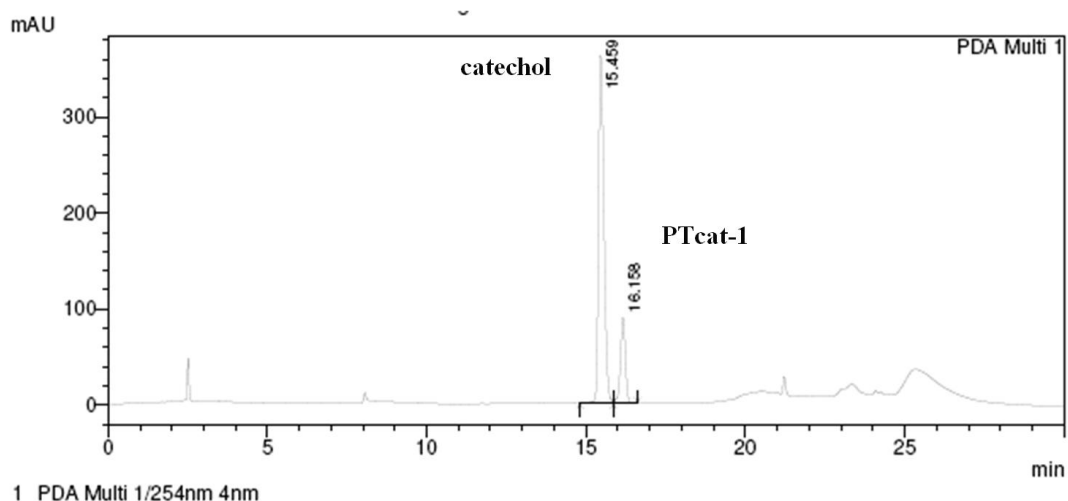
Figure 3.80 HPLC profile of 10 mM catechol oxidized by tyrosinase (4.26 U/μg) for 1 h at 25 °C

Table 3.18 Retention times and areas of the reaction products of catechol oxidized by tyrosinase for 1 h at 25 °C

Peak	Retention time	Area %
1 (catechol)	15.4	81.53
2 (PTcat-1)	16.1	18.74
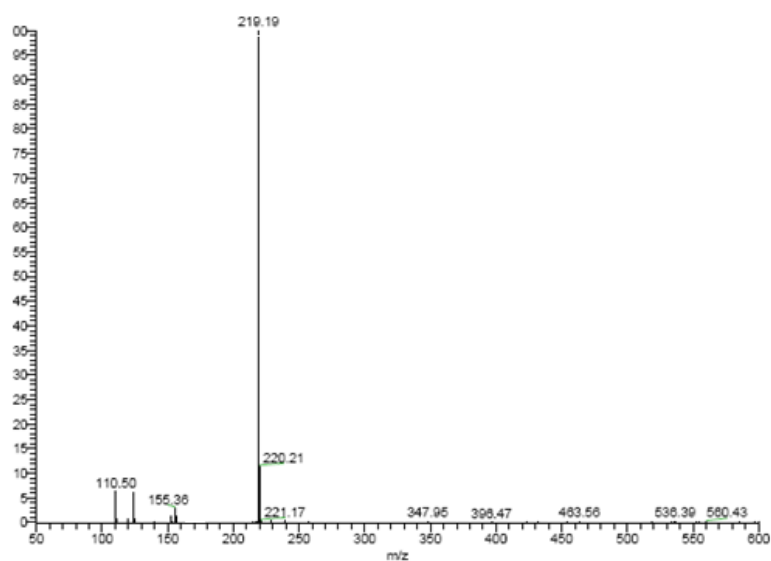
Figure 3.81 Mass spectra of product at RT: 16 min (PTcat-1) (main peak m/z ratio: 219)

PTcat-1 has m/z ratio of 219.1, which could be a dimer of catechol (Figure 3.81). The retention time of PTcat-1 does not show any similarly to any product of catechol oxidized by CATPO or laccase. Different elution time and higher polarity of PTcat-1 than Pcat-1 and PLcat-1 is suggesting that, the dimer structure of PTcat-1 is different from the dimer structure of Pcat-1 and PLcat-1. PTcat-1 exhibited strong absorbance at 288 nm (Figure 3.82). This type of an absorbance profile also support the structure difference between the PTcat-1 and Pcat-1.

Unlike laccase and CATPO, any other oxidation product was not observed during 1 h of reaction. This could depend on unexplained irreversible inactivation of tyrosinase, which occurs during oxidation of catechols. One of the proposed mechanisms about the inactivation of the enzyme is a mechanism that involves the catechol substrate preventing itself at the active site as a cresol (monophenol) called 'cresolase presentation'. This leads to the catechol being oxidized to form a product able to undergo deprotonation and reductive elimination, resulting in inactivation of the enzyme through the formation of copper(0) at the active site (Land *et al.,* 2004). On the basis the mechanism, it is proposed that the inactivation of tyrosinase during catechol oxidation is due to the catechol being capable of alternative cresolase presentation.

The study about the oxidative products that result from the biocatalysis of tyrosinase directed by Madani *et al.,* (1999) confirm our results. Oxidation of catechol by commercial mushroom tyrosinase was done for 10 min at 25 °C. The results of HPLC showed that the oxidation of catechol by tyrosinase resulted in the appearance of one end product. However, the characterization of this product was unperformed. On the other hand, some studies about the oxidation of catechol by tyrosinase confirm the formation of phenylene units by coupling of C-C. (Dawson and Tarpley, 1963). PTcat-1 m/z ratio indicates the formation of catechol dimer but to understand the structure of the dimer further analysis should be done.
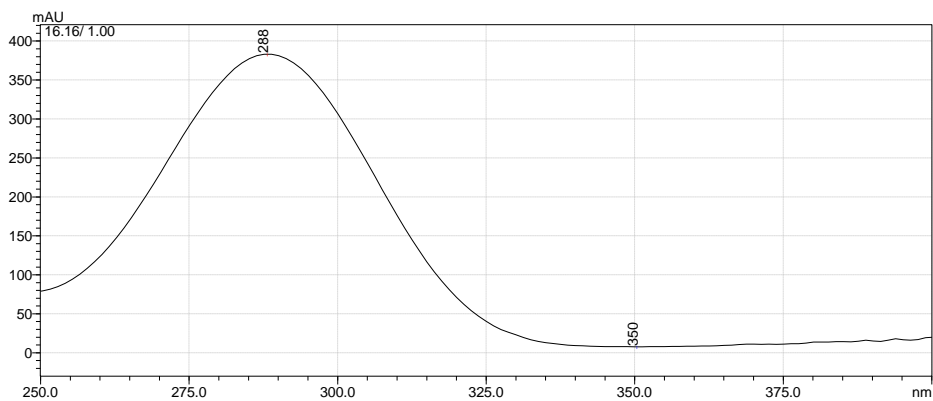
Figure 3.82 UV-Vis spectra of PTcat-1 (lambda max. at 288 nm)

3.5.2 Oxidation of Catechin by Tyrosinase

Three major products were observed during the oxidation of catechin by tyrosinase (Figure 3.83). HPLC profile showed that, PTcath-1 is more polar than catechin, which suggests that this product could be a hydrophilic dimer. PTcath-2 and Pcath-3 are less polar than catechin and this suggest the formation of hydrophobic dimer and maybe trimer or tetramer. UV-Vis spectrum of PTcath-1 is similar to Pcath-1 and PLcath-1 and show max. absorbance at 279 nm. Similarly, UV-Vis spectrum of PTcath-2 and PTcath-3 are compatible with Pcath-2, Pcath-3, PLcath-2 and PLcath-3.
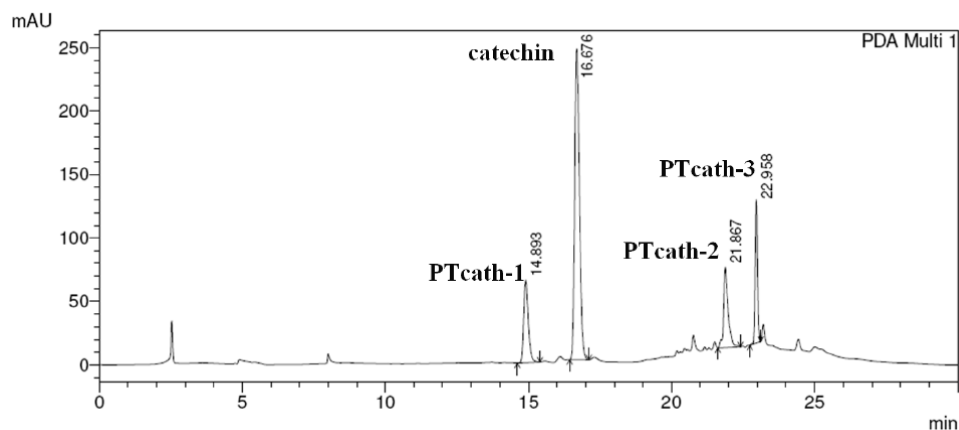
Figure 3.83 HPLC profile 10 mM catechin oxidized by tyrosinase (4.26 U/µg) for 1 h at 25 °C

121

Table 3.19 Retention times and areas of the reaction products of catechin oxidized by tyrosinase for 1 h at 25 $^{\circ}$C

Peak	Retention time	Area %
1 (PTcath-1)	14.8	14.6
2 (catechin)	16.6	58.2
3 (PTcath-2)	21.8	14.3
4 (PTcath-3)	22.9	12.7
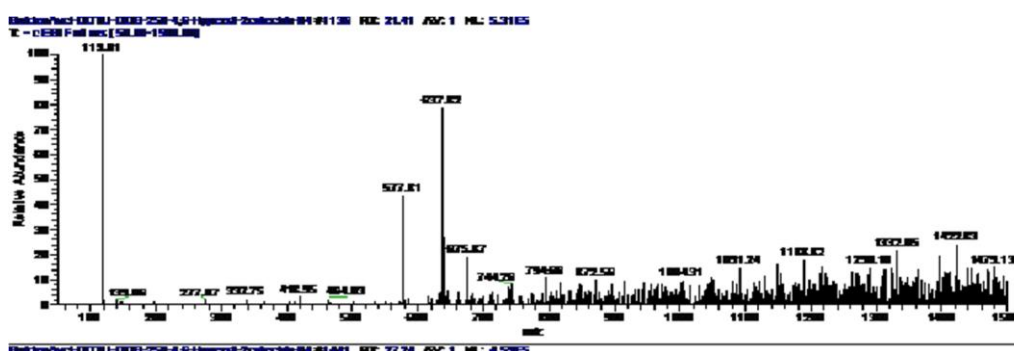
Figure 3. 84 Mass spectra of product at RT: 14.8 (the base peak m/z ratio: 577)
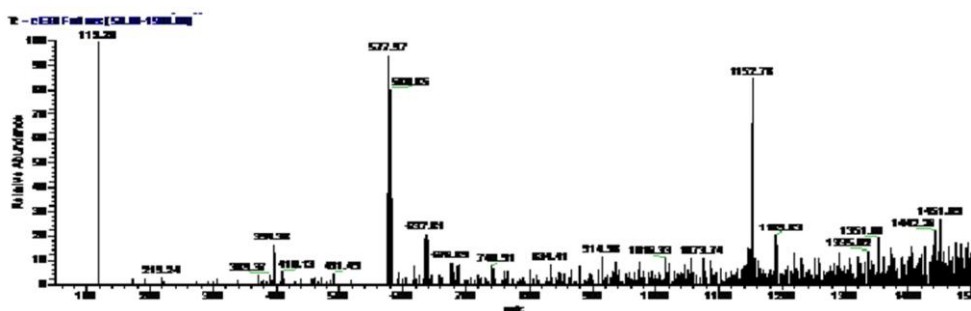
Figure 3.85 Mass spectra of product at RT: 21.8 (the main peak m/z ratio: 1152 and base peak m/z ratio: 577)
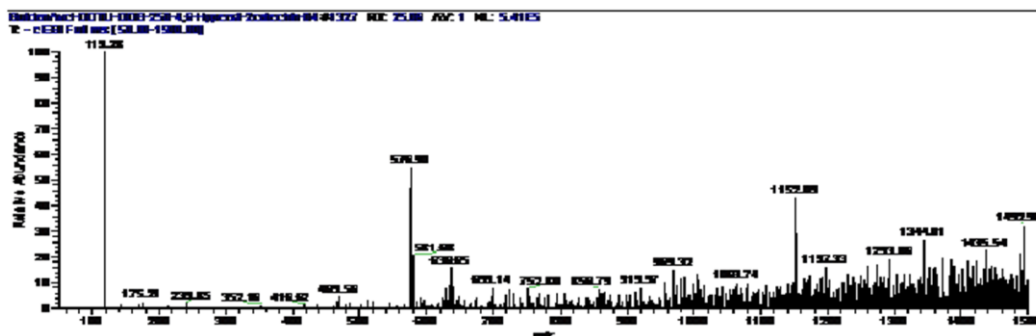
Figure 3.86 Mass spectra of product at RT: 22.9(main peak m/z ratio: 1152 and base peak m/z ratio: 577)

Three major products were observed during oxidation of catechin by tyrosinase for 1-hour at 25 °C (Figure 3.83). The dimer appeared at 14. min during oxidation of catechin by tyrosinase and gave a 577 m/z ratio on ESI/LC-MS (A type dimer of catechin) (Figure 3.84). PTcath-2 m/z ratio of main fragment is 577 (hydrophobicdimer of catechin), and PTcath-3 m/z ratio of main fragment is 1152 (tetramer of catechin) (Figure 3.84 and 3.85). According to these results, the two types of dimers (type A and type B) and tetramers were appeared from catechin oxidation by tyrosinase similarly to laccase and CATPO.
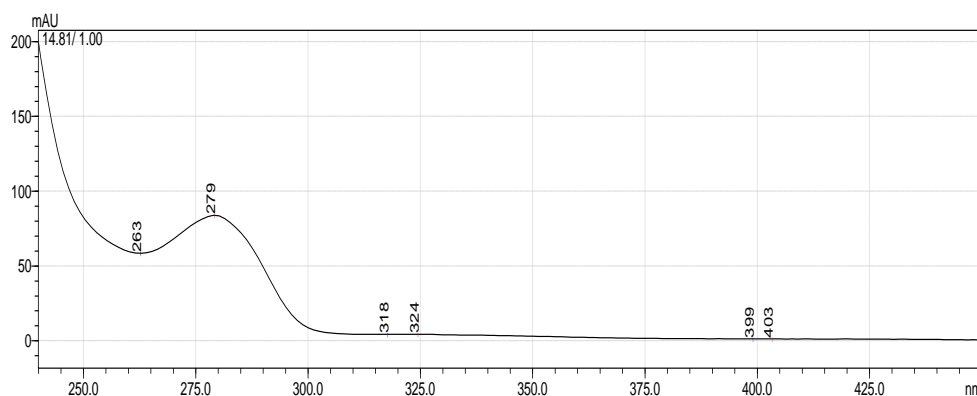
Figure 3.87 UV-Vis spectrum of PTcath-1 (lambda max. at 279 nm)
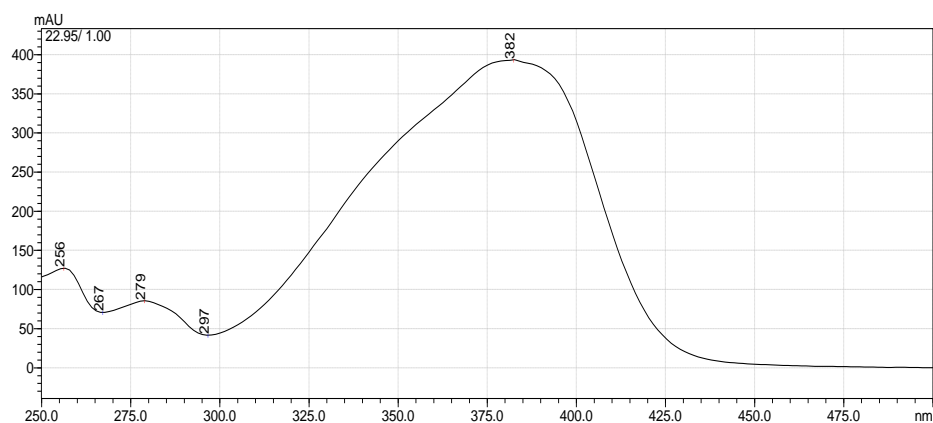
Figure 3.88 UV-Vis spectrum of PTcath-2 and PTcath-3 (lambda max. at 382 nm)

3.6 Comparative Discussion of Conversion of Phenolic Compounds by Catalase Phenol Oxidase, Laccase and Tyrosinase

As a result of the oxidation of catechol, chlorogenic acid, catechin and caffeic acid, differences were observed both at the efficiency of oxidation and the products. After 1 h of oxidation of catechol under the specified conditions, 35% conversion of catechol for CATPO (10 μg) was observed. While this was 50% for laccase (10 μg) and 18% for tyrosinase (10 μg). Only CATPO was able to oxidize chlorogenic acid into a single product with 52% conversion. The highest activity for catechin was found with CATPO (63% conversion). Laccase and tyrosinase were also able to oxidize catechin, but with lower efficiencies (58% conversion by laccase and 32% conversion by tyrosinase). Both laccase and CATPO were able to oxidize caffeic acid (28% conversion by CATPO and 30% conversion by laccase). Whereas, tyrosinase was not able to oxidize caffeic acid (Figure 3.90).
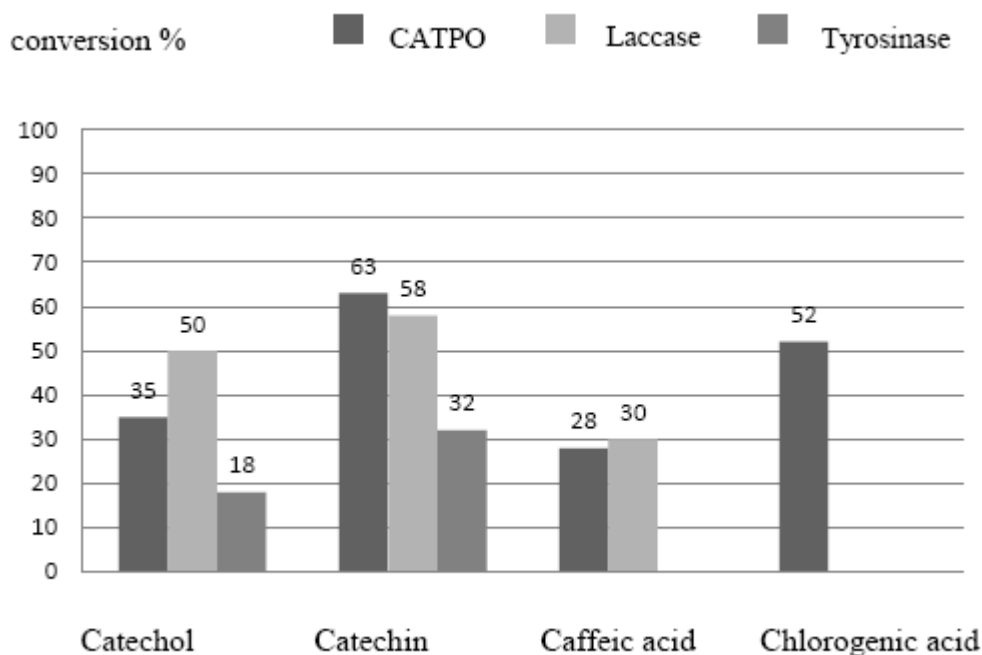
Figure 3.89 Conversion efficiency of CATPO (10 μg) at 1 h incubation with 10 mM phenolic compounds at 60 $^{\circ}$C in 0.1 M potassium phosphate buffer, pH 7.0, compared with conversion efficiency of laccase (10 μg) determined at 1 h incubation with 10 mM phenolic compounds at 25 $^{\circ}$C in 0.1 M potassium citrate buffer, pH 4.8 and conversion efficiency of tyrosinase (10 μg) at 1 h incubation with 10 mM phenolic compound at 25 $^{\circ}$C in 0.1 M potassium phosphate buffer, pH 6.5.

Two oxidation products of catechol (Pcat-1 and Pcat-2) were observed after 1 h incubation with CATPO. Whereas, three products (PLcat-1, PLcat-2 and PLcat-3) were observed after 1 h incubation with laccase and one product was observed after 1 h incubation with tyrosinase. The m/z ratios of Pcat-1 and PLcat-1 were 214.9 indicated the dimer formation. The m/z ratio of PTcat-1 was 219 also indicate the dimerization. However, the retention time of PTcat-1 does not show any similarly to any product of catechol oxidized by CATPO or laccase. Higher polarity on HPLC and different UV-Vis spectrum of PTcat-1 is suggesting that, the structure of PTcat-1 is different from the structure of Pcat-1 and PLcat-1. The m/z ratio of Pcat-1 (856) and PLcat-1 (977) indicate the oligomerization was performed by CATPO and laccase respectively.

Four major products (Pcath-1, Pcath-2, Pcath-3 and Pcath-4) were observed after oxidation of catechin by CATPO for 1 h and similarly four major products (PLcath-1, PLcath-2, PLcath-3 and PLcath-4) were observed after oxidation of catechin by laccase. On the other hand, three major products (PTcath-1, PTcath-2, and PTcath-3) were detected after 1-h incubation of catechin with tyrosinase. The UV-Vis spectra, LC-ESI-MS results of catechin catalyzed reaction by CATPO, laccase and tyrosinase showed that, first, catechin was oxidized to semiquinone and *o*-quinone then, *o*-quinone reduced to hydrophilic dimer (type B dimer, Pcath-1, PLcath-1 and PTcath-1). Type B dimer enzimatically oxidized to the hydrophobic dimers (Pcath-2, PLcath-2 and PTcath-2). Once formed, the hydrophobic dimers were further oxidized by the enzyme to an o-quinone which, most likely, condensed with catechin to form the reduced trimer and then, oxidized tetramer (Pcath-3, PLcath-3 and PTcath-3) or reduced tetramer (Pcath-4 and PLcath-4).

Two major products (Pcaf-1 and Pcaf-2) were detected after 1 h incubation of caffeic acid by CATPO. Three major fragments were observed by HPLC, during the oxidation of caffeic acid by laccase for 1-hour (PLcaf-1, PLcaf-2 and PLcaf-3). PLcaf-2 and PLcaf-3 exhibited the same UV-Vis spectra with Pcaf-1 and Pcaf-2. PLcaf-2, PLcaf-3, Pcaf-1 and Pcaf-2 exhibited spectra similar to those of caffeicins, with a different ratio between the absorbance at 297 and 324 nm suggesting a partial loss of the side-chain conjugation during oxidation (C-O coupling). On the other hand, spectra relevant to the PLcaf-1 exhibited lambda max. at 324 nm similar to that caffeic acid and this similarity suggests that the side chain conjugation of the oxidation precursor is still present in this molecule. They could be then related to caffeic acid dimers arising from the C-C type coupling of the caffeic acid.

CHAPTER 4

CONCLUSIONS

- The phenol oxidase activity of CATPO (catalase-phenol oxidase) from *S. thermophilum* was confirmed by the spectroscopic and chromatographic analysis of the oxidation products.

- Among 14 phenolic compounds, only in catechol, cholorogenic acid, catechin and caffeic acid distinct oxidation products were observed by HPLC. This result showed that the range of phenolic compounds oxidized by CATPO is not limited to catechol, but larger MW polyphenolic compounds are also oxidized. Interestingly, all the 4 compounds oxidized by CATPO are well known for their strong antioxidant capacities.

- The common feature of catechol, catechin, caffeic acid and chlorogenic acid, appears to be the presence of two hydroxyl groups in the *ortho-* position. This suggests that the phenol oxidase activity of CATPO requires the presence of two hydroxyl groups in the *ortho-* position, although this is clearly not the only criteria for oxidation to take place.

- Epicatechin is an isomer of catechin but it was not oxidized by CATPO. This indicates that, CATPO shows stereospecificity on the substrates.

- While the maximum conversion efficiency, within 1 hr of reaction, was observed with catechin, minimum conversion efficiency was attained by caffeic acid, under the specified conditions.

- The oxidation products of catechol, caffeic acid, chlorogenic acid and catechin were characterized by LC-ESI-MS analysis. Dimer, trimer, tetramer and oligomer formation was detected.

- The enzyme was incapable of oxidizing tyrosinase and laccase-specific substrates tyrosine and ABTS respectively. However, depends on the oxidizing spectrum of substrates indicate that the nature of phenol oxidation by CATPO appears to resemble mainly those of laccase.

CHAPTER 5

RECOMMENDATIONS

For future studies; NMR and FT-IR should be performed to understand the exact bonding pattern and coupling mechanisms of oxidation products. Different phenolic compounds could be analyzed as CATPO substrates. The effects of different conditions on oxidation pattern and oxidation products of catechin, chlorogenic acid and caffeic acid can be analyzed. The role of CATPO in lignin degradation could be analyzed to understand the extracellular role of the enzyme. EPR (Electron paramagnetic resonance) could be performed to identify reaction intermediates in catalytic cycle(s) of CATPO.

REFERENCES

Aguirre, J., Rios-Momberg, M., Hewitt, D., Hansberg, W., 2005, "Reactive oxygen species and development in microbial eukaryotes", *Trends in Microbiology*, 13: 111-118.

Akagawa, M., Shigemitsu, T., Suyama, K., 2003, "Production of hydrogen peroxide by polyphenols and polyphenol-rich beverages under quasiphysological conditions", *Bioscience, Biotechnology and Biochemistry*, 67(12): 2632-2640.

Aktas, N., Tanyolac, A., 2003a., "Kinetics of laccase-catalyzed oxidative polymerization of catechol, *Journal of Molecular Catalysis B: Enzymatic,* 22: 61–69. 2003b., "Reaction conditions for laccase catalyzed polymerization of catechol", *Bioresource Technology,* 87: 209–214.

Aktas, N., Sahiner, N., Kantoglu, O., Salih, B., Tanyolac, A., 2003, "Biosynthesis and Chracterization of Laccase Catalyzed Poly(Catechol)", *Journal of Polymers and the Environment*, 11: 123.

Alexandre G., Zulin I.B., 2000, "Laccases are widespread in bacteria", *Trends Biotechnology* 18:41-42.

Alfonso-Prieto, M., Borovik, A., Carpena, X., Murshudov, G., Melik-Adamyan, W., Fita, I., Rovira, C., Loewen, P.C., 2007, *Journal of American Chemical Society,* 129: 4193-4205.

Allgood, G.S., Perry, J., 1986, *J.J. Bacteriol,* 168: 563

Angelova, M.B., Pashova, S.B., Spasova, B.K., Vassilev, S.V., Slokoska, L.S., 2005, "Oxidative stress response of filamentous fungi induced by hydrogen peroxide and paraquat", *Mycological Research*, 109: 150-158

Aoshima, H. Ayabe, S., 2007, "Prevention of the deterioration of polyphenol-rich beverages", *Food Chemistry*, 100: 350-355.

Arakane, Y., Muthukrishnan S., Beeman, R.M., Kanost, M.R., Kramer, K.J., 2005, *"Laccase 2 Is The Phenoloxidase Gene Required For Beetle Cuticle Tanning"*, Proceedings , *Annual Meeting*

Bento, I., Arménia Carrondo, M., Lindley, P.F., 2006, "Reduction of dioxygen by enzymes containing copper", *Journal of Biological Inorganic Chemistry*, 11:539.547.

Berthet, S., Nykyri, L.M., Bravo, J., Mate, M., Berthet-Colominas, C., Alzari, P.M., Koller, F., Fita, I., 1997, ''Crystallization and preliminary structural analysis of catalase A from *Saccharomyces cerevisiae'' Protein Science*, 6:481-483.

Bertrand, T., Jolivalt, C., Briozzo, P., Caminade, E., Joly, N., Madzak, C., Mougin, C., 2002, "Crystal structure of a four-copper laccase complexed with an arylamine: insights into substrate recognition and correlation with kinetics", *Biochemistry*, 41:7325-7333.

Billman-Jacobe, H., Sloan, J., Coppel, R.L., 1996, ''Analysis of isoniazid-resistant transposon mutants of *Mycobacterium smegmatis'', Fems Microbiology Letters*, 144: 47-52.

Boerjan, W., Ralph, J., Baucher M., 2003, ''Lignin Biosynthesis'', *Annual Reviews Plant Biology*, 54: 519–46.

Bollag J.M., Leonowicz A., 1984, "Comparative Studies of Extracellular Fungal Laccases" *Applied Environment Microbiolog*y, 48(4): 849-854.

Bourbonnais, R., Paice, M. G., Reid, I. D., Lanthier, P., Yaguchi M., 1995, "Lignin Oxidation by Laccase Isozymes from *Trametes versicolor* and Role of the Mediator 2,29-Azinobis (3-Ethylbenzthiazoline- 6-Sulfonate) in Kraft Lignin Depolymerization" *Applied And Environmental Microbiology*, 61 (5): 1876–1880.

Bradford, M.M., 1976, "A rapid and sensitive method for the quantitation of microgram quantities of protein utilizing the principle of protein-dye binding", *Analytical Biochemistry*, 72: 248-254.

Bravo, J., Verdaguer, N., Tormo, J., Betzel, C., Switala, J., Loewen, P.C., Fita, I., 1995, ''Crystal structure of catalase HPII from Escherichia coli'', *Structure,* 3: 491-502.

Burton, S.G., 2003, "Laccases and phenol oxidases in organic synthesis-a review", Current Organic Chemistry, 7: 1317-1331. *of the Microscopy Society Of America*, 102:11337-11342.

Chelikani, P., Fita, I., Loewen, P.C., 2004, "Diversity of structures and properties among catalases", *CMLS Cellular and Molecular Life Sciences*, 61: 192-208.

Cimpoiu, C., 2006, "Analysis of Some Natural Antioxidants by Thin-Layer Chromatography and High Performance Thin-Layer Chromatography", *Journal of Liquid Chromatography & Related Technologies*, 29: 1125-1142.

Claus, L.,2003, "Laccases and their occurrence in prokaryotes", *Archieves of Microbiolology*, 179: 145-150.

Cooney, D.G., Emerson, R., 1964, "Thermophilic Fungi: An Account of Their Biology, Activities and Classification", W.H. Freeman Publishers, San Francisco, USA.

Coseteng, M.Y., Lee, C.Y., J., 1987, "Changes in apple polyphenol oxidase and polyphenol concentrations in relation to degree of browning", *Journal of Food Science* 52:985-989.

Dawson, C. R., Tarpley, W. B., 1963, "On the Pathway of the Catechol-Tyrosinase Reaction", Annals *of the New York Academy of Sciences,* 100: 937–950

De, Marco, A., Roubelakis-Angelakis, K.A., 1997, "Laccase activity could contribute to cell-wall reconstitution of regenerating protoplasts", *Phytochemistry,* 46: 421–425.

Della-Cioppa, G., Garger, S.J., Holtz, R.B., McCulloch, M.J., Sverlow, G.G., 1998a, Method for making stable extracellular tyrosinase and synthesis of polyphenolic polymers therefrom. US Patent 5801047.

Díaz, A., Muñoz-Clares, R.A., Rangel, P., Valdés, V.J., Hansberg, W., 2005, "Functional and structural analysis of catalase oxidized by singlet oxygen", *Biochimie*, 87: 205-214.

Díaz, A., Horjales, E., Rudiño-Piñera, E., Arreola, R., Hansberg, W., 2004, "Unusual Cys-Tyr Covalent Bond in a Large Catalase", *Journal of Molecular Biology*, 342: 971-985

Dittmer, N.T., Suderman, R.J., Jiang, H., Zhu, Y.C., Gorman, M.J., Kramer, K.J., Kanost, M.R., 2004, "Characterization of cDNA encoding putative laccase-like multicopper oxidases and developmental expression in the tobacco hornworm, Manduca sexta, and the malaria mosquito, Anopheles gambia",. *Insect Biochemistry* and *Molecular Biology,* 34:29–41.

Dressler H, 1994, ''Resorcinol, its uses and derivatives'', *Polymer International*, 1: 74

Dubey, S., Singh, D., Misra, R. A., 1998, "Enzymatic Snythesis and Various Properties of Poly(Catechol)", *Enzyme and Microbial Technology,* 23: 432-437

Dugan, L., Simic, M.G., Karel. M., 1980, "Autooxidation in Food and Biological Systems", Plenum Press, New York, p. 261.

Duncan, W. R., Prezhdo, O.V., 2005, "Electronic Structure and Spectra of Catechol and Alizarin in the Gas Phase and Attached to Titanium", *J. Phys. Chem. B*, 109, 365-373.

Durán, N., Rosa, M.A., D'Annibale, A,, Gianfreda, L., 2002, " Applications of laccases and tyrosinases (phenoloxidases) immobilized on different supports: a review" *Enzyme and Microbial Technology,* 31:907–931.

Eicken, C., Krebs, B., Sacchettini, J. C., 1999, "Catechol oxidase-structure and activity", *Current Opinion in Structural Biology,* 9:677-683

Enguita, F. J., martins, L. O., Henriques, A. O., Carrondo, M. A., 2003, "Crystal structure of a bacterial endospore coat component a laccase with enhanced thermostability properties", *J.Biol. Chem.* 278**,** 19416–19425.

Farver, O., Pecht, J., 1984, "In copper proteins and copper enzymes (CRC. ,Boca raton) " 1: 183

Feofilova, E.P., Tereshina, V. M., 1999, "Thermophilicity of Mycelial Fungi in the Context of Biochemical Adaptation to Thermal Stress", *Applied Biochemistry and Microbiology*, 35: 486-494.

Fiegel, H., Voges, H. W., Hamamoto, T., Umemura, S., Iwata, T., Miki, H., Fujita, Y., Buysch, H. J., Garbe, D., Paulus, W., 2002, "Phenol Derivatives" in Ullmann's Encyclopedia of Industrial Chemistry, Wiley-VCH, DOI: 10.1002/14356007.a19_313.

Fiegel, H., Voges, H.W., Hamamoto, T., Umemura, S., Iwata, T., Miki, H., Fujita, Y., Buysch, H.J., Garbe, D., Paulus, W., 2002, *"Phenol Derivatives" Ullmann's Encyclopedia of Industrial Chemistry*

Fita, I., Silva, A.M., Murthy, M.R.N., Rossmann, M.G., 1986, "The refined structure of beef liver catalase at 2.5 ▢ resolution", *Acta Crystallogrophica- Section B: Structural Crystallogtraphy and Crystal Chemistry*, 42: 497-515.

Fraaije, M.W., Roubroeks, H.P., Hagen, W.R., Van-Berkel, W.J., 1996, ''Purification and Characterization of an Intracellular Catalase-Peroxidase from *Penicillium Simplicissimum''* *European Journal of Biochemistry*, 235: 192-198.

Fridovich, I., 1995, Superoxide radical and superoxide dismutases., *Annu Rev Biochem,* 64: 97-112

Garcia-Molina, F., Hiner, A.N.P., Fenoll, L.G., Rodriguez-Lopez, J.N., Garcia- Ruiz, P.A., Garcia-Canovas, F., Tudela, J., 2005, "Mushroom tyrosinase: Catalase activity, inhibition and suicide inactivation", *Journal of Agricultural and Food Chemistry*, 53: 3702-3709.

Gerdemann, C., Eicken, C., Magrini, A., Meyer, H.E., Rompel, A., Spener, F., Krebs, B., 2001, "Isoenzymes of *Ipomoea batatas* catechol oxidase differ in catalase-like activity", *Biochemica et Biophysica Acta*, 1548: 94-105.

Gerdemann, C., Eicken, C., Krebs, B., 2002, "The crystal structure of catechol oxidase: new insight into the function of type-3 copper proteins" Accounts of *Chemical Research* 35(3):183-91.

Gienfreda, L., Bollag, J-M., 2002, "Isolated enzymes fort he transformation and detoxification of organic pollutant", *In Enzymes in the Environment: Activity, Ecology, and Applications;* 495-538.

Gianfreda, L., Iamarino, G., Scelza, R.,and Rao, M.A., 2006, Oxidative catalysts for the transformation of phenolic pollutants: *Biocatalysis and Biotransformation*, 24, 3, 177-187

Gianfreda L.,, Xu F., Bollag J.M., 2010, "Laccases: A Useful Group of Oxidoreductive Enzymes", *Bioremediation Journal* 3:1-26.
.
Gouet, P., Jouve, H.-M., Dideberg, O., 1995, "Crystal structure of *Proteus mirabilis* PR catalase with and without bound NADPH", *Journal of Molecular Biology*, 249: 933-954

Griffith, G.W., 1994, "Phenoloxidases", *Progress in Industrial Microbiology*, 29: 763-788.

Gukasyan, G.S., 1999, "Purification and some properties of tyrosinase from *Aspergillus flavipes*", *Biochemistry*, 64:417-420.

Halaouli S., Asther, Mi., Kruus K., Guo, L., Hamdi M., Sigoillot J.-C., Asther M., Lomascolo A., 2005, "Characterization of a new tyrosinase from *Pycnoporus* species with high potential for food technological applications", *Journal of Applied Microbiology* 98:332-343.

Hamilton, A.J., Gomez, B.L., 2002, "Melanins in fungal pathogens", *Journal of Medical Microbiology*, 51, 189–191.

Hearing, V.J., Tsukamoto, K., 1991, "Enzymatic control of pigmentation in mammals", *FASEB Journology,* 5:2902-2909.

Heim, K.E., Tagliaferro, A.R., Bobilya, D.J., 2002, "Flavonoid antioxidants: chemistry, metabolism and structure-activity relationships", *The Journal of Nutritional Biochemistry*, 13: 572-584.

Herrmann, K., 1976, "Flavonols and flavones in food plants", *Journal of Food Technology*, 11:433.

Hudnall P. M., 2002, "Hydroquinone" *Ullmann's Encyclopedia of Industrial Chemistry.*

Huttermann, A., Mai, C., Kharazipour, A., 2001, "Modification of lignin for the production of new compounded materials", *Applied Microbiology and Biotechnology,* 55: 387–394.

Jacobson, E.S., 2000, "Pathogenic roles for fungal melanins", *Clinical Microbiology*, 13, 708–717.

Jassim, S.A.A., Naji, M.A., 2003, "Novel antiviral agents: a medicinal plant perspective". *Journal of Applied Microbiology* 95 (3): 412–427.

Jolley, R., Nelson, R., Robb, D., 1969, "The Multiple Forms of Mushroom Tyrosinase. Structural Studies on the Isozymes ", *J Biol Chem*, 244, 3251

Jolley, R.L. Jr., Evans, L.H., Makino, N., Mason, H.S., 1974, "Oxytyrosinase", *The Journal of Biological Chemistry*, 249(2): 335-345.

Kaptan, Y., 2004, "Utilization of *Scytalidium thermophilum* phenol oxidase in bioorganic synthesis", M.Sc. Thesis, METU, Ankara, Turkey.

Klotz, M.G., Loewen, P.C., 2003, "The molecular evolution of catalatic hydroperoxidases: Evidence for multiple lateral transfer of genes between Prokaryota and from Bacteria into Eukaryota", *Molecular Biology and Evolution* 20: 1098-1112.

Kocabas, D.S., Bakir, U., Phillips, S.E.V., McPherson, M.J., Ogel, Z.B., 2008, "Purification, characterization, and identification of a novel bifunctional catalasephenol oxidase from *Scytalidium thermophilum*", *Applied Microbiology and Biotechnology*, 79: 407-415.

Koller, F., Fita, I., 1999, "Structure of catalase A from *Saccharomyces cerevisiae*", *Journal of Molecular Biology*, 286: 135-139.

Kong K.H., Lee J.L., Park H.J., Cho S.H., 1998, "Purification and characterization of the tyrosinase isozymes of pine needles", *Biochemistry & Molecular* Biology *International,* 45:717-724.

Krastanov A., 2000, "Removal of phenols from mixtures by co-immobilized laccase/tyrosinase and polyclar adsorption", *Journal of Industrial Microbiology and Biotechnology*, 24, 383–388.

Kwon-Chung, K.J., Polacheck, I., Popkin, T.J., 1982, "Melanin-lacking mutants of *Cryptococcus neoformans* and their virulence for mice", *The Journal of Bacteriology*, 150, 1414–1421.

Kwon, B.S., Haq, A.K., Pomerantz, S.H., Halaban, R., 1987, "Isolation And Sequence Of A Cdna Clone For Human Tyrosinase That Maps At The Mouse C-Albino Locus", *Proceedıngs of The National Academy of Sciences of The United States of America-Physical Sciences* 84(21):7473-7.

Kwon, B.S., Wakulchik, M., Haq, A.K., Halaban, R., Kestler, D., 1988, "Sequence analysis of mouse tyrosinase cDNA and the effect of melanotropin on its gene expression", Biochemical and Biophysical Research *Communications* 153:1301-1309.

Land, E.J., Ramsden, C.A., Riley, P.A., 2004, " Quinone chemistry and melanogenesis", *Methods Enzymol.*, 378:88.109.

Land, E.J., Ramsden, C.A., Riley, P.A., 2007, "The mechanism of suicide-inactivation of tyrosinase: a substrate structure investigation", *Tohoku J. Exp. Med.*, 212, 341-348

Land, E.J., Ramsden, C.A., Riley, P.A.,Stratford , M.R.L., 2008, " Studies of para-quinomethane formatinon during the tyrosinase-catalysed oxidation of 4-alkylcatechols", *Arkivoc*, 258- 267

Langfelder K., Streibel M.,, Jahn B., Haase G., Brakhage A.A**.,** 2003, "Biosynthesis of fungal melanins and their importance for human pathogenic fungi", *Fungal Genetics and Biology*, 38 (2): 143-158.

Leatham G.F., Stahmann M.A., 1981, "Studies on the laccase of lentinus edodes: specificity, localization and association with the development of fruiting bodies", *Journal of General Microbiology*, 125: 147-157.

Lerch K., 1983, *Neurospora tyrosinase*: structural, spectroscopic and catalytic properties. *Molecular Cell*, 52(2):125.138.

Levy, E., Eyal, Z., Hochman, A., 1992, ''Purification and characterization of a catalase-peroxidase from the fungus *Septoria tritici*'', *Archives of Biochemistry And Biophysics*, 296: 321-7.

Loewen, P.C., Switala, J., von Ossowski, I., Hillar, A., Christie, A., Tattrie, B., Nicholls, P., 1993, "Catalase HPII of *Escherichia coli* catalyzes the conversion of protoheme to cis-heme *d*", *Biochemistry*, 32: 10159-10164.

Loewen, P.C., 1997, "Bacterial catalases", *Oxidative Stress and the Molecular Biology of Antioxidant Defences*, 273-308.

Loewen, P.C., Klotz, M.G., Hassett, D.J., 2000, "Catalase- an "old" enzyme that continues to surprise us", *American Society for Microbiology News*, 66:76-82

Lule, S.U., Xia, W.S., 2005, "Food phenolics, pros and cons: a review", *Food Reviews International*, 21: 367-388.

Macheix, J.J., Fleuriet, A., Billot, J., 1989, "Fruit Phenolics", CRC Press, Boca Raton, FL.

Madani, W., Kermasha, S., A. Versari, A., 1999, "Characterization of Tyrosinase- and Polyphenol Esterase-Catalyzed End Products Using Selected Phenolic Substrates" *J. Agric. Food Chem*, 47: 2486-2490

Maga, J.A., 1978, "Simple phenol and phenolic compounds in food flavor", *Critical Reviews in Food Science* and *Nutrition*, *10: 323.*

Maheshwarı, R., Bharadwaj, G., Bhat, M.K., 2000, *Thermophilic Fungi, Their Physiology and Enzymes*, 64 (3): 461–488.

Manach, C., Scalbert, A., Morand, C., Rémésy, C., Jiménez, L., 2004, "Polyphenols: food sources and bioavailability", *The American Journal of Clinical Nutrition*, 79: 727

Makino, N., McMahill, P., Mason, H.S., 1974, "The oxidation state of copper in resting tyrosinase", *Journal of Biological Chemistry*, 249(19):6062-6066.

Martins, L.O., Soares, C.,M, Pereira, M.M., Teixeira, M., Costa, T., Jones, G.H., Henriques, A.O., 2002, The *Journal of Biological* Chemistry, 277: 18849–18859.

Mason, H.S., 1948, "The chemistry of melanin. III. Mechanism of the oxidation of dihydroxyphenylalanine by tyrosinase" *Journal of Biological Chemistry*, 172:83.92.

Maté, M.J., Zamocky, M., Nykyri, L. M., Herzog, C., Alzari, P.M., Betzel, C., Koller, F., Fita, I., 1999, "Structure of catalase A from *Saccharomyces cerevisiae*", *Journal of Molecular Biology*, 286: 135-139.

Mate, M., Murshudov, G., Bravo, J., Melik-Adamyan, W., Loewen, P.C, Fita, I., 2001, "Heme-catalases", *Handbook of proteins*.

Matoba, Y., Kumagai, T., Yamamoto, A., Yoshitsu, H., Sugiyama, M., 2006, *Journal of Biological Chemistry*, 281:8981-8990.

Matheis G., Chem. Mikrobiol. Technol. Lebensm. G. 1987b, "Polyphenol oxidase and enzymatic browning of potatoes (Solanum tuberosum) II. Enzymatic browning and potato constituents", *Food Chemistry Microbiology Technology,* 11: 33-41.

Mayer, A.M., 1987, "Polyphenol oxidases in plant" *Recent Progress Phytochemistry* 26:11-20.

Mayer, A.M., Staples, R.C., 2002, "Laccase: new function for an old enzyme", *Phytochemistry*, 60: 551-565

Mayer, A.M., 2006, "Polyphenol oxidases in plant and fungi: going places? A review", *Phytochemistry*, 67: 2318-2331.

Melik-Adamyan, W.R., Barynin, V.V., Vagin, A.A., Borisov, V.V., Vainshtein, B.K., Fita, I., Murthy, M.R., Rossmann, M.G., 1986, ''Comparison of beef liver and Penicillium vitale catalases'', *Journal of Molecular Biology,* 188: 63-72.

Merle, P.L., Sabourault, C., Richier, S., Allemand, D., Furla, P., 2007, "Catalase characterization and implication in bleaching of a symbiotic sea anemone", *Free Radical Biology and Medicine*, 42: 236-246.

Mete, S., 2003, "Scytalidium thermophilum polyphenol oxidase: production and partial characterization", M.Sc. Thesis, METU, Ankara, Turkey.

Moore, B., 2004, "Bifunctional and moonlighting enzymes: lighting the way to regulatory control", *Trends in Plant Science,* 9: (5) 221-228.

Morton L.M., Caccettah R.A.A., Ian B. Croft P., Croft K. D., 2000, *Clinical and Experimental Pharmacology and Physiology* 27: 152–159.

Mullen R.T., Lee M.S., Trelease R.N., 1997, ''Identification of the peroxisomal targeting signal for cottonseed catalase'', *Plant Journal* 12: 313-322.

Murshudov, G. N.; Melik adamyan, W.R.; Barynin, V.V; Vagin, A.A.; Grebenko, A.I.; Barynin, V.V.; Vagin, A.A.;Vainshtein , B.K.; Dauter, Z.; Wilson, K., 1992, *Federation of European Biochemical Societies* 312: 127-131.

Muñoz-Muñoz, J.L., García-Molina. F., García-Ruiz, P.A., Arribas, E., Tudela, J., García-Cánovas. F., Rodríguez-López J.N., 2009, "Enzymatic and chemical oxidation of trihydroxylated phenols", *Food Chemistry*, 113: 435-444.

Murthy, M.R.N., Reid, T.J., Sicignano, A., Tanaka, N. and Rossmann, M.G., 1981, ''Structure of beef liver catalase'', *Journal of Molecular Biology* 152: 465-49.

Nagai, M., Kawata, M., Watanabe, H., Ogawa, M., Saito, K., Takesawa, T., Kanda K., Sato, T., 2003, "Important role of fungal intracellular laccase for melanin synthesis: purification and characterization of an intracellular laccase from Lentinula edodes fruit bodies", *Microbiology,* 149: 2455-2462**.**

Nagy, J.M., Cass A. E. G Brown, K. A., 1997, "Purification and Characterization of Recombinant Catalase-Peroxidase, Which Confers Isoniazid Sensitivity in *Mycobacterium tuberculosis*[*] *The Journal of Biological Chemistry,* 272, 31265-31271

Nicholls, P., Fita, I., Loewen, P.C., 2001, "Enymology and structure of catalases", *Advances in Inorganic chemistry*, 51: 51-106.

Obinger, C., Regelsberger, G., Strasser, G., Burner, U., Peschek, G.A., 1997b, ''Purification and characterization of a homodimeric catalase-peroxidase from the cyanobacterium *Anacystis nidulans*'', *Biochemical and Biophysical Research Communication,* 371:810-3.

Olthof M.R., Hollman PC, Katan M.B., 2001, "Chlorogenic acid and caffeic acid are absorbed in humans", *Journal of Nutrition*, 131: 66–71.

Osman, A. M., Wong, K. K. Y., Fernyhough, A., 2007, The laccase/ABTS system oxidizes (+)- catechin to oligomeric products" *Enzyme and Microbial Technology*, 40: 1272-1279

Osman, A., Agha, A. E., Makris, D. P., Kefalas, P., 2009, "Chlorogenic Acid Oxidation by a Crude Peroxidase Preperation: Biocatalytic Characteristics and Oxidation Products, *Food Biprocess Technol*. DOI 1007 /s11947-009-0241-8

Ögel, Z.B., Yüzügüllü, Y., Mete, S., Bakir, U., Kaptan, Y., Sutay, D., Demir, A.S., 2006, "Production, properties and application to biocatalysis of a novel extracellular alkaline phenol oxidase from the thermophilic fungus Scytalidium thermophilum", *Applied Microbiology and Biotechnology*, 71: 853-862.

Paynter, N. P., Yeh, H.C., Voutilainen, S., Schmidt, M.I., Heiss, G., Folsom, A.R., Brancati, F.L., Kao, W. H. L., 2006, *American Journal of Epidemiology*, 164: 1075–1084

Pati, S., Losito, I., Palmisano, F., Zambonin, P. G., 2006, "Characterization of Caffeic Acid Enzymatic Oxidation By-Products by Liquid Chromatography Coupled to Electrospray Ionization Tandem Mass Spectrometry", *Journal of Chromatography A*, 1102: 184-192.

Pierpoint W.S., 1966, "The enzymic oxidation of chlorogenic acid and some reactions of the quinone produced", *Biochemical Journal*, 98(2):567–580.

Piontek K., Antorini M., Choinowski T., 2002, "Crystal strucrure of a laccase from the fungus *Trametes versicolor* at 1.90-A resolution containing a full complement coppers", *The journal of Biological Chemistry*, DOI 10.1074.

Pourcel, L., Routaboul, J.-M., Cheynier, V., Lepiniec, L., Debeaujon, I., 2006, "Flavonoid oxidation in plants: from biochemical properties to physiological functions", *Trends in Plant Science*, 12: 29-36.

Reinhammar, B., Malstrom, B.G., 1981, "Blue" coppercontaining oxidases", *Copper Proteins, Metal Ions in Biology,* 3: 109-149.

Rice-Evans C.A., Miller, N.J., Paganga G., 1996, "Structure-antioxidant activity relationships of flavonoids and phenolic acids", *Free Radical Biology and Medicie*, 20: 933-956.

Sakaguchi, N, Inowe, M., Ogihara, Y., 1998, "Reactive oxygen species and intracellular Ca2+, common signals for apoptosis induced by gallic acid", *Biochemical Pharmacology*, 55: 1973-1981.

de Sotillo, D.R., Hadley, M., Wolf-Hall, C., 1998, *J. Food Sci.* 63 (5): 907

Scandalios, J.G., 1994, "Regulation and properties of plant catalases", *Causes of Photooxidative Stress and Amelioration of Defense Stress and Amelioration of Defense Systems in Plants*. 275-315.

Schmidtlein, H., Herrmann, K., 1975a, "On the phenolic acids of vegetables. I. Hydroxycinnamic acids and hydroxybenzoic acids of Brassica species and leaves of other Cruciferae", *Z. Lebensm. Unters. Forsch,* 159:139.

Schutt, C., Netzly , D.,1991, " Effect of apiforol and apigeninidin on the growth of selected fungi", *Journal of Chemical Ecology*, 17: 1122-1125

Siegbahn, E. M., 2004, "The catalytic cycle of catechol oxidase" *Journal of Biological Inorganic Chemistry,* 9: 577-590

Singh, R., Wiseman, B., Deemagarn, T., Jha, V., Switala, J., Loewen, P.C., 2008, Comparative study of catalase-peroxidases (KatGs), *Archives of Biochemistry and Biophysics* 471, 207–214.

Sharma, K.K., Kuhad, R.C., 2008, "Laccase:enzyme revisited and function redefined", *Indian Journal of Microbiology*, 48:309-316.

Smejkalova, D., Conte, P., Piccolo, A., 2007, "Structural Characterization of Isomeric Dimers from the Oxidative Oligomerization of Catechol with a Biomimetic Catalyst", *Biomacromolecules*, 8: 737-743

Smejkalova, D., Piccolo, A.,Spiteller, M., 2006, "Oligomerization of Humic Phenolic Monomers by Oxidative Coupling under Biomimetic Catalysis", *Environ. Sci. Technol.* 40: 6955-6962

Solomon, E.I., Sundaram, U.M., Machonkin, T.E., 1996, "Multicopper oxidases and oxygenases" *Chemical Reviews,* 96:2563-2606.

Sotillo, D.R.; Hadley, M.; Wolf-Hall, C., 1998, "Potato Peel Extract a Nonmutagenic Antioxidant with Potential Antimicrobial Activity", *Journal of Food Science* 63 (5): 907.

Spritz, R.A., Oh, J., Fukai, K., Holmes, S.A., Ho, L., Chitayat, D., France, T.D., Musarella, M.A., Orlow, S.J., Schnur, R.E., Weleber, R.G., Levin, A.V., 1997, *Human Mutation* 0:171.174.

Sutay, D., 2007, "Purification, characterization, crystallization and preliminary X-ray structure determination of *Scytalidium thermophilum* bifunctional catalase and identification of its catechol oxidase activity", Ph.D. Thesis, METU, Ankara, Turkey.

Sun W, Kadima T.A., Pickard M.A., Dunford H.B., 1994, "Catalase activity of chloroperoxidase and its interaction with peroxidase activity" *Biochemistry* and *Cell Biology*, 72: 321-31.

Stohr, A., Herrmann, K., 1975b., "The phenols of fruits. V. the phenols of strawberries and their changes during development and ripeness of fruits". *Z. lebesm. Unters. Forsch.,* 158:341.

Steyn W.J., 2009, "Anthocyanin production in cranberry leaves and fruit related to cool temperatures at a low light intensity" *Biomedical and Life Sciences Anthocyanins*, 1-21.

Tepper, A.W.J.W., 2005, "Structure and mechanism of the type-3 copper protein tyrosinase" Doctoral Thesis, Leiden University. 165.

Thomas J.A., Morris D.R., Hager L.P., 1970, "Chloroperoxidase VII. Classical peroxidatic, catalytic and halogenating forms of the enzyme". *The Journal of Biological Chemistry*, 245: 3129–3134.

Thurston, C.F., 1994, "The structure and function of fungal laccases", *Microbiology* 140: 19–26.

Vainshtein, B.K., Melik-Adamyan, W.R., Barynin, V.V., Vagin, A.A., Grebenko, A.I., 1981, "Three-dimensional structure of the enzyme catalase" *Nature* 293: 411-412.

Vetrano, A.M., Heck, D.E., Mariano, T.M., Mishin, V., Laskin, D.L., Laskin, J.D., 2005, "Characterization of the oxidase activity in mammalian catalase", *The Journal of Biological Chemistry*, 280(42): 35372-35381.

Waldo, G.S., Fronko, R.M., Penner-Hahn, J. E., 1991, *Biochemistry*, 30: 10486.

Walker, J.R., Ferrar, P.H., 1998, "Diphenol oxidases, enzyme-catalysed browning and plant disease resistance" *Biotechnology & Genetic Engineering Reviews* 15:457.498.

Wayne, F., Beyer, Jr., Fridovich, I., 1985, "Pseudocatalase from Lactobacillus plantarum: evidence for a homopentameric structure containing two atoms of manganese per subunitv", *Biochemistry*, 1985, 24 (23), 6460–6467

Wichers, H.J., Gerritse, Y.A., Chapelon, C.G.J., 1996, "Tyrosinase isoforms from the fruitbodies of *Agaricus bisporus*", *Phytochemistry*, 43:333-337.

Wiegant, W. M., 1992, *Applied and Environmental Microbiology*, 58: 1301-1307.

Wheeler, M.H., Bell, A.A., 1988, "Melanins and their importance in pathogenic fungi", *Current Topics in Medical Mycology*, 338– 387.

Yamazaki, S., Morioka, C., Itoh, S., 2004, "Kinetic evaluation of catalase and peroxygenase activities of tyrosinase", *Biochemistry*, 43: 11546-11553.

Yüzügüllü. Y., 2010, "Functional and structural analysis of catalase-phenol oxidase from *Scytalidium thermophilum.*

Zámocký, M., Koller, F., 1999, "Understanding the structure and function of catalases: clues from molecular evolution and *in vitro* mutagenesis", *Progress in Biophysics & Molecular Biology*, 72: 19-66.

Zhang X.; van Leeuwen J.; Wichers H. J.; Flurkey W. H., 1999, "Characterization of tyrosinase from the cap flesh of Portabella mushrooms" *Journal of Agricultural Food Chemistry*. 47: 374-378.

APPENDIX A

CHEMICALS, ENZYMES AND THEIR SUPPLIERS

Table A.1 Chemicals and Enzymes

Chemical or Enzyme	Supplier
Acetonitril	Merck
Acetic acid	Merck
Agar	Merck
Calcium Chloride	Merck
Catechol	Sigma
Caffeic acid	Sigma
Chlorogenic acid	Sigma
Coumaric acid	Sigma
Catechin	Sigma
CuSO4	Sigma
Epicatechin	Sigma
Ethanol	Merck
Gallic acid	Sigma
Glucose	Merck
Hydrocholoric Acid	Merck
Hydroquinone	Sigma
KCL	Merck
K2HPO4	Merck
KH2PO4	Merck

Table A.1 Chemicals and Enzymes (continued)

Chemical or Enzyme	Supplier
Methanol	Merck
Myrisetin	Sigma
MgCl2.7H2O	Merck
NaCl	Merck
NaOH	Merck
Phenillactic acid	Sigma
Resorcinol	Sigma
Resveratrol	Sigma
SDS	Merck
Sodium Acetate	Merck
Sodium Citrate	Merck
Soluble Starch	Sigma
Quercetina	Sigma
Vanillic acid	Sigma
Yeast Extract	Merck

GROWTH MEDIA, BUFFERS AND SOLUTIONS PREPARATIONS

Ethanol (70%, 100 mL)

70 mL absolute ethanol is mixed with 30 mL distilled sterile water.

LB Broth (per Liter)

10 g tryptone

5 g yeast extract

10 g NaCl

Final volume is adjusted to 1 liter with distilled water and pH is adjusted to 7.0 with NaOH and autoclaved. 100 μg/ mL ampicilin is added whenever it is used. The medium is stored at 4 °C.

NaOH (10 N, 100 mL)

40 g of NaOH pellets is added slowly to 80 mL of H2O. When the pellets have dissolved completely, the volume is adjusted to 100 mL with H2O. The solution is stored at room temperature.

Phosphate (Sodium) Buffer

Stock solution A: 2 M monobasic sodium phosphate, monohydrate (276 g/L)

Stock solution B: 2 M dibasic sodim phosphate (284 g/L)

Mixing an appropriate volume (mL) of A and B as shown in the table below and diluting to a total volume of 200 mL, a 1 M phosphate buffer of the required Ph at room temperature.

TAE Buffer (50X, per Litre)

242 g of Tris base is dissolved in 600 mL distilled waster. The pH is adjusted to 8.0 with approximately 57 mL glacial acetic acid. Then, 100 mL 0.5 M EDTA (pH 8.0) is added and the volume is adjusted to 1 L.

TE Buffer

10 mM Tris1 mM EDTA (pH 8.0)

Tris HCl Buffer (50 mM, pH 8.0)

6 g Tris base is dissolved in 800 mL of distilled water. The pH is adjusted to the desired value with concentrated hydrochloric acid. The solution is cooled to room temperature before making final adjustment to pH. The volume of the solution is then adjusted to 1 L with distilled water and sterilized by autoclaving.

YpSs Agar

4.0 g/L Yeast extract
1.0 g/L K2HPO4
0.5 g/L MgSO4.7H2O
15.0 g/L Soluble starch
20.0 g/L Agar

YpSs Broth

4.0 g/L Yeast extract
1.0 g/L K2HPO4
0.5 g/L MgSO4.7H2O

10 g/L Glucose

Preculture Medium

4.0 g/L Yeast extract
1.0 g/L K2HPO4
0.5 g/L MgSO4.7H2O
10.0 g/L Glucose
HCl (pH 8.0)

Mainculture Medium

4.0 g/L Yeast extract
1.0 g/L K2HPO4
0.5 g/L MgSO4.7H2O
0.1 g/L CuSO4.5H2O
40 g/L Glucose
(0.17 g/L Gallic acid)

SDS (10% w/v, per Liter)

100 g of SDS is dissolved in 900 mL of H2O. The solution is heated to 68 °C and stirred with a magnetic stirrer to assist dissolution. If necessary, pH is adjusted to 7.2 by adding a few drops of concentrated HCl. The volume of the solution is adjusted to 1 liter with H2O. It is stored at room temperature.

PROTEIN MEASUREMENT BY BRADFORD METHOD

Bovine serum albumin (BSA) was used as the protein standard according to Bradford (1976) (Figure C.2.). To prepare 1 mg/mL stock BSA solution, 25 mg BSA was dissolved in 25 mL of 100 mM pH 7 sodium phosphate buffer. To measure the protein content, 0.5 mL BSA solution and 5 mL of Bradford reagent (Sigma) were mixed in a glass test tube. Ten minutes later absorbances at 595 nm were measured by using a spectrophotometer and BSA standard curve was achieved (Figure B.1). Protein concentrations of other samples were analyzed by the same method and protein concentrations were calculated using the BSA standard curve. Figure C.1. BSA standard curve for Bradford Method.
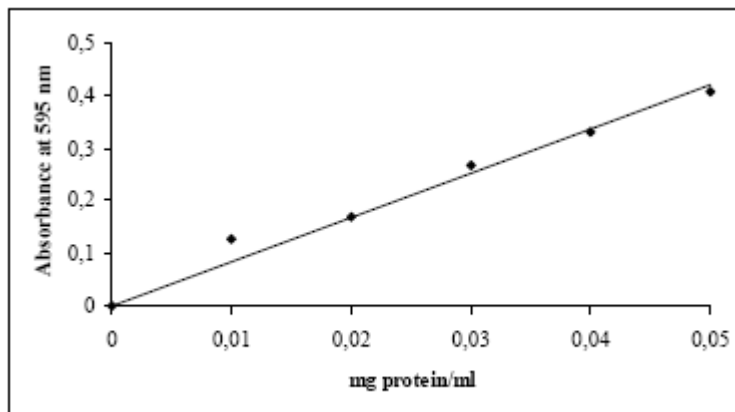

Figure C.2 BSA standard curve for Bradford Method

Table C.1 Standard protocol of Bradford Assay

Tube number	BSA standard (µL)	Distilled water (µL)	Bradford solution (µL)	Protein (mg/mL)
1	-	500	5	0
2	5	495	5	0.01
3	10	490	5	0.02
4	15	485	5	0.03
5	20	480	5	0.04
6	25	475	5	0.05

SODIUMDODECYLSULPHATE POLYACRYLAMIDE GEL ELECTROPHORESIS (SDS-PAGE) PROTOCOL

SDS-Polyacrylamide Gel Electrophoresis was performed using NuPAGE® Novex® Bis-Tris gels according to the instructions provided from www.invitrogen.com web site (Table D.1 and Table D.2)

Table D 1 Standard protocol of preparation of Stacking gel

Components	Stacking gel (mL) (7.5%) (x1)	Stacking gel (mL) (7.5%) (x2)
Stacking Gel Buffer	0.6	1.2
30 % Acrylamide stock solution	0.4	0.8
H_2O	1,4	2.8
Ammonium persulphate (25%)	0,02	0.04
TEMED	0,002	0.004
Total	2.4	4.8

Table D.2 Standard protocol of preparation of Separating gel

Components	Separating gel (mL) (12.5%)(x1)	Separating gel (mL) (12.5%)(x2)
Separating Gel Buffer	1,2	2.4
30 % Acrylamide stock solution	2,1	4.2
H_2O	1,7	3.4
Ammonium persulphate (25%)	0,03	0.06
TEMED	0,003	0.006
Total	5	10

Sample Loading

Load the appropriate concentration of protein (of interest) on the gel.

Buffer Loading

Fill the Upper Buffer Chamber with 200 mL 1X NuPAGE® SDS Running Buffer. For reduced samples, use 200 mL 1X NuPAGE® SDS Running Buffer containing 500 μL NuPAGE® Antioxidant. Fill the Lower Buffer Chamber with 600 mL 1X NuPAGE® SDS Running Buffer.

Running Conditions

Voltage: 200 V constant
Run time: 35 min (MES Buffer), 50 min (MOPS Buffer)
Expected current: 100-125 mA/gel (start), 60-80 mA/gel (end)

APPENDIX E

COOMASSIE-BASED GEL STAINING PROTOCOL

Simply Blue Safe Stain Microwave Protocol (Invitrogen) for staining 1.0 and 1.5 mm mini NuPAGE Gels (ınvitrogen) was described below. Table F.1. Simply Blue Safe Stain Microwave Protocol

E.1 Step Protocol Time

1. Place the gel in 100 mL ultrapure water and microwave on high (950-1100 watts) 1 min
2. Shake the gel on an orbital shaker. Discard wash 1 min
3. Repeat Steps 1 and 2 twice. 1 min each
4. Add 20-30 mL SimplyBlue SafeStain and microwave 45 sec to 1 min
5. Shake the gel on an orbital shaker. Discard stain. 5-10 min
6. Wash the gel in 100 mL ultrapure water on an orbital shaker. 10 min
7. Add 20 mL 20% NaCl and shake the gel on an orbital shaker 5-10 min
8. Optional: Repeat Step 6 for a clear background 1 h

AREA VERSUS CONCENTRATION CURVE OF PHENOLS OF DIFFERENT MOLARITIES

The calibration curve is a graph showing the response of an analytical technique to know quantities of analyte. Based on these chromatograms showing the different molarities of phenolics, concentration versus area curve was drawn (Figure G.1, G.2, G.3).
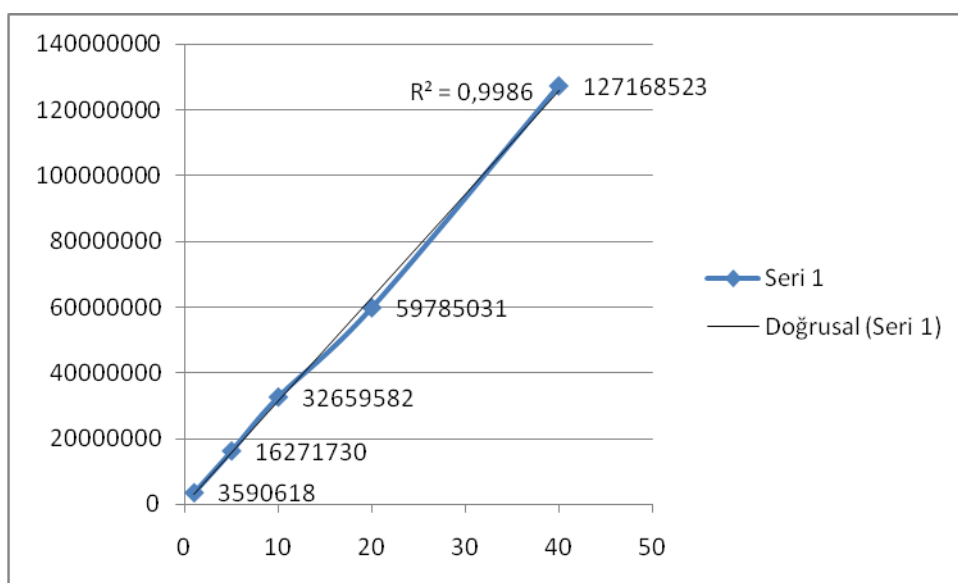
Figure F.1 Area versus concentration curve of chlorogenic acid of different molarities
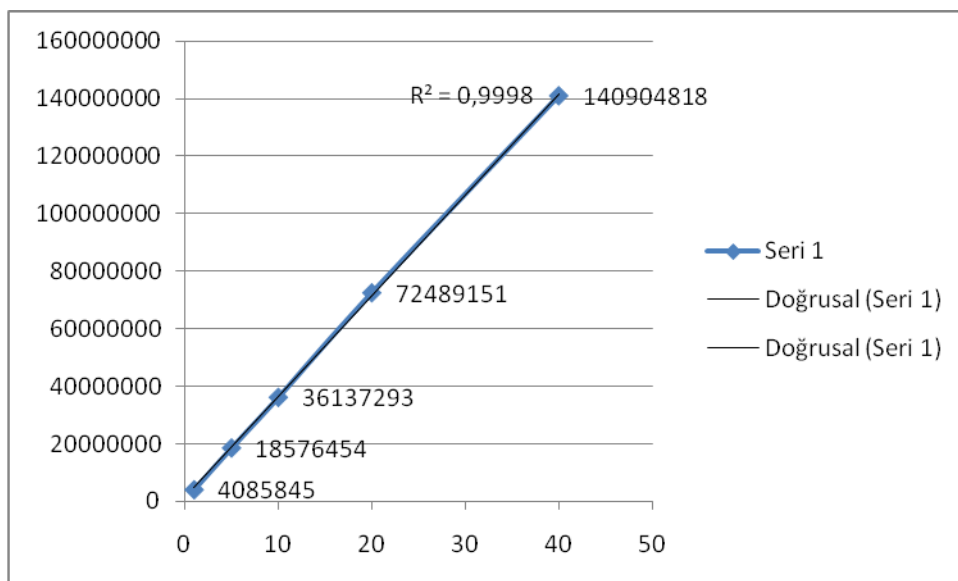
Figure F.2 Area versus concentration curve of caffeic acid of different molarities
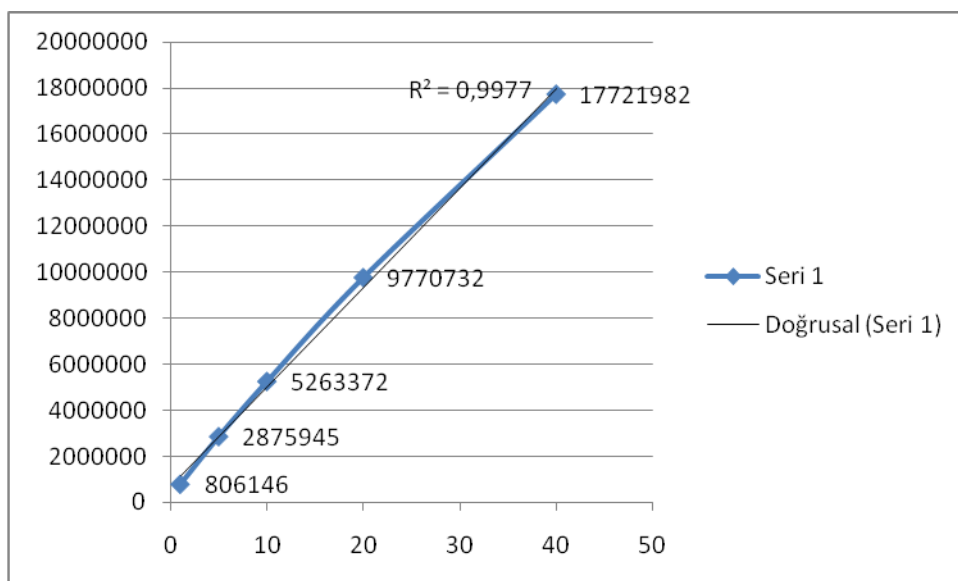
Figure F.3 Area versus concentration curve of catechin of different molarities Figure H 1

CHROMATGRAMS SHOWING EFFECTS OF DIFFERENT CONDITIONS
ON CATECHOL OXIDATION
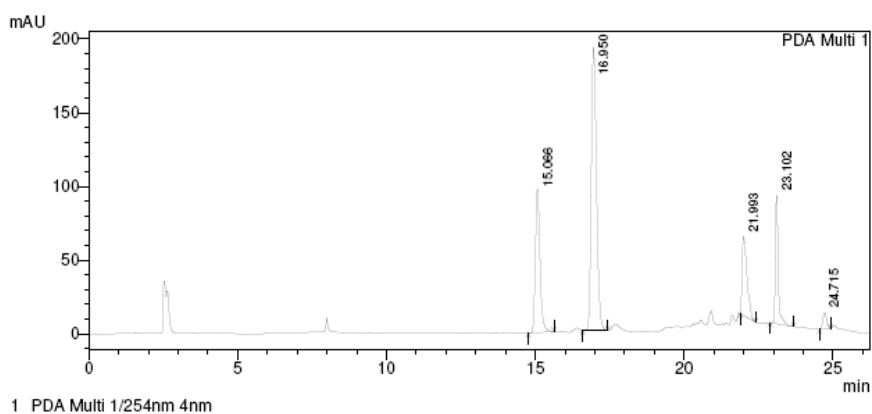
Figure G.1 24 Auto-oxidation profile of 10 mM catechol for 24 hs at 60 ^{o}C and pH 7
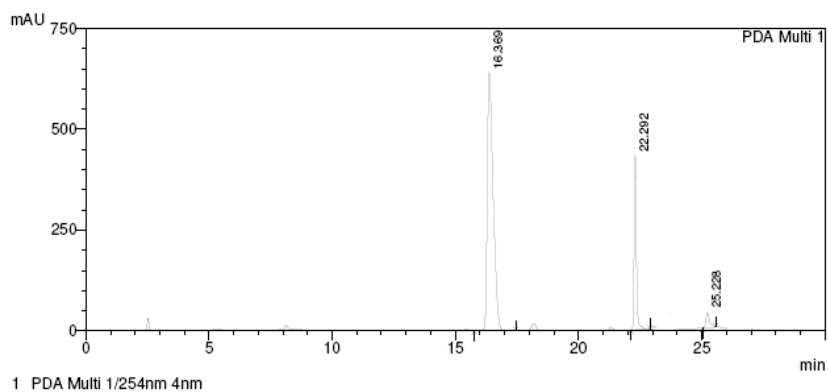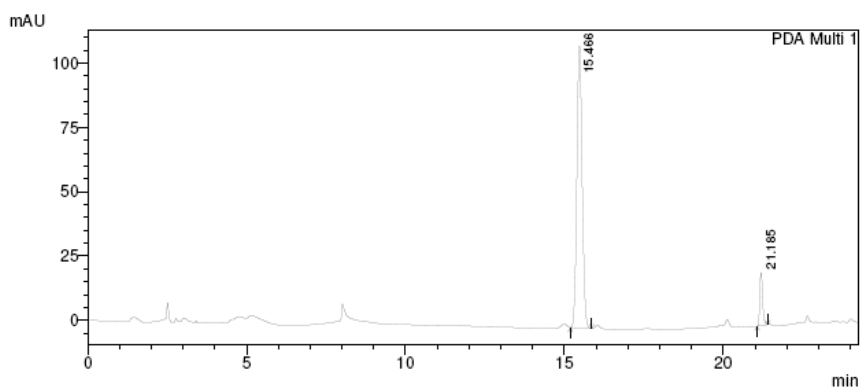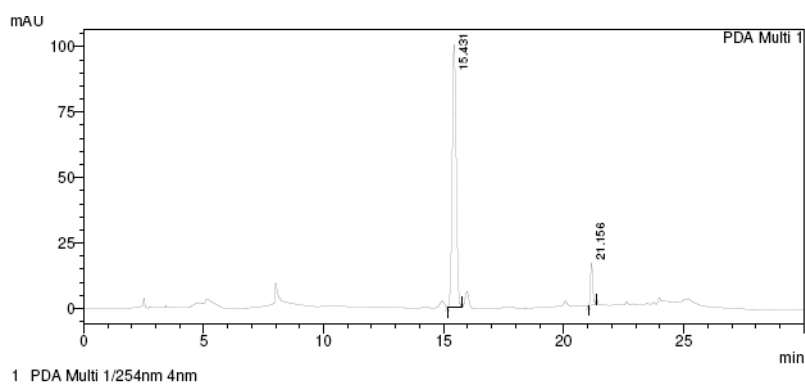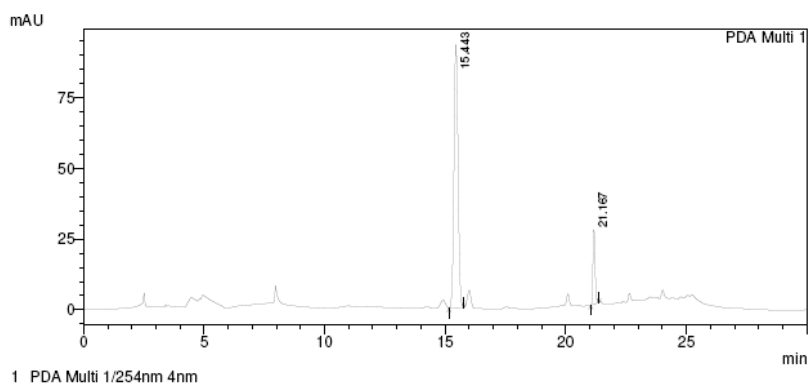

Figure G.1 HPLC profile of 100 mM catechol oxidized by CATPO (3.63 U/µg) for 1 h at 60 ^{o}C and pH 7
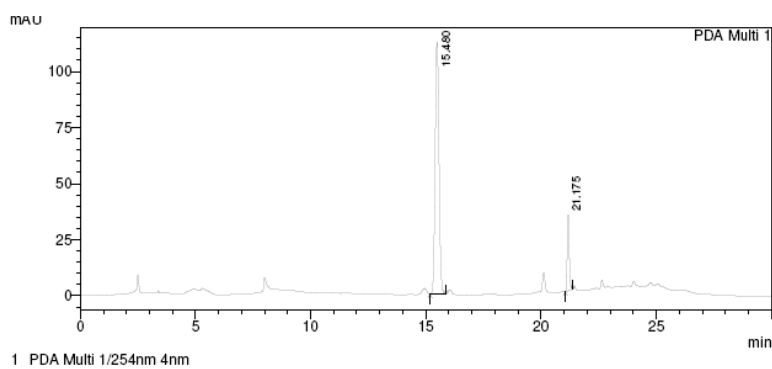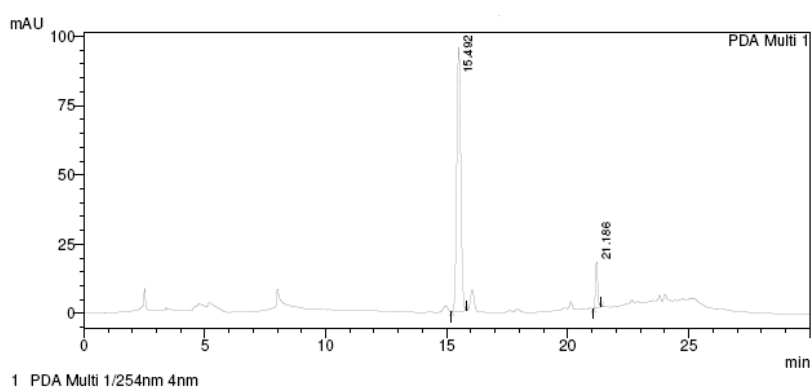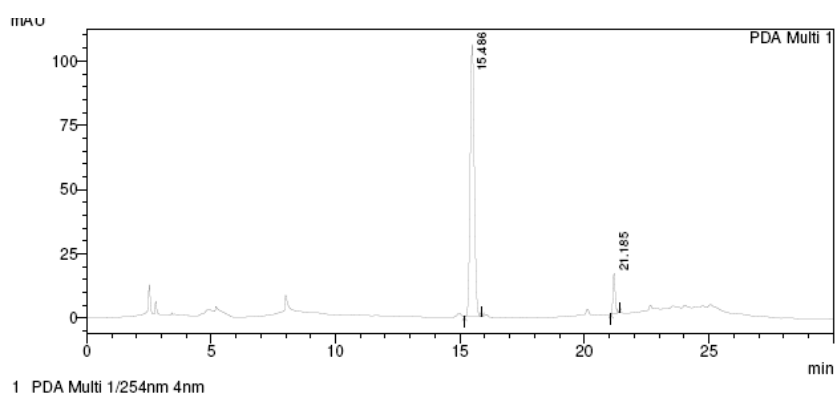
(a)

(b)

(c)

Figure G.2 HPLC profile of 10 mM catechol oxidized by CATPO (3.63 U/µL) for 1 h at 40 ^{o}C (a), 50 ^{o}C (b) and 70 ^{o}C (c) and pH 7

(d)

(e)

(f)

Figure G.3 HPLC profile of 100 mM catechol oxidized by CATPO (3.63 U/μg) for 1 h at 60 $^{\circ}$C and pH:6 (d), pH:8 (e) and pH 9 (f)

CIRRICULUM VITALE

PERSONAL INFORMATION

Surname, Name: Avcı, Gülden

Nationality: Turkish (TC)

Date and Place of Birth: 29.05.1979 Ankara

Phone: +90 532 498 92 50

Email: biogulden@hotmail.com

EDUCATION

Degree	Institution	Year of Graduation
MS	METU Biotechnology	2006
BS	Ankara University Biology	2001
High School	Fethiye Kemal Mumcu Anatolian High School	1997

FOREIGN LANGUAGES

Advanced English

CONFERENCES

16th National Biotechnology Conference (December 13-16, 2009, Antalya)

International Symposium on Biotechnology, (September 27-30, 2009), Ankara-Turkey

GRANTS

Tubitak Research Grant, 1001 funding; Production and biocatalytic properties of the bifunctional catalase/catechol oxidase enzyme of the thermophilic fungus *Scytalidium thermophilum* in the presence of phenolic compounds (2007-2009), $114,424